## SECTION C

# BEHAVIOUR OF WELLS IN CONFINED AQUIFER AND WELL DESIGN PROCEDURES.

by

P. S. Huyakorn

## Summary

Following the theoretical and numerical methods described in Section B, two finite element programs were written in Fortran IV language to solve the general problem of two regime axisymmetric confined flow toward a single well. Both programs were used to analyse steady state behaviour of flow through a typical confined aquifer.

The basic procedures for program usage and the performance of various types of well design in extracting water from the aquifer are described in this section. Permeability data obtained for unconsolidated materials, and graphs showing the effects of well design factors, hydraulic properties of aquifer material and radius of influence are presented. Hydraulic considerations and procedures in well design are also discussed.

## Table of Contents


| | Page No. |
|---|---|
| 1. Introduction | C1. |
| 1.1 General | C1. |
| 1.2 Basic Approach to the Problem | C1. |
| 2. Analysis of Flow by Finite Element Programs | C3. |
| 2.1 General | C3. |
| 2.2 Input Data | C3. |
| 2.2.1 Reading and Printing of Data | C3. |
| 2.2.2 General Data | C5. |
| 2.2.3 Mesh Preparation and Automatic Generation of Mesh Data | C5. |
| 2.3 Processing of Output | C6. |
| 2.3.1 Printed Output | C6. |
| 2.3.2 Graphical Output | C7. |
| 2.4 Validity Check and Accuracy of Results | C8. |
| 3. Steady Flow Behaviour and Well Design Data | C10. |
| 3.1 General | C10. |
| 3.2 Permeability Data obtained for Unconsolidated Materials | C10. |
| 3.3 Drawdown-distance Curves and Non-Darcy Zones | C14. |
| 3.3.1 Fully Screened Wells | C14. |
| 3.3.2 Partially Screened Wells | C15. |
| 3.4 Drawdown-discharge Relationships | C16. |
| 3.4.1 Effects of Well Design Factors | C16. |
| 3.4.2 Effects of Properties of Aquifer Material | C18. |
| 3.4.3 Effects of Radius of Influence | C18. |
| 3.5 Proposed Empirical Drawdown-discharge Relationships | C20. |
| 4. Hydraulic Consideration and Procedures in Well Design | C21. |
| 4.1 General | C21. |
| 4.2 Hydraulic Performance of Well | C21. |
| 4.2.1 Specific Capacity | C21. |
| 4.2.2 Entrance Velocity | C22. |
| 4.2.3 Well Loss and Hydraulic Efficiency | C23. |
| 4.3 Selection of Screen and Casing Dimensions | C25. |
| 4.3.1 Screen Diameter | C25. |
| 4.3.2 Casing Diameter | C25. |
| 4.3.3 Screen Open Area and Slot Size | C26. |

Table of Contents (cont'd.)


| | Page No. |
|---|---|
| 4.4 Selection of Gravel Pack | C28. |
| 4.4.1 General | C28. |
| 4.4.2 Grading of Pack | C29. |
| 4.4.3 Thickness of Pack | C30. |
| 5. Conclusions and Further Work | C32. |
| Appendix I - Mathematical Solution of Steady Radial Flow toward a Fully Screened Well | C33. |
| List of References | C37. |

## List of Tables


| Table No. | Title | Page No. |
|---|---|---|
| 0 | Flow Chart of Main Program | C4. |
| 1 | Comparison of Drawdowns Computed by various methods | C9. |
| 2 | Comparison of Well Discharges computed by various methods | C9. |
| 3 | List of Permeability Data for Unconsolidated Materials | C11. |
| 4 | Permeability Data for Gravel Materials | C12. |
| 5 | Hydraulic Coefficients - Theoretical Curves | C13. |
| 6 | Results for Fully Screened Wells | C14. |
| 7 | Comparison of Discharges and Velocities for Various Well Radii | C16. |
| 8 | Effect of Screen Position | C17. |
| 9 | Effect of Gravel Pack Properties | C19. |
| 10 | Suggested Casing Diameters (after Johnson, E.E. Inc.) | C26. |
| 11 | Surescreen, Stainless Steel Standard and Medium Pattern Screens (by courtesy of Surescreen Manufacturing Co., Brisbane, Australia) | C27. |

## List of Figures


| Figure No. | Title | Follows Page No. |
|---|---|---|
| (1-1) | Strata section of unconsolidated sediments | C2. |
| (1-2) | Design features of selected wells | C2. |
| (1-3) | Constructed digital flow model for computer analysis | C3. |
| (2-1) | Triangular mesh pattern for a well fully penetrating two layered aquifers | C6. |
| (2-2) | Triangular mesh pattern for a partially penetrating well | C6. |
| (2-3) | One-dimensional mesh consisting of 3-node elements | C6. |
| (3-1) | Velocity-gradient lines for typical unconsolidated materials | C10. |
| (3-2) | Velocity-gradient lines for typical gravel pack materials | C10. |
| (3-3) | Theoretical velocity-gradient curves constructed for studying effects of hydraulic coefficients | C10. |
| (3-4) | Sieve analysis curves of materials tested by Dudgeon (1965) | C10. |
| (3-5) | Drawdown-distance curves for fully screened well | C14. |
| (3-6) | Drawdown-distance curves for a partially screened well | C14. |
| (3-7) | Non-Darcy zones in the vicinity of well screen for various drawdowns | C15. |
| (3-8) | Non-Darcy zones in the vicinity of well screen for various drawdowns | C15. |
| (3-9) | Drawdown-discharge curves showing effect of well radius | C16. |
| (3-10) | $s_w/Q$ Vs. Q curves showing effect of well radius | C16. |
| (3-11) | Drawdown-discharge curves showing effect of screen length | C17. |
| (3-12) | $s_w/Q$ Vs. Q curves showing effect of screen length | C17. |
| (3-13) | Discharge of partially screened well as function of screen length/aquifer thickness ratio | C17. |

List of Figures (cont'd.)


| Figure No. | Title | Follows Page No. |
| --- | --- | --- |
| (3-14) | Drawdown-distance curves showing effect of gravel pack | C18. |
| (3-15) | Drawdown-discharge curves showing effect of material properties | C18. |
| (3-16) | $s_w/Q$ Vs. Q curves showing effect of material properties | C18. |
| (3-17) | Discharge ratio Vs. radius ratio for a fully screened well | C20. |
| (4-1) | Flow through screen opening and well loss | C23. |
| (4-2) | Adjusted value of screen loss coefficient as a function of $\frac{CL}{D}$ (after Petersen, et al) | C24. |
| (4-3) | Discharge Vs. well drawdown showing component of losses | C24. |
| (I-1) | Mathematical model of confined well-aquifer system | C33. |
| (I-2) | Theoretical $s_w/Q$-Q relationship | C35. |

# 1. Introduction

## 1.1 General

Following the theoretical and numerical methods described in Section B of this report, two finite element programs were written in Fortran IV computer language to solve the general problem of two regime axi-symmetric confined flow toward a single well.

The first program employs one-dimensional elements to treat the simplest case of radial flow toward a fully screened well completely penetrating a single confined aquifer. The second is a more general program which employs triangular elements to handle two-dimensional flow.

The two programs were used to analyse steady state flow through a thin aquifer of simple hydrogeological setting as shown in Fig. (1-1). The example chosen is of similar dimensions and materials to the aquifer tested by the Queensland Irrigation and Water Supply Commission at Murgon (Ref. 8). The aquifer is approximately 13 ft. thick and composed of unconsolidated sand and gravel. The overlying and underlying beds consist of clay bound sand and multi-coloured clay which may be assumed to be impermeable. The water table is 45 ft. above the bottom boundary of the aquifer. The available drawdown to the top boundary is 32 ft., which should be sufficient to induce non-Darcy flow having significant effects on the discharge and the head distribution near the well.

The flow behaviour was examined for various selected well designs shown in Fig. (1-2), which include fully and partially screened and gravel packed wells. The effects of several factors on the well discharge and specific capacity were evaluated. These factors include well diameter, degree of penetration, properties of the aquifer material and radius of influence.

## 1.2 Basic approach to the Problem

In solving the flow problem by using the computer programs, it is necessary to construct a digital flow model incorporating simplifying assumptions, and simulate the various flow cases which are to be analysed. A sketch of the constructed steady flow model is shown in Fig. (1-3). The following assumptions were made:

(i) The aquifer is of constant thickness, overlain and underlain by horizontal impermeable beds and intercepted at a radius of influence by a large body of water, the level of which is unaffected by pumping.

(ii) The aquifer is homogeneous and isotropic.

(iii) The well is pumped at a constant water level above the top of the aquifer.

(iv) The flow is steady and hydraulic losses through the screen and inside the well are negligible.

With the introduction of these assumptions, the programs were applied. The drawdown distribution and the total discharge were calculated for selected values of prescribed well drawdown.

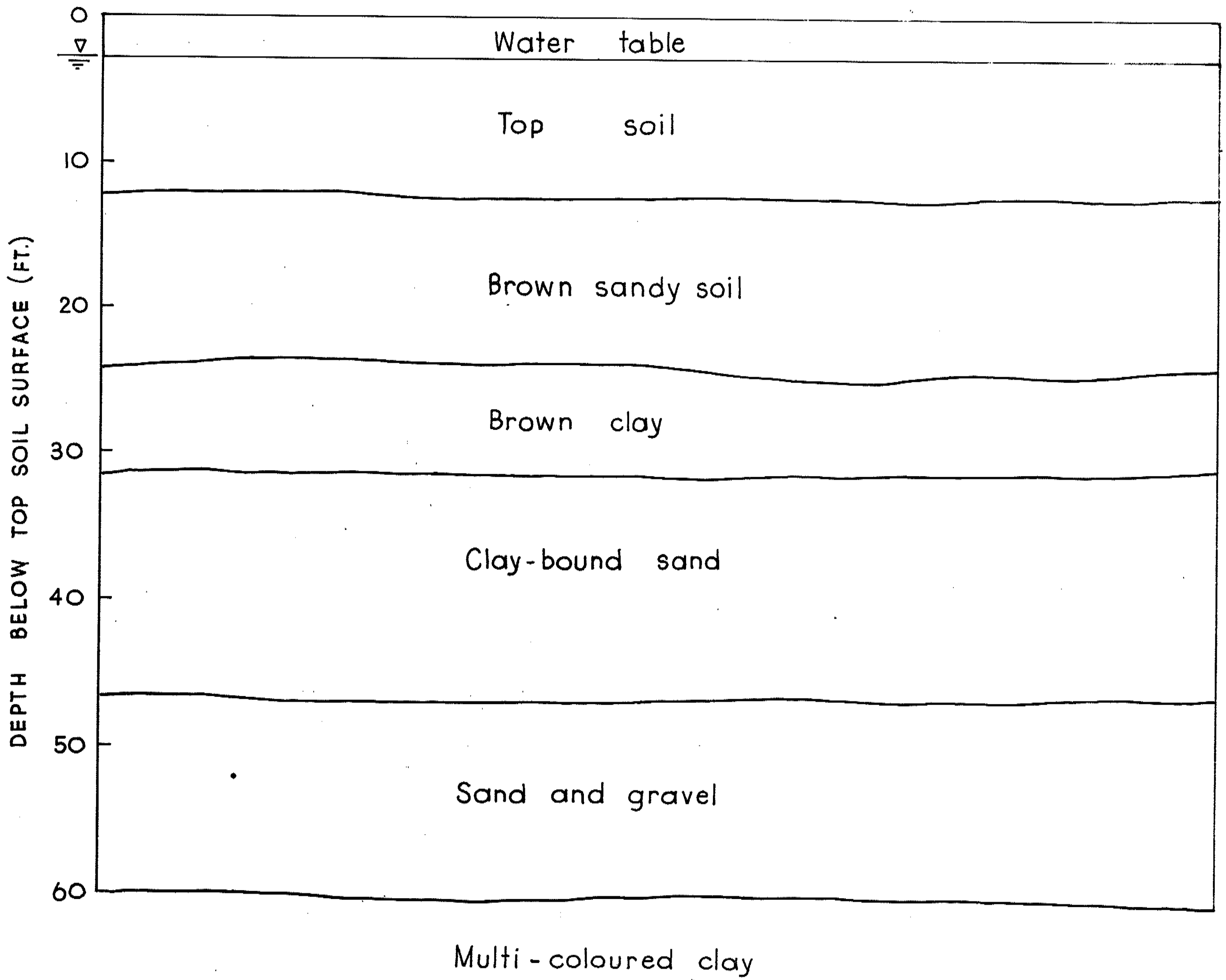


Fig.(1-1): Strata section of unconsolidated sediments.

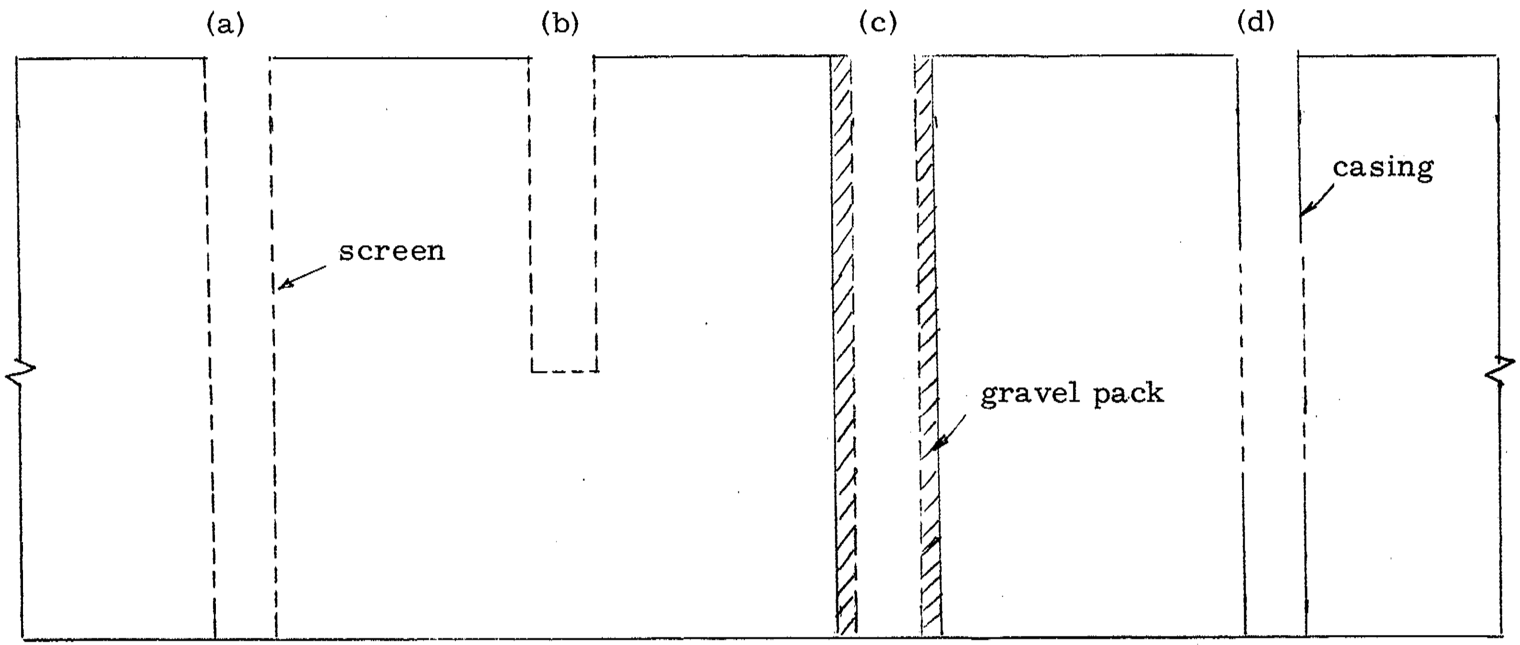


Fig. (1-2): Design features of selected wells.

## 2. Analysis of Flow by Finite Element Programs

### 2.1 General

The detailed description of the two computer programs is not presented. A schematic flow chart showing the major operations in the main program is shown in Table 0.

The general two-dimensional program was written in such a way that the complication resulting from the following factors could be readily handled.

(i) Partial penetration, partial screening or the use of multiple screens.

(ii) Gravel packed wells.

(iii) Multi-layered aquifers.

(iv) Anisotropy and non-homogeneity of aquifer.

To employ the two programs, the user only needs to familiarise himself with the preparation of input data, processing of output and validity check and interpretation of the computed results.

### 2.2 Input Data

#### 2.2.1 Reading and Printing of Data

The bulk of input data consists of the following:-

(i) General data, which are data essential for complete definition of the flow problem.

(ii) Mesh data, which consist of coordinates of nodal points and elements with their defining node numbers.

The above data are printed as soon as they have been read in. Thus, the results of analysis are always preceded by the input data, which makes checking easier in case some errors have been introduced in the data preparation. Also, these data will generally be useful for future reference. Another salient feature in the programs is the self-checking system for the number of cards that have been read in, to avoid the error

C4.

Table 0: Flow Chart of Main Program

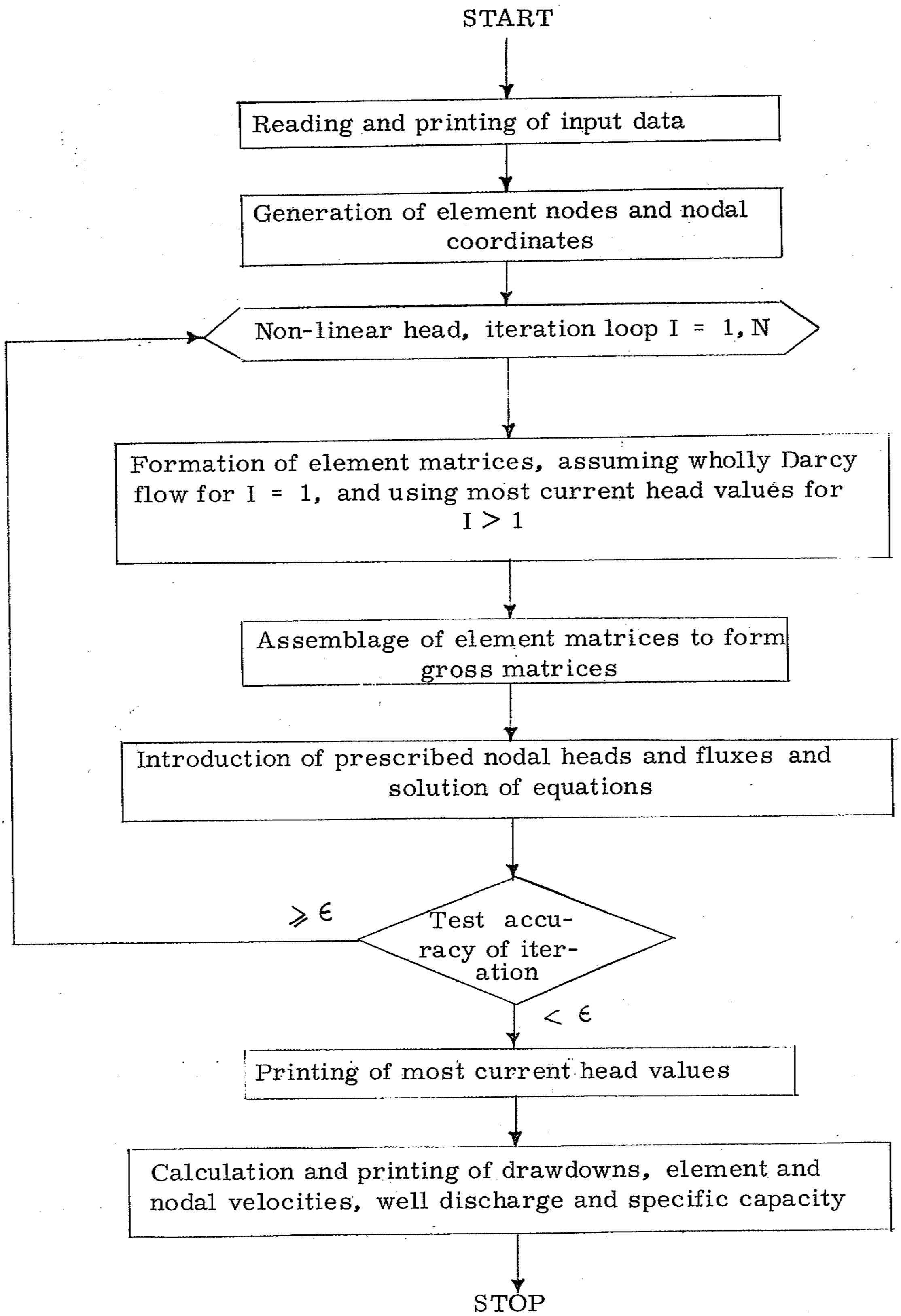

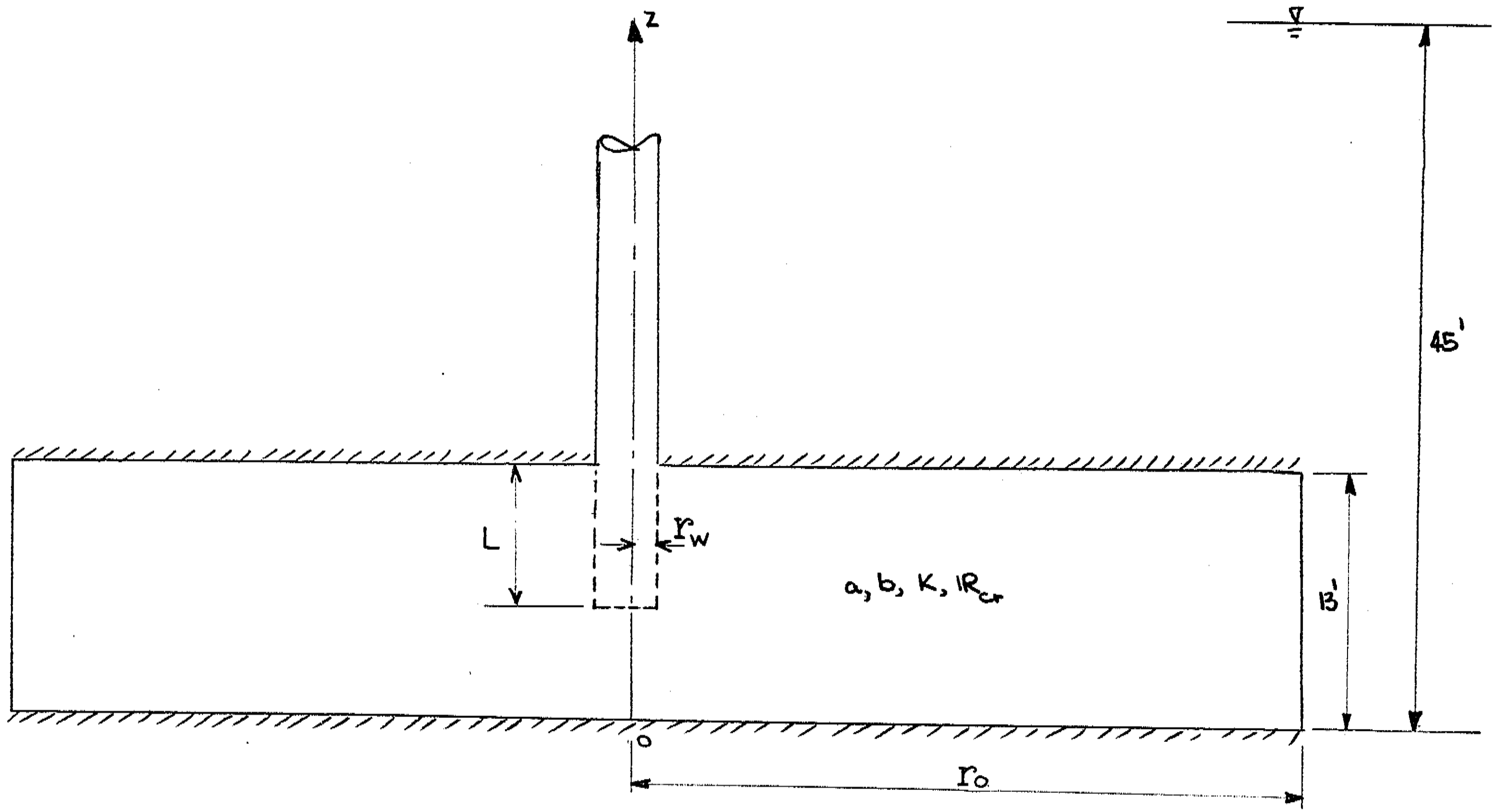


Fig. (1-3): Constructed digital flow model for computer analysis.

of having an incorrect number of data cards in a particular set. As any such error will cause the computer to stop, only little execution time will be wasted, and the position where the error has occurred can be pin-pointed exactly.

### 2.2.2 General Data

The general data required by the programs are as follows:

(i) Dimensions of the well structure. These include the well radius, penetration length, length and position of screen and, for the gravel packed well, the thickness and depth of pack.

(ii) Geological setting of the aquifer, which is described in terms of its thickness, height of water table and radius of influence.

(iii) Hydraulic properties of the aquifer material, which are the Forchheimer coefficients a and b, critical flow velocity corresponding to the critical Reynolds number and the coefficient of hydraulic conductivity K.

(iv) The water level in the well, in the case of pumping at constant drawdown.

(v) The total discharge into the well, in the case of pumping at constant discharge.

### 2.2.3 Mesh Preparation and Automatic Generation of Mesh Data

The finite element method requires subdivision of the entire flow region into a network of finite elements. The network is usually referred to as "mesh". The detailing of the mesh to be used in the analysis has to be decided by the program user. Experience and careful judgement is necessary in order that the required solution may be obtained at reasonable accuracy and cost. The general guides for a proper choice of the mesh are to use many small elements in the near well zone where the hydraulic gradient is steep and a smaller number of larger elements in the outer zone of the aquifer, and to grade the mesh appropriately in between. A general knowledge of the head distribution should be attained before deciding upon the mesh detail. In choosing the total number of nodes and elements, consideration should be given to the accuracy and detail of the solution required and the resulting cost.

A salient feature of the existing programs is the automatic generation of the mesh by their subroutines. This is desirable as the labour involved in preparing and checking of input data is considerably reduced and the occurrence of errors in the preparation is greatly diminished.

Typical mesh patterns adopted for various types of well boundary and stratification of the aquifer are shown in Figs. (2-1) to (2-3).

To employ the discretisation subroutines in the two-dimensional program, the user has to divide the entire flow region into a number of rectangular zones, termed "regular subregions", as shown in Fig. (2-1), and feed in the data describing them, namely the height and width of the rectangle and the node number and nodal coordinates of its bottom left corner. One subroutine is then called to discretise each subregion into a regular grid pattern of triangular elements each of which is identified by 3 nodes connected in an anti-clockwise sense. The numbers of horizontal and vertical lines characterising the rectangular grid have to be specified before discretisation. Another subroutine is called to determine the coordinates of all the nodes in the subregion. A graded zone is employed to connect two adjacent regular subregions, which facilitates the use of finer mesh near the well and coarser mesh in the outer portion of the aquifer. The graded zone is discretised by the third subroutine.

The numbering of the nodes in the entire flow region starts from bottom to top of the aquifer in increasing order along a vertical line.

In the one-dimensional program, the flow region is divided into a number of line segments each of which is further subdivided into a number of 3-node elements as shown in Fig. (2-3). The radial coordinate of all the nodes in the flow region are also generated.

## 2.3 Processing of Output

### 2.3.1 Printed Output

The flow problem is analysed for a number of values of the prescribed drawdown in the well. For each drawdown value, the nodal head values and the velocities at the centroids of the elements are calculated. The heads are subtracted from the elevation of the water table to give the nodal drawdowns, and the element velocities are averaged to result in the nodal velocities. To assess the performance of the well facility in extracting water from the aquifer, the total well discharge and

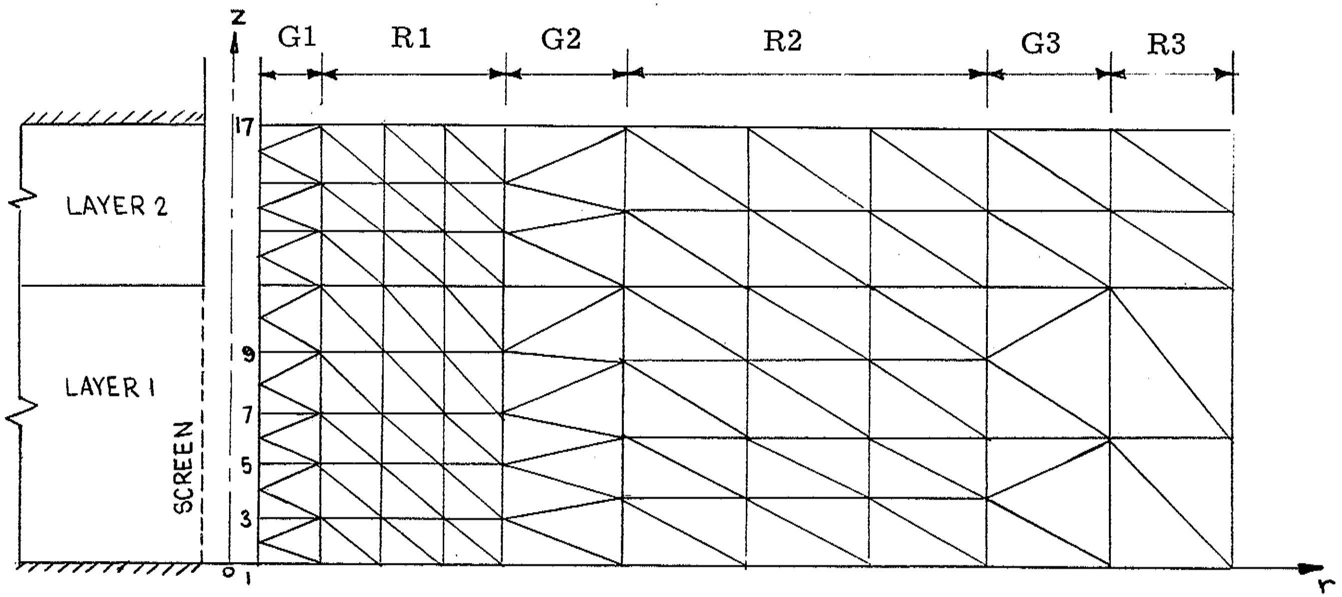


R1 to R3 are regular subregions 1 to 3
G1 to G3 are graded regions 1 to 3


Fig. (2-1): Triangular mesh pattern for a well fully penetrating two layered aquifers.

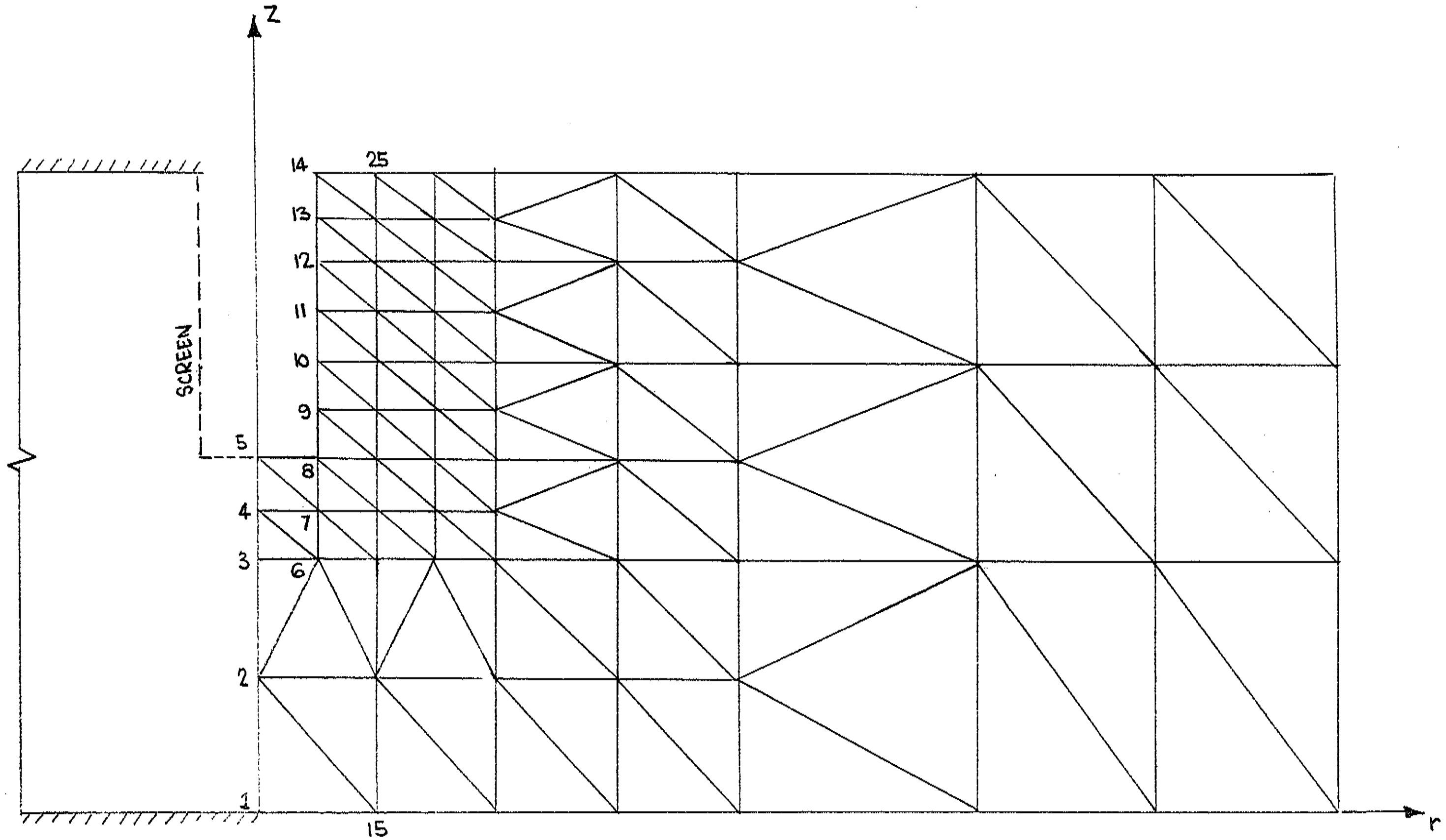


Fig. (2-2): Triangular mesh pattern for a partially penetrating well.

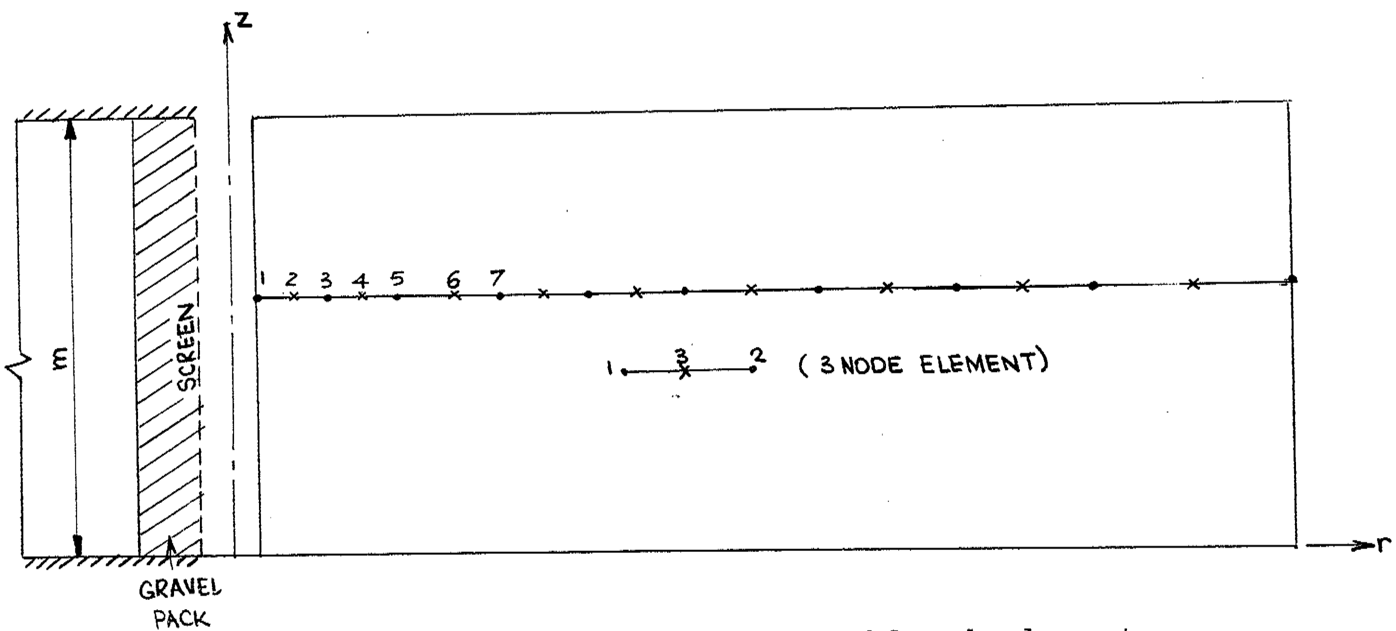


Fig. (2-3): One-dimensional mesh consisting of 3-node elements.

specific capacity are computed and related to the prescribed well draw-down.

The bulk of printed output consists of the following:-

(i) General data and mesh data.

(ii) Node numbers, coordinates, nodal heads and drawdown values.

(iii) Element numbers, connected nodes and element centroids and velocities.

(iv) Node numbers, coordinates and nodal velocities.

(v) Total well discharge and specific capacity.

In the majority of practical flow cases, the engineer is not particularly interested in the flow velocities. A command statement may be invoked to delete their print-out. However, a knowledge of velocity distribution along the well screen is useful for the approximate computation of an additional screen loss which is proportional to the entrance velocity through a screen raised to some power, and a loss due to axial flow inside the well. Knowing these losses, the computed drawdown-discharge relationship for the well may then be adjusted.

### 2.3.2 Graphical Output

Automatic plotting of the problem data and computed results is accomplished by calling plotting subroutines which have been written to perform the following plots using the IBM360/50 plotter.

(i) Plot of well-aquifer model showing the detail of aquifer stratification and well boundary and screen pattern.

(ii) Mesh pattern of discretised flow region.

(iii) Contour lines of equal heads or drawdowns.

(iv) Cone of depression

(v) Localised non-Darcy zone near the screen.

(vi) Velocity distributions, velocity vector field and flow lines in the vicinity of the well.

The use of these subroutines is optional. Their use is particularly suitable for problems involving several hundred nodes and elements as manual plotting is tedious and subject to inaccuracy.

## 2.4 Validity Check and Accuracy of Results

To ensure the validity of the two finite element programs, a validity check was performed which consisted of comparison of numerical results and exact mathematical solution and assessment of accuracy.

A test problem of steady radial flow through a confined aquifer toward a 4-inch radius, fully screened well was selected. The aquifer, shown in Fig. (1-3), is 13 ft. thick and composed of unconsolidated sand and gravel having the hydraulic properties as listed in Table 3 (curve No. 5). The radius of influence was assumed to be 100 ft.

Tables 1 and 2 compare the drawdown values and well discharges computed by various methods respectively. It is seen that both the one-dimensional and triangular element solutions check quite closely with the exact solution, and that a much greater number of nodes is required, in the mesh pattern shown in Fig. (2-1), for the triangular element program to result in a certain prescribed degree of accuracy. Thus for the simpler case of one-dimensional flow, the one-dimensional program should preferably be used whilst for more general two-dimensional flow the triangular element program should be resorted to.

As a final check to ensure convergence of the finite element solutions, a number of networks shown in Figs. (2-1) and (2-3) were used and the resulting solutions compared. It was noted that starting from the coarsest network and refining the network, the numerical results were considerably improved and converged to the exact solution. However, for a particular mesh pattern, increasing the total number of nodes beyond a certain value led to accumulated round-off errors which destroyed the accuracy thus obtained.

Table 1: Comparison of Drawdowns Computed by Various Methods

| Radial Coordinate (ft.) | Drawdown value (ft) computed by | | |
|---|---|---|---|
| | Analytical solution | 1-dimensional elements | Triangular elements |
| 0.33 | -30.000 | -30.00 | -30.00 |
| 0.43 | -27.719 | -27.72 | -27.71 |
| 0.63 | -24.894 | -24.90 | -24.90 |
| 0.83 | -23.111 | -23.11 | -23.17 |
| 1.23 | -20.843 | -20.84 | -20.91 |
| 1.63 | -19.357 | -19.36 | -19.43 |
| 2.23 | -17.800 | -17.80 | -17.86 |
| 3.23 | -16.050 | -16.06 | -16.13 |
| 4.23 | -14.788 | -14.80 | -14.87 |
| 5.23 | -13.795 | -13.80 | -13.87 |
| 7.23 | -12.280 | -12.29 | -12.36 |
| 9.23 | -11.138 | -11.15 | -11.22 |
| 11.73 | -10.016 | -10.03 | -10.08 |
| 16.73 | - 8.455 | - 8.47 | - 8.42 |
| 21.73 | - 7.132 | - 7.14 | - 7.20 |
| 26.73 | - 6.163 | - 6.17 | - 6.22 |
| 31.73 | - 5.361 | - 5.37 | - 5.41 |
| 41.49 | - 4.109 | - 4.12 | - 4.15 |
| 51.24 | - 3.122 | - 3.13 | - 3.16 |
| 60.99 | - 2.308 | - 2.31 | - 2.33 |
| 70.74 | - 1.615 | - 1.62 | - 1.63 |
| 80.50 | - 1.013 | - 1.02 | - 1.02 |
| 90.25 | - 0.480 | - 0.48 | - 0.48 |
| 100.00 | - 0.000 | - 0.00 | - 0.00 |

Table 2: Comparison of Well Discharges computed by Various Methods

| Method used | No. of nodes | Well discharge (c.f.m.) |
|---|---|---|
| Analytical solution | 24 | 137.94 |
| 1-dimensional elements | 47 | 137.50 |
| Triangular elements | 235 | 139.85 |

## 3. Steady Flow Behaviour and Well Design Data

### 3.1 General

Steady flow toward a pumped well occurs when there is equilibrium between the discharge of the well and the aquifer recharge replenished by an outside source. In the foregoing construction of the steady flow model, the recharge source was assumed to be a large body of surface water surrounding the aquifer at the radius of influence. Although such an assumption is rarely met in the field situation, it is justified in practice, as over a relatively long period of time a steady state is approximately reached when it is impossible to observe the deepening or expanding of the cone of depression during short-time interval of pumping. Accordingly, the steady flow analysis is useful in providing valuable information for well design in which the engineer is particularly concerned with the long term hydraulic performance of the well. Assessment and comparison of the well performance and efficiency on the steady state basis leads to criteria for selecting the dimensional factors and materials for the well structure.

The purpose of this section is to develop an understanding of the steady state behaviour of two-regime well flow through the unconsolidated aquifer previously described. Particular emphasis is laid on the effects of non-Darcy flow in close proximity to the well and well design factors on the discharge and specific capacity.

### 3.2 Permeability Data for Unconsolidated Materials

Values of the cofficient of hydraulic conductivity $K$, the Forchheimer coefficients a and b and the critical Reynolds number $\mathbb{R}_{cr}$ are required in the numerical analysis of flow. At present the only reliable way of determining these values is to carry out permeameter tests. Limited data for unconsolidated materials are available in the literature. Tables 3 and 4 present the result of some data for sands, gravels and crushed metals analysed by the author using the curve fitting technique suggested by Sunada (1965).

The logarithmic plots of velocity against hydraulic gradient are shown in Figs. (3-1) to (3-3). The first portion of the curves is a $45^{\circ}$ straight line as the hydraulic gradient is proportional to the first power of the flow velocity. Definite departure from this line is at the critical velocity where the slope of the curves changes abruptly. The slope of the upper branch of the curve increases gradually with increase in velocity.

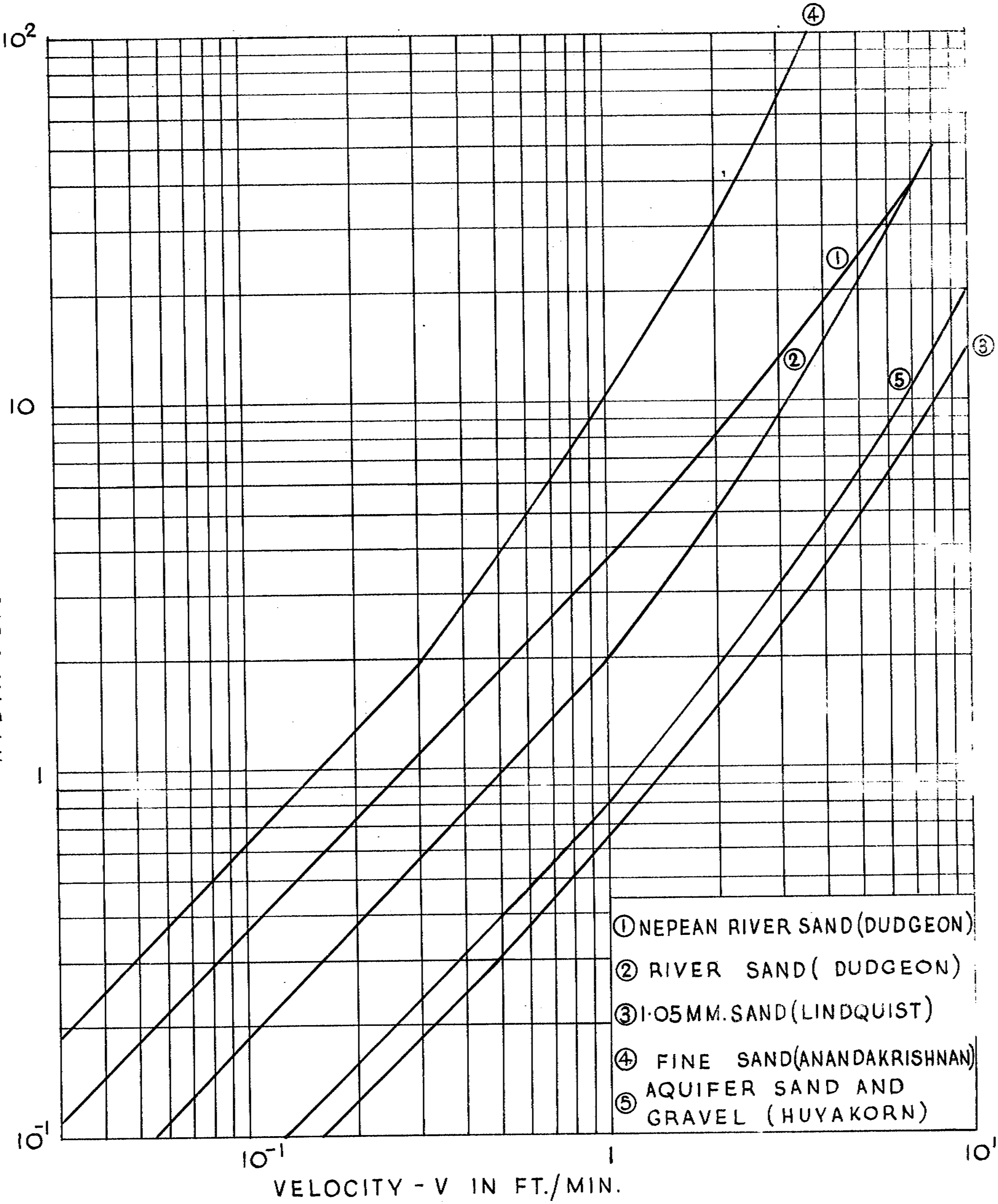


Fig. (3-1): Velocity-gradient lines for typical unconsolidated materials.

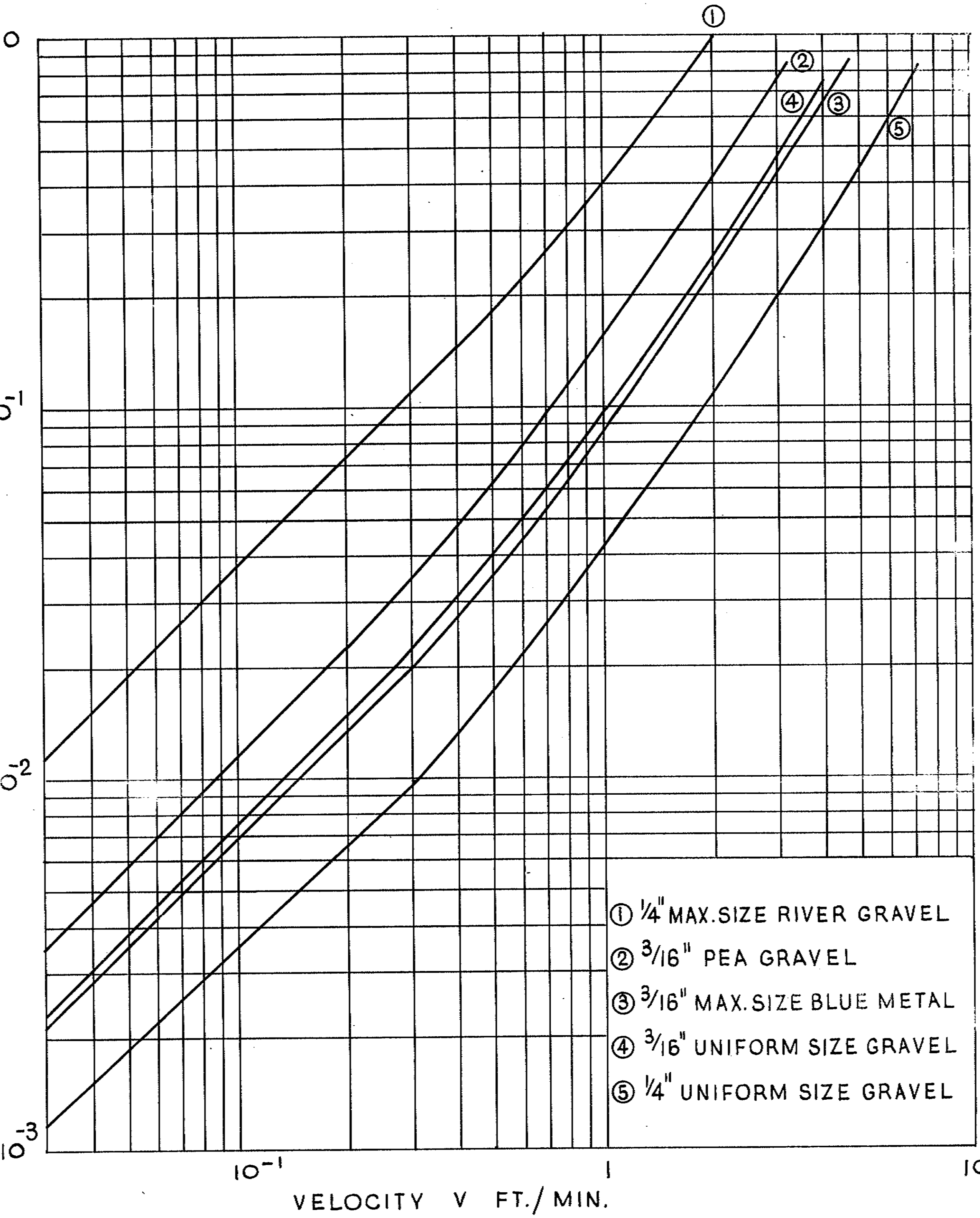


Figure (3-2): Velocity-gradient lines for typical gravel pack materials.

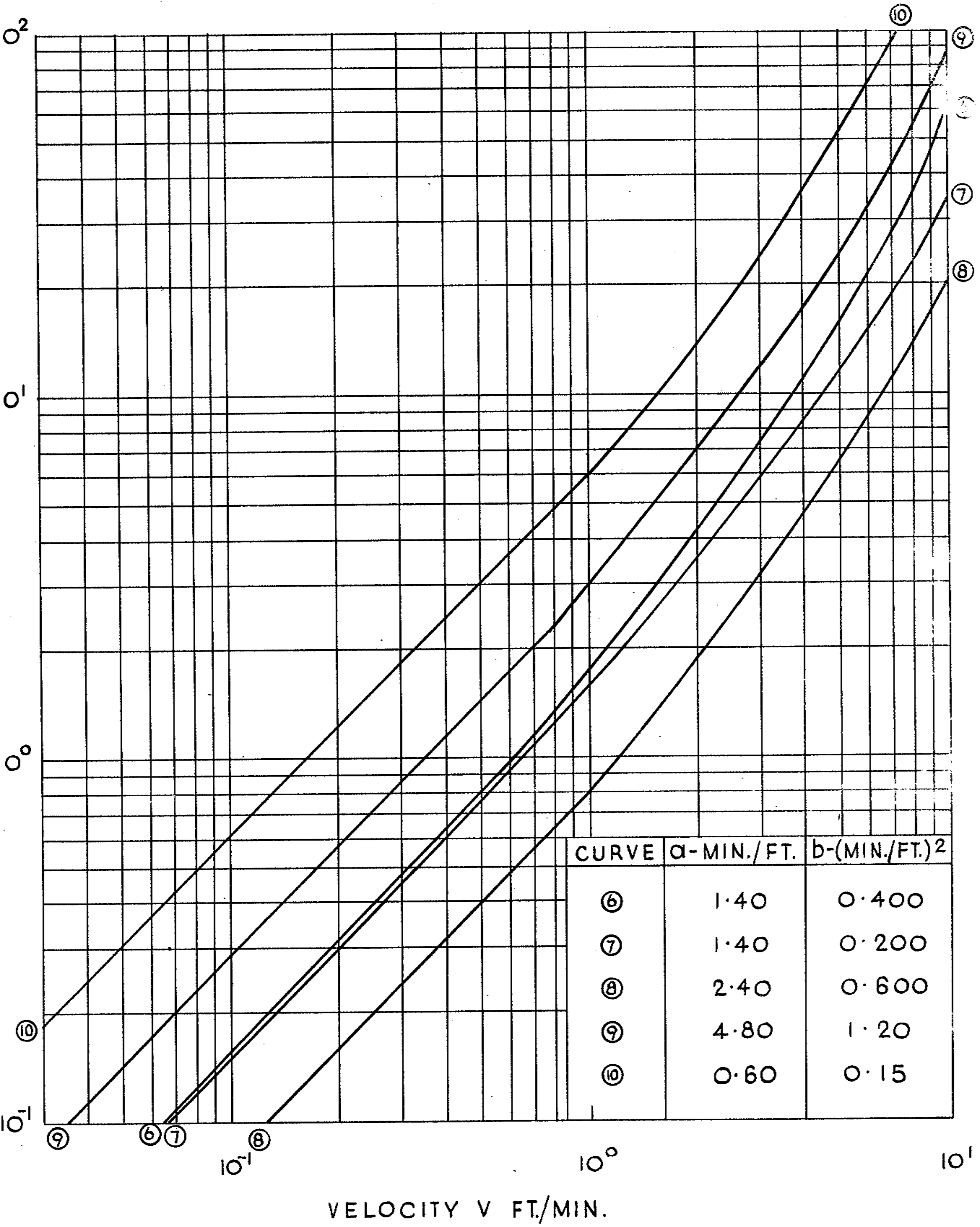


Figure (3-3): Theoretical velocity-gradient curves constructed for studying the effects of hydraulic coefficients.

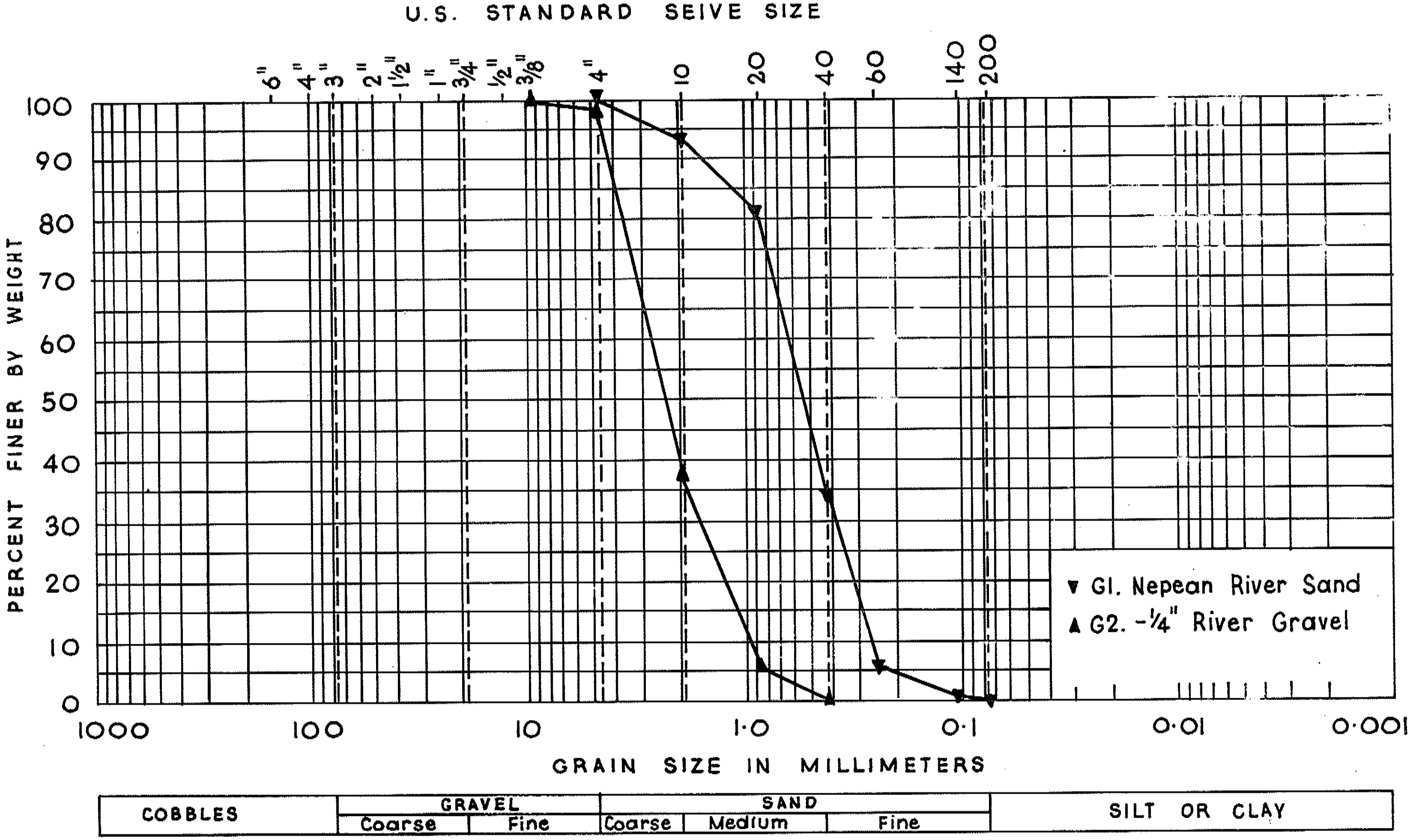


Fig. (3-4): Sieve analysis curves of materials tested by Dudgeon (1965).

Table 3

List of Permeability Data for Unconsolidated Materials

| Curve No. | Investigator | Material | $\bar{d}$ (ft.) | a min./ft. | b min.$^2$/ft.$^2$ | K ft./min. | $\mathbb{R}_{cr}$ |
|---|---|---|---|---|---|---|---|
| 1 | Dudgeon | Nepean River Sand | $.87 \times 10^{-3}$ | 3.32 | 0.327 | 0.273 | 1.7 |
| 2 | Dudgeon | Medium Sand | $1.08 \times 10^{-3}$ | 1.4 | 0.60 | 0.50 | 1.1 |
| 3 | Linquist | 1.05 mm Sand | $3.06 \times 10^{-3}$ | 0.59 | 0.077 | 1.6 | 2.6 |
| 4 | Anandakr-ishnan | Fine Sand | $0.99 \times 10^{-3}$ | 4.9 | 5.4 | 0.153 | 0.5 |
| 5 | Huyakorn | Aquifer Sand and Gravel | $2.75 \times 10^{-3}$ | 2.4 | 0.6 | 0.348 | 3.5 |

$\bar{d}$ = diameter of grain such that 10% by weight of the sample is of smaller grains

$\mathbb{R}_{cr}$ = critical Reynolds number

Table 4

Permeability Data for Gravel Materials

| Curve No. | Investigator | Material | d (ft.) | a (min./ft.) | b $(min.^2/ft.^2)$ | K (ft./min.) | $\mathbb{R}_{cr}$ |
|---|---|---|---|---|---|---|---|
| 1 | Dudgeon | $\frac{1}{4}$" River Gravel | $3.5 \times 10^{-3}$ | 0.337 | .069 | 2.80 | 1.75 |
| 2 | Lane | 3/16" Pea Gravel | $5.5 \times 10^{-3}$ | 0.102 | .055 | 8.60 | 1.70 |
| 3 | Dudgeon | 3/16" Blue Metal | $6.56 \times 10^{-3}$ | .0578 | .0281 | 15.5 | 2.50 |
| 4 | Huyakorn | 3/16" Gravel | $6.10 \times 10^{-3}$ | .067 | .030 | 14.4 | 1.50 |
| 5 | Dudgeon | $\frac{1}{4}$" Gravel | $9.85 \times 10^{-3}$ | .026 | .0155 | 32.6 | 0.50 |

$\bar{d}$ = diameter of grain such that 10% by weight of the sample is of smaller grains

$\mathbb{R}_{cr}$ = critical Reynolds number

Table 5: Hydraulic Coefficients - Theoretical Curves (Figure 3-3)

| Curve No. | a (min/ft) | b ($min^2/ft^2$) | k (ft/min) | $v_{cr}$ (ft/min) |
|---|---|---|---|---|
| 6 | 1.400 | 0.400 | 0.610 | 0.60 |
| 7 | 1.400 | 0.200 | 0.675 | 0.60 |
| 8 | 2.400 | 0.600 | 0.350 | 0.80 |
| 4 | 4.800 | 1.200 | 0.167 | 1.00 |
| 10 | 0.600 | 0.150 | 1.480 | 0.50 |

$v_{cr}$ = critical velocity

Sieve analyses of the materials tested by Dudgeon (1965) are shown in Fig. (3-4). The 10% finer grain size was used to determine the critical Reynolds number, the values of which lie between 1 and 4 for all materials listed in Tables 2 and 4.

To study the effects of the material properties, namely coefficients a, b and K, additional theoretical curves were constructed as shown in Fig. (3-3).

Table 5 lists the values of the coefficients corresponding to each curve.

### 3.3 Drawdown-distance Curves and Non-Darcy Zones

#### 3.3.1 Fully Screened Wells

The flow toward an 8-inch diameter fully screen well in an aquifer composed of medium sand (see Table 3) was analysed. The semi-logarithmic drawdown-distance curves are shown in Fig. (3-5). Each curve is a straight line in the outer zone of the aquifer where Darcy flow occurs. The non-Darcy zone extends from a radius, termed critical radius, inward to the screen boundary. The curve becomes distorted in this zone to the extent shown by the difference between the broken line and the solid line.

The computed values of the critical radius, well discharge, specific capacity and maximum velocity at the screen, which correspond to prescribed well drawdowns in the well are tabulated below.

Table 6: Results for Fully Screened Well

| Drawdown $s_w$ (ft.) | Critical Radius $r_{cr}$ (ft.) | Discharge Q(gpm) | Specific Capacity $Q/s_w$ (gpm/ft) | Velocity at Screen ft/min. |
|---|---|---|---|---|
| 5 | 0.93 | 248 | 49.6 | 1.48 |
| 10 | 1.69 | 471 | 47.1 | 2.82 |
| 15 | 2.36 | 670 | 44.6 | 4.00 |
| 20 | 2.97 | 850 | 42.5 | 5.10 |
| 25 | 3.52 | 1020 | 40.9 | 6.10 |
| 30 | 4.04 | 1175 | 39.2 | 7.05 |

From Table 6, the following points are noted:

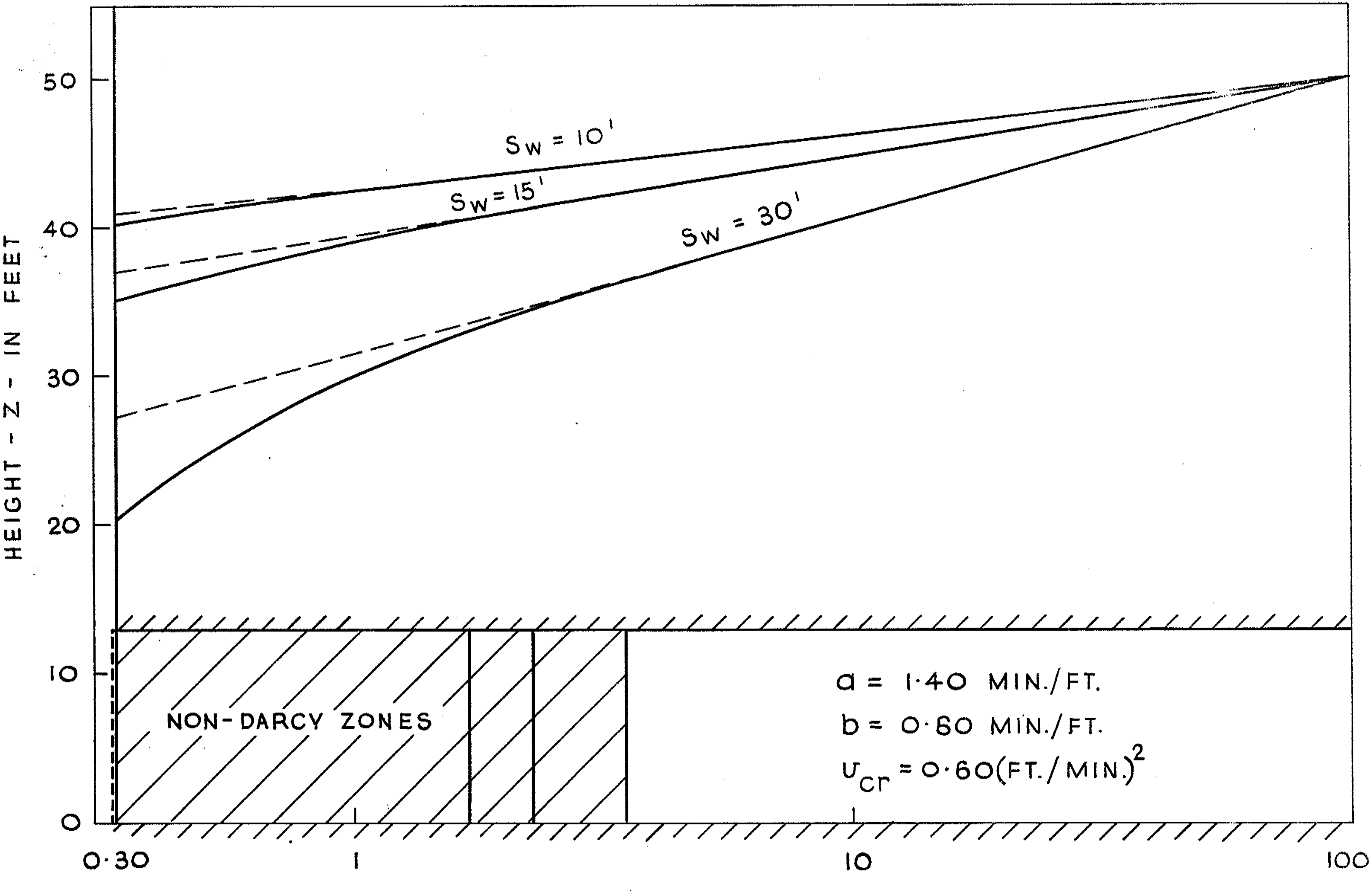


Fig. (3-5): Drawdown-distance curves for a fully screened well.

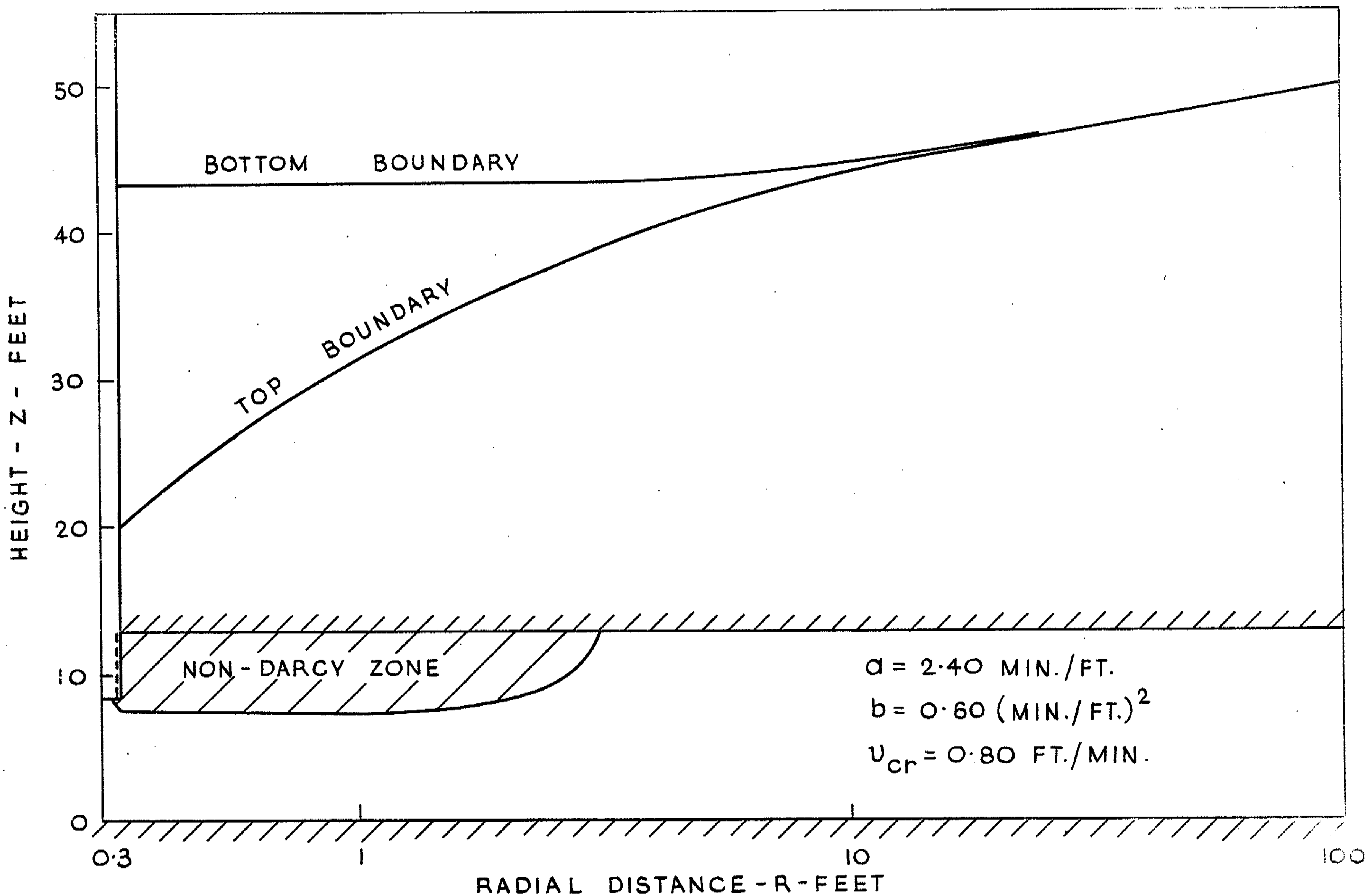


Fig. (3-6): Drawdown-distance curves for a partially screened well.

(i) The specific capacity of the well $Q/s_w$ decreases appreciably as well drawdown $s_w$ increases due to the effect of non-Darcy flow.

(ii) The value of the critical radius, $r_{cr}$, for the non-Darcy zone is directly proportional to the well discharge. The maximum value at 30 ft. drawdown is only a few feet from the screen, indicating that the extent of the non-Darcy zone is in close proximity of the well, and to reduce or minimise the non-Darcy effect, treatment should be given to the material in the immediate surroundings of the well to improve its hydraulic properties.

(iii) Neglecting additional losses due to flow through screen openings into the well and flow inside the well, the maximum discharge at 30 ft. well drawdown is approximately 1175 gpm. If the above losses are a sizable fraction of the total well drawdown, the discharge actually measured will be somewhat less than the computed value.

### 3.3.2 Partially Screened Wells

The flow toward a partially penetrating well and two fully penetrating but partially screened wells was studied. The selected aquifer material is a mixture of medium sand and gravel having the hydraulic properties as listed in Table 3.

Fig. (3-6) shows the sketch of the partially penetrating well, the drawdown-distance curves along the top and bottom boundaries of the aquifer and the non-Darcy zone. It is noted that the drawdown near the well varies with depth in the aquifer. The variation is most pronounced adjacent to the screen and disappears with increasing radius from the well. Inside a radius slightly less than the thickness of the aquifer, the bottom boundary curve is relatively flat whilst the top curve shows a steep gradient, particularly near the screen. The two curves approximately coincide at a radial distance about 1.5 times the aquifer thickness. The non-Darcy zone extends to a depth slightly greater than the screen length. The maximum critical radius is only 3.10 ft. for 30 ft. well drawdown.

For the two partially screened wells, the non-Darcy zones resulting from various well drawdowns are shown in Figs. (3-7) and (3-8). It is seen that the non-Darcy zone extends in the radial and vertical directions as the well drawdown is increased and its shape depends on the screen pattern.

## 3.4 Drawdown-discharge Relationships

### 3.4.1 Effects of Well Design Factors

#### (i) Well Radius

The drawdown-discharge and $s_w/Q$-discharge curves for fully screened wells having radii of 3", 4" and 8" are compared in Figs. (3-9) and (3-10) respectively, where $s_w/Q$ is the reciprocal of the specific capacity. The non-linearity of the drawdown-discharge curves is caused by non-Darcy flow in the vicinity of the screen, which becomes more significant at greater well drawdown and for a smaller well radius. The curve for the 8" radius well is linear up to 20 ft. drawdown, indicating that non-Darcy flow does not exist or is not appreciable until this drawdown value is exceeded.

The drawdown - $s_w/Q$ curves are closely approximated by straight lines of different positive slopes. The greater slope corresponds to the smaller well radius. The value of $s_w/Q$ for the 8" radius well is constant at discharges lower than a certain value where non-Darcy flow commences.

For a prescribed value of the well drawdown, enlarging the well radius results in an appreciable percentage increase in the well discharge and specific capacity, and a close to proportional percentage reduction in the velocity approaching the well screen. Table 7 compares results for the 4-inch and 8-inch wells with that obtained for the 3-inch well.

Table 7: Comparison of Discharges and Velocities for Various Well Radii

| Well Drawdown (ft.) | Discharge Ratio, % | | | Velocity Ratio, % | | |
|---|---|---|---|---|---|---|
| | 3" Well | 4" Well | 8" Well | 3" Well | 4" Well | 8" Well |
| 5 | 100 | 105 | 120 | 100 | 79.0 | 45.0 |
| 10 | 100 | 106 | 122 | 100 | 79.5 | 46.0 |
| 15 | 100 | 106.5 | 124.5 | 100 | 80 | 46.7 |
| 20 | 100 | 107 | 126.5 | 100 | 80.2 | 47.5 |
| 25 | 100 | 107.5 | 128 | 100 | 80.5 | 48.0 |
| 30 | 100 | 108 | 130 | 100 | 81.0 | 48.7 |

It is seen that the percentage increase in discharge and specific capacity of the larger wells increases with increasing drawdown as a result of the more predominant role of non-Darcy flow in reducing the discharge from the 3" well, the increase being as high as 10% for the 8-inch well.

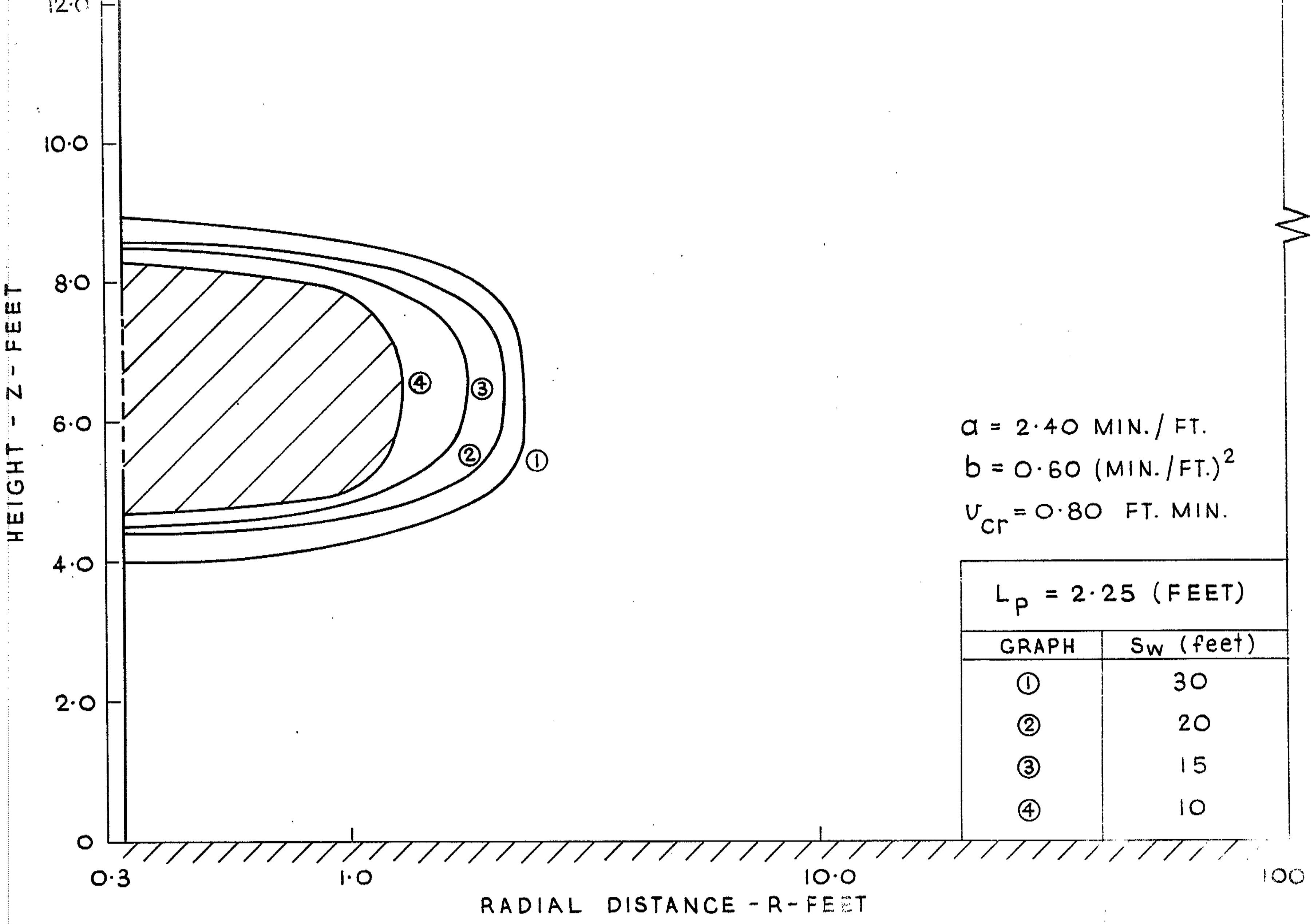


Fig. (3-7): Non-Darcy zones in the vicinity of well screen for various drawdowns.

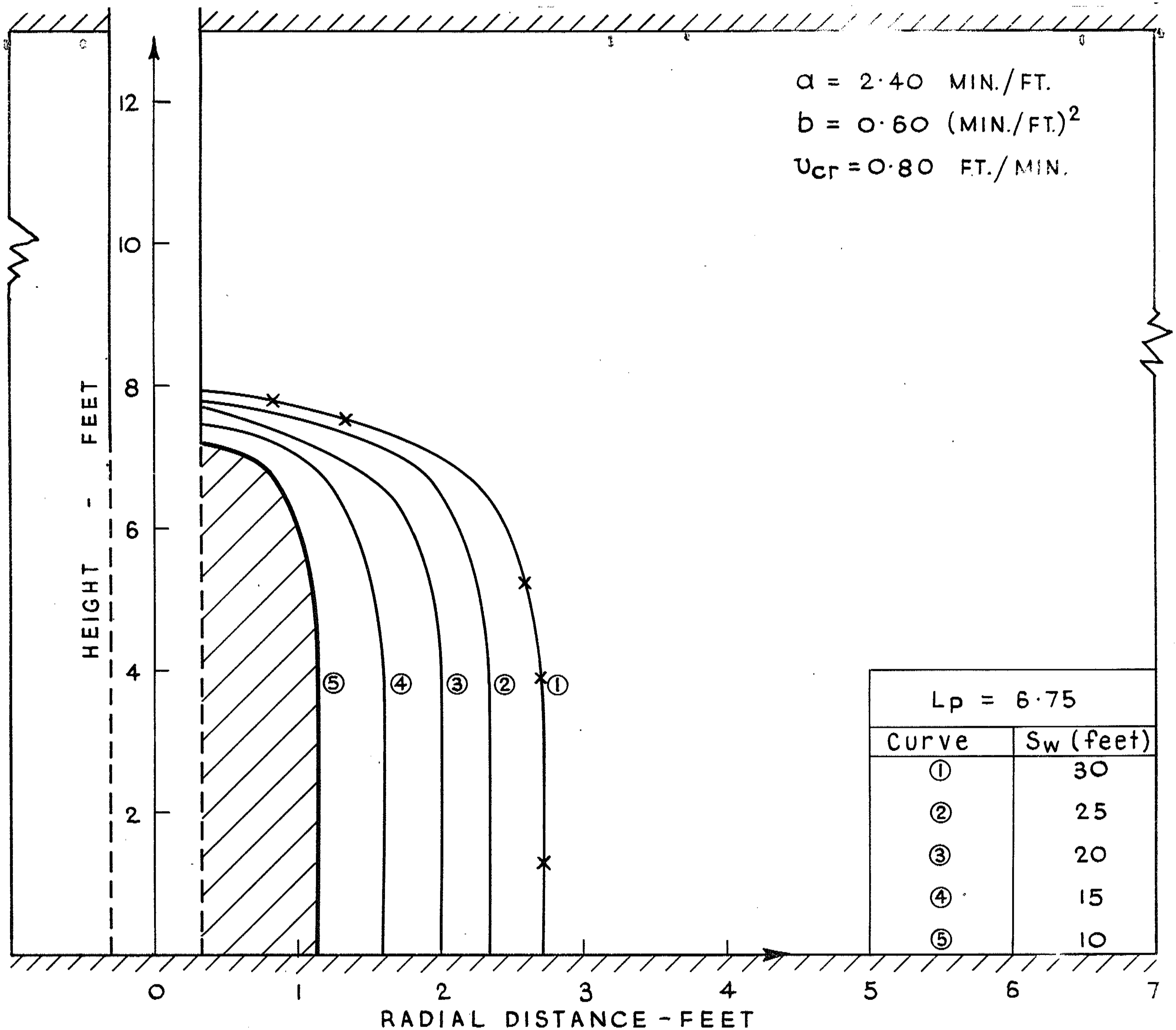


Fig. (3-8): Non-Darcy zones in the vicinity of well screen for various well drawdowns.

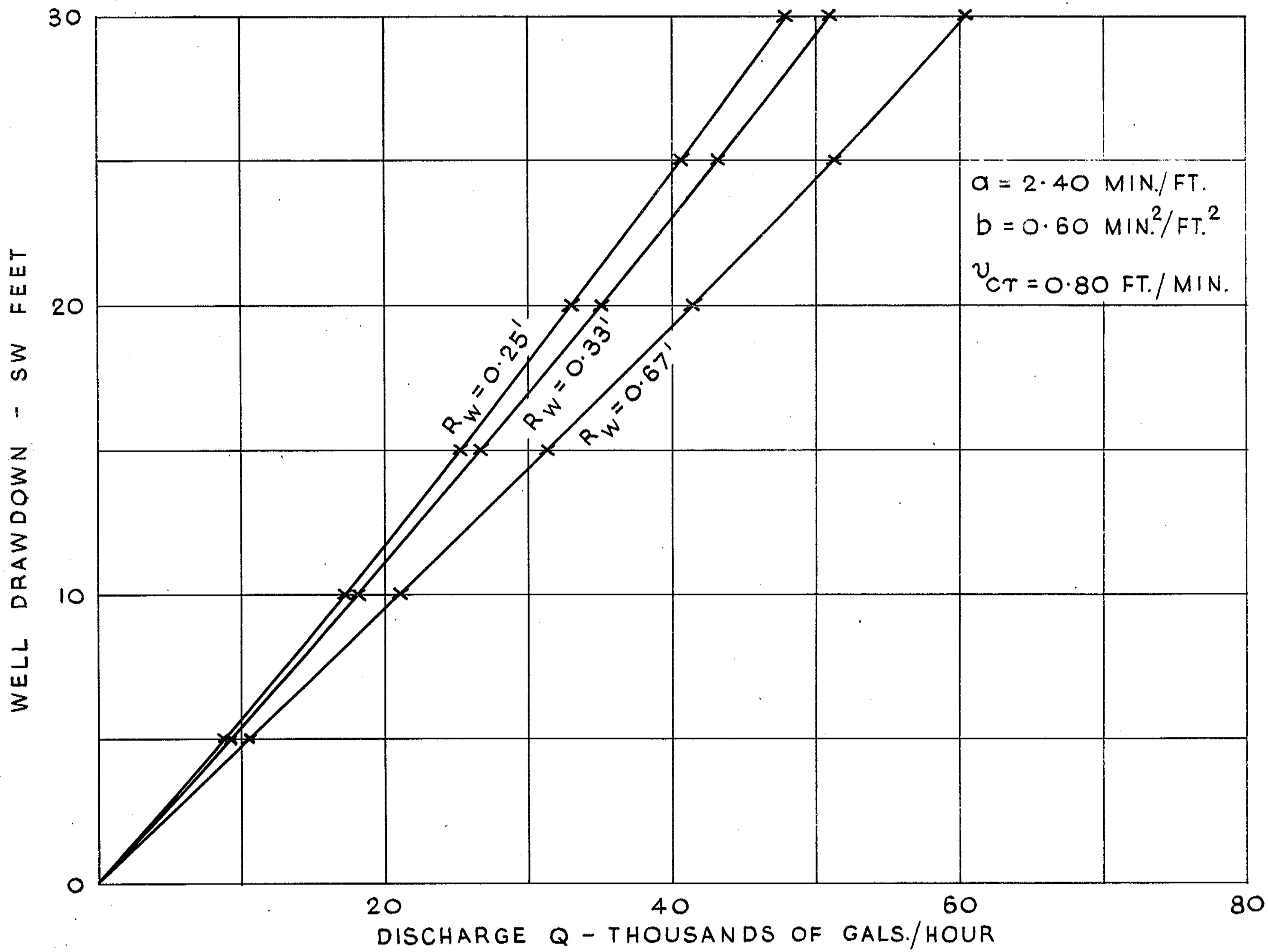


Fig. (3-9): Drawdown-discharge curves showing effect of well radius.

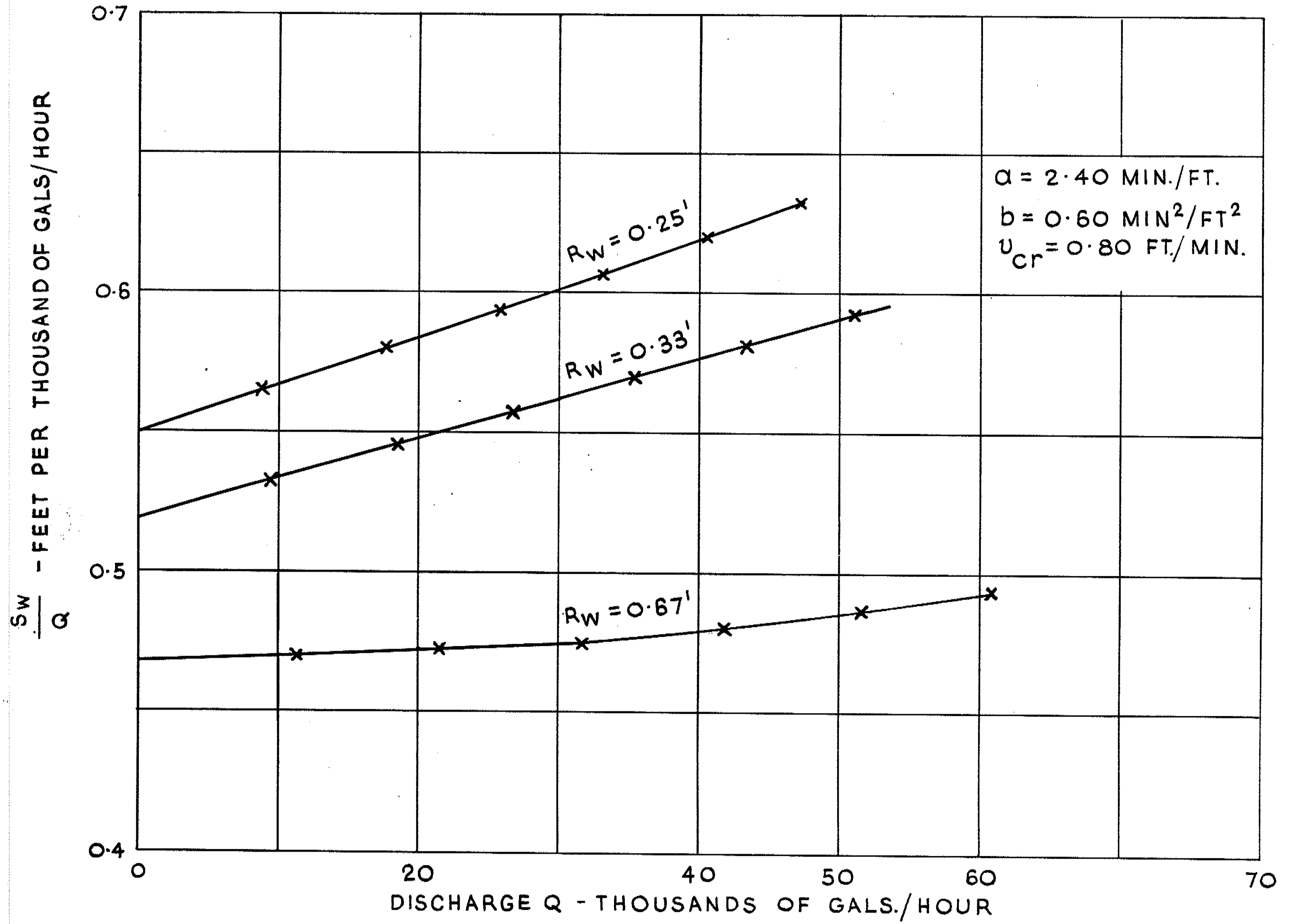


Fig. (3-10): $^{s_w}/_Q$ Vs Q curves showing effect of well radius.

(ii) Screen Length and Position

To show the effect of screen length, a partially penetrating well of 4-inch radius similar to that shown in Fig. (3-8) was considered. Figs. (3-11) and (3-12) show the drawdown-discharge and the $s_w/Q$-discharge plots for various ratios of screen length to aquifer thickness. From Fig. (3-11), it is evident that the effects of non-Darcy flow and departure from radial flow are more pronounced for smaller screen length ratios, causing the well drawdown to increase rapidly with discharge. The $s_w/Q$-discharge plots in Fig. (3-12) are straight lines of different slopes and intercepts. The greater slope and intercept correspond to the smaller screen length ratio. The relationship between discharge and screen length ratio is shown in Fig. (3-13). Each curve corresponds to a prescribed value of the well drawdown.

Apart from depending on the screen length ratio, the discharge and specific capacity of a partially screened well also depends on the space position of the screen.

The discharge and specific capacity of two wells having the screens positioned as shown in Figs. (3-8) and (3-7) respectively are compared in Table 8. Both wells penetrate the same aquifer material and have the same radius of 4 inches and screen length of 2.25 ft.

Table 8: Effect of Screen Position

| Drawdown ft. | Discharge (gpm) | | Specific Capacity | |
|---|---|---|---|---|
| | Well (1) | Well (2) | Well (1) | Well (2) |
| 10 | 110.0 | 138.0 | 11.00 | 13.80 |
| 15 | 156.0 | 194.0 | 10.40 | 12.90 |
| 20 | 194.5 | 244.0 | 9.73 | 12.20 |
| 25 | 230.0 | 288.0 | 9.25 | 11.50 |
| 30 | 264.0 | 330.0 | 8.80 | 11.00 |

It is seen that the discharge and specific capacity of the second well is considerably greater as it is more efficient in tapping the lower and upper portions of the aquifer.

(iii) Gravel Pack Properties

Gravel packed wells of 8-inch screen diameter and 6-inch thick gravel envelope were considered. The flow behaviour of the wells was studied and compared with that of a non-gravel pack well of the same diameter.

Fig. (3-14) shows the effect of hydraulic properties of the pack material on the drawdown-distance curves obtained for 30 ft. well drawdown. Curve 1 in the figure corresponds to a non-gravel packed well in an undisturbed aquifer formation whilst curve 2 and curve 3 correspond to a well packed with clean, well-rounded $\frac{1}{4}$" river gravel and the same well but with badly clogged gravel envelope respectively. It is seen that the hydraulic loss in the envelope zone depends on the characteristics of the pack material. Clean pack material results in low values of the coefficients of hydraulic resistance and a very small hydraulic loss in the pack envelope, as indicated by the relatively flat portion of curve 2, whilst clogging of the pack material results in high values of the coefficients of hydraulic resistance and excessive loss.

To show how the well performance is affected, Table 9 compares the discharge and specific capacity of various wells having different pack materials. It is evident that the use of clean gravel packs improves the well discharge and specific capacity considerably and that the improved values of the discharge and specific capacity change very slightly with different choices of the pack material. For the well having clogged gravel pack, the discharge and specific capacity are significantly low when compared to that of the non-gravel pack well.

### 3.4.2 Effect of Hydraulic Properties of Aquifer Material

Plots of velocity-hydraulic gradient relationships for a range of aquifer material properties are shown in Fig. (3-3). The hydraulic coefficients and other relevant data for the materials are given in Table 5. Flow through the aquifer towards a fully screened well of 4-inch radius has been analysed and plots of drawdown-discharge and $s_w/Q$-discharge are shown in Figs. (3-15) and (3-16) respectively. It is seen in Fig. (3-16) that for the two materials having the same value of coefficient 'a' but different value of coefficient 'b', the intercepts of the $s_w/Q$-Q lines are nearly the same, but the slope is steeper for the larger value of b.

### 3.4.3 Effect of Radius of Influence

The discharge and specific capacity of a well obtained from

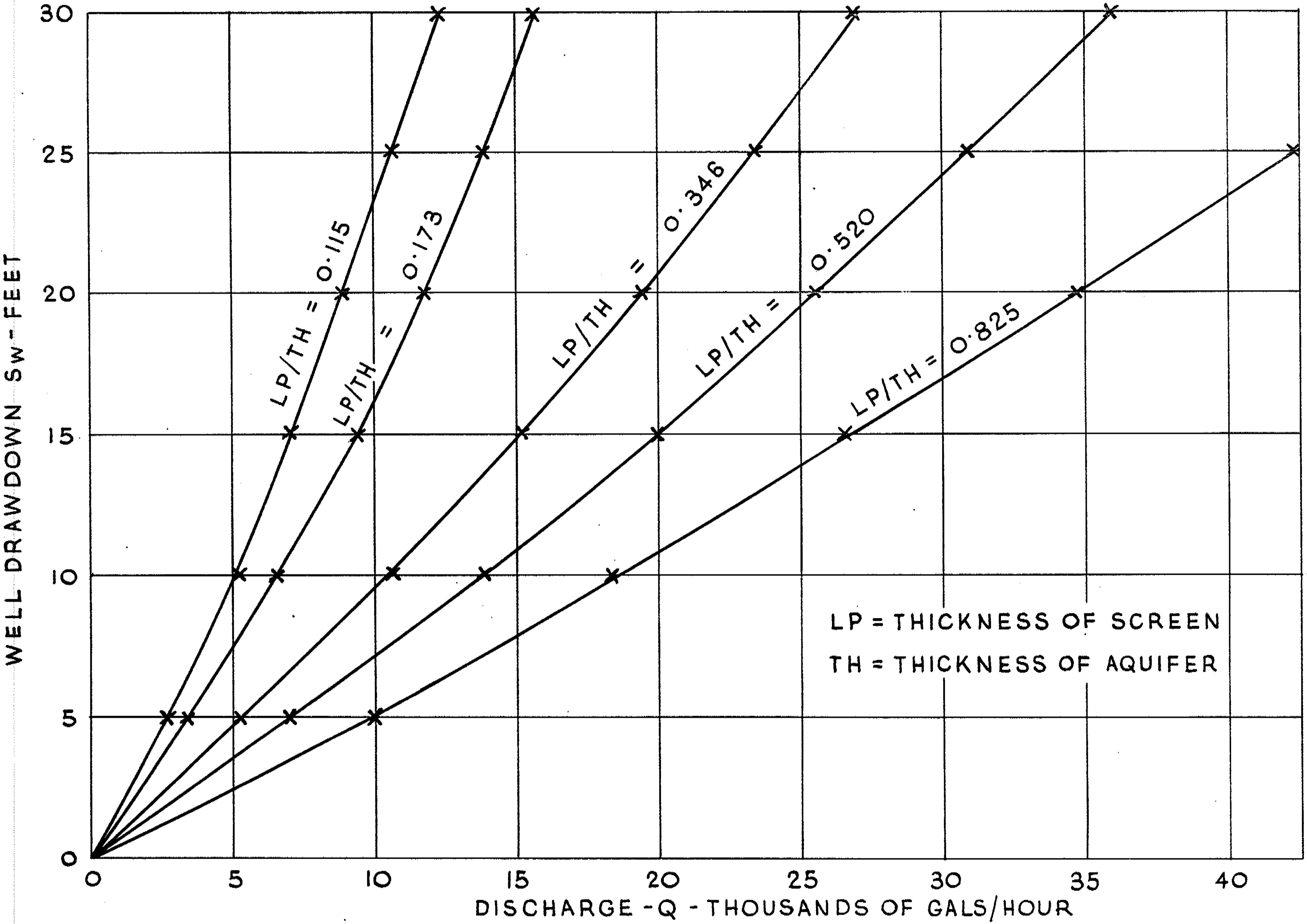


Fig. (3-11): Drawdown-discharge curves showing effect of screen length.

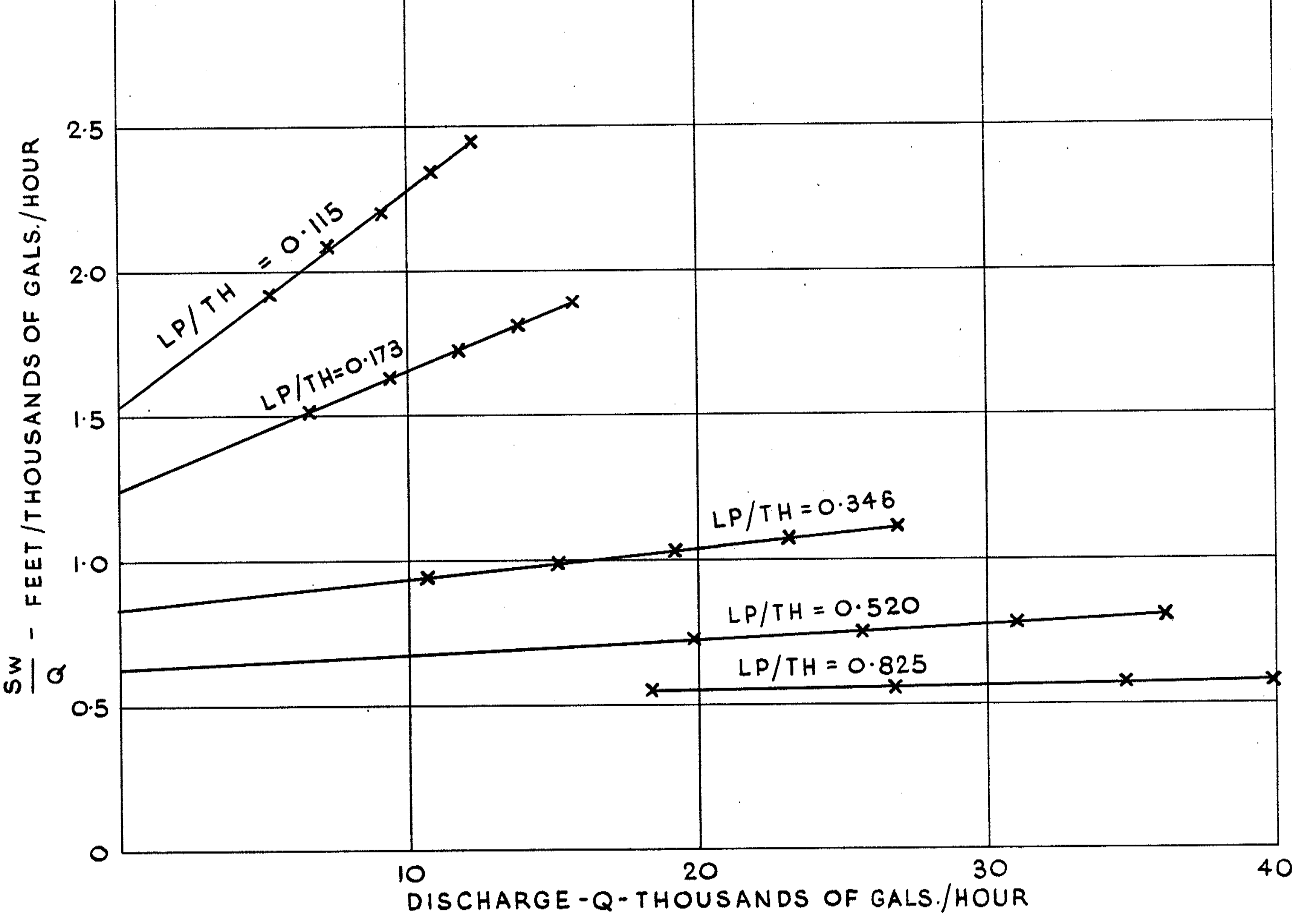


Fig. (3-12): $\frac{s_W}{Q}$ Vs Q curves showing effect of screen length.

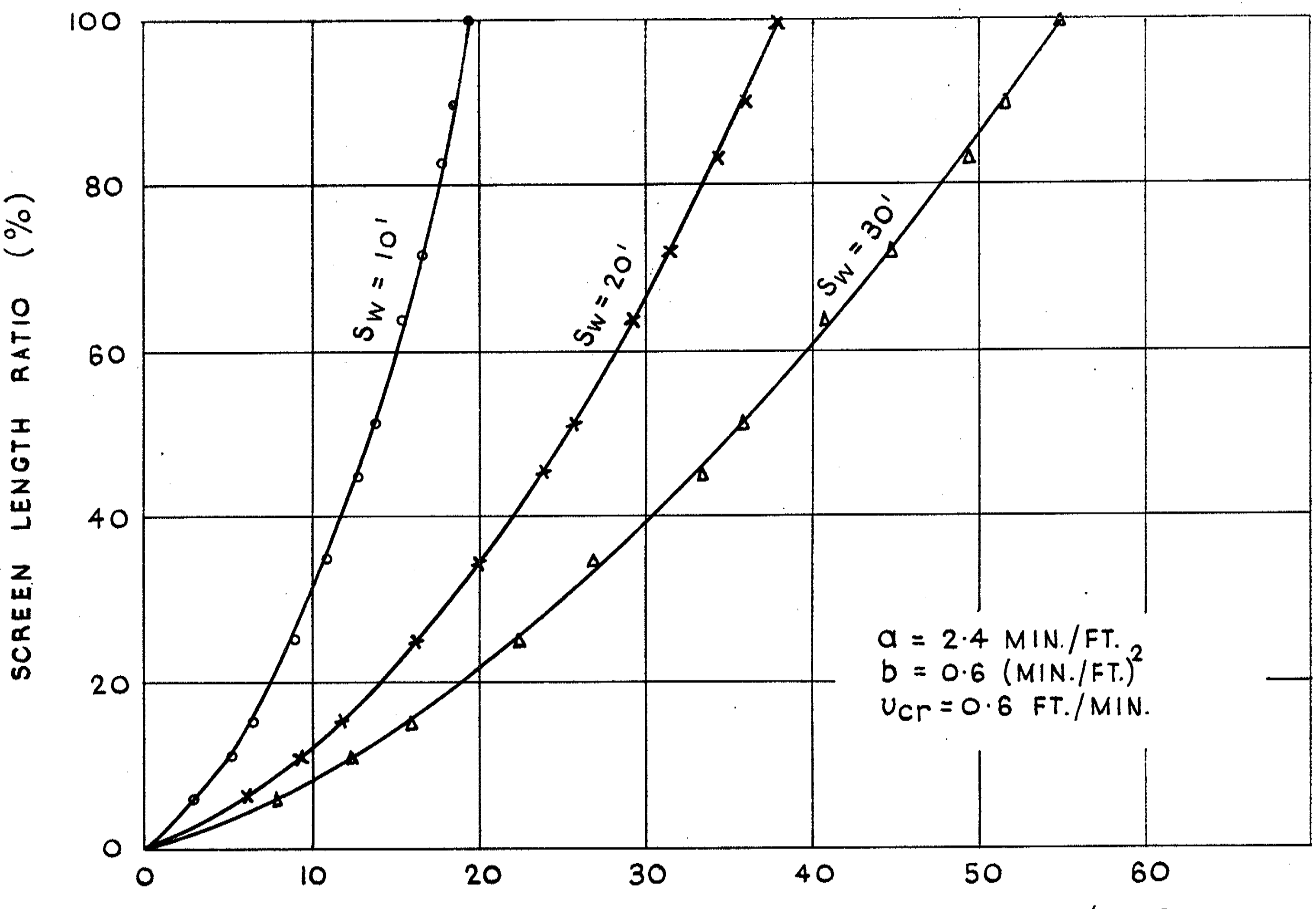


Fig. (3-13): Discharge of partially screened well as function of screen length/ aquifer thickness ratio.

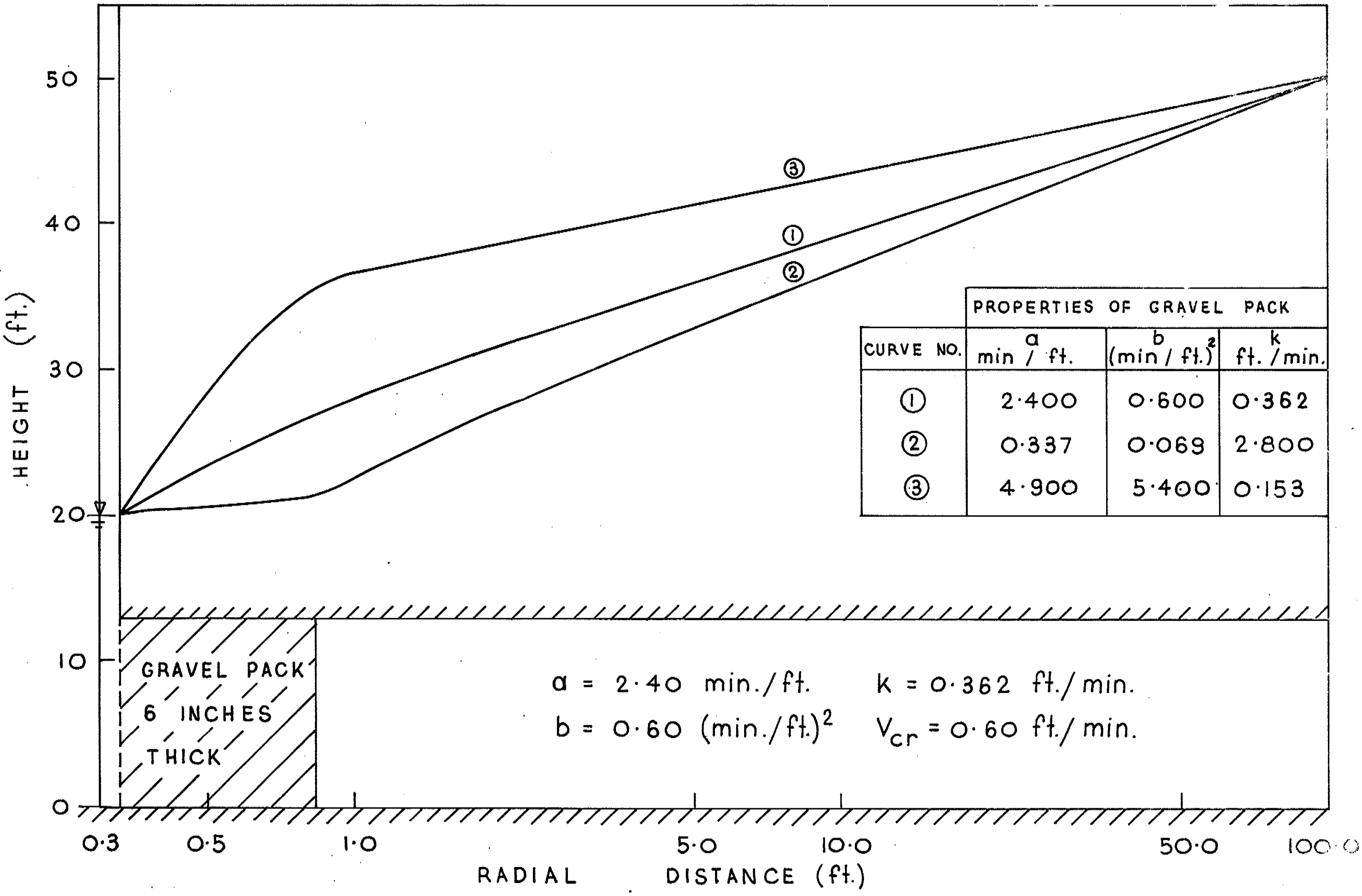


Fig. (3-14): Drawdown-distance curves showing effect of gravel pack.

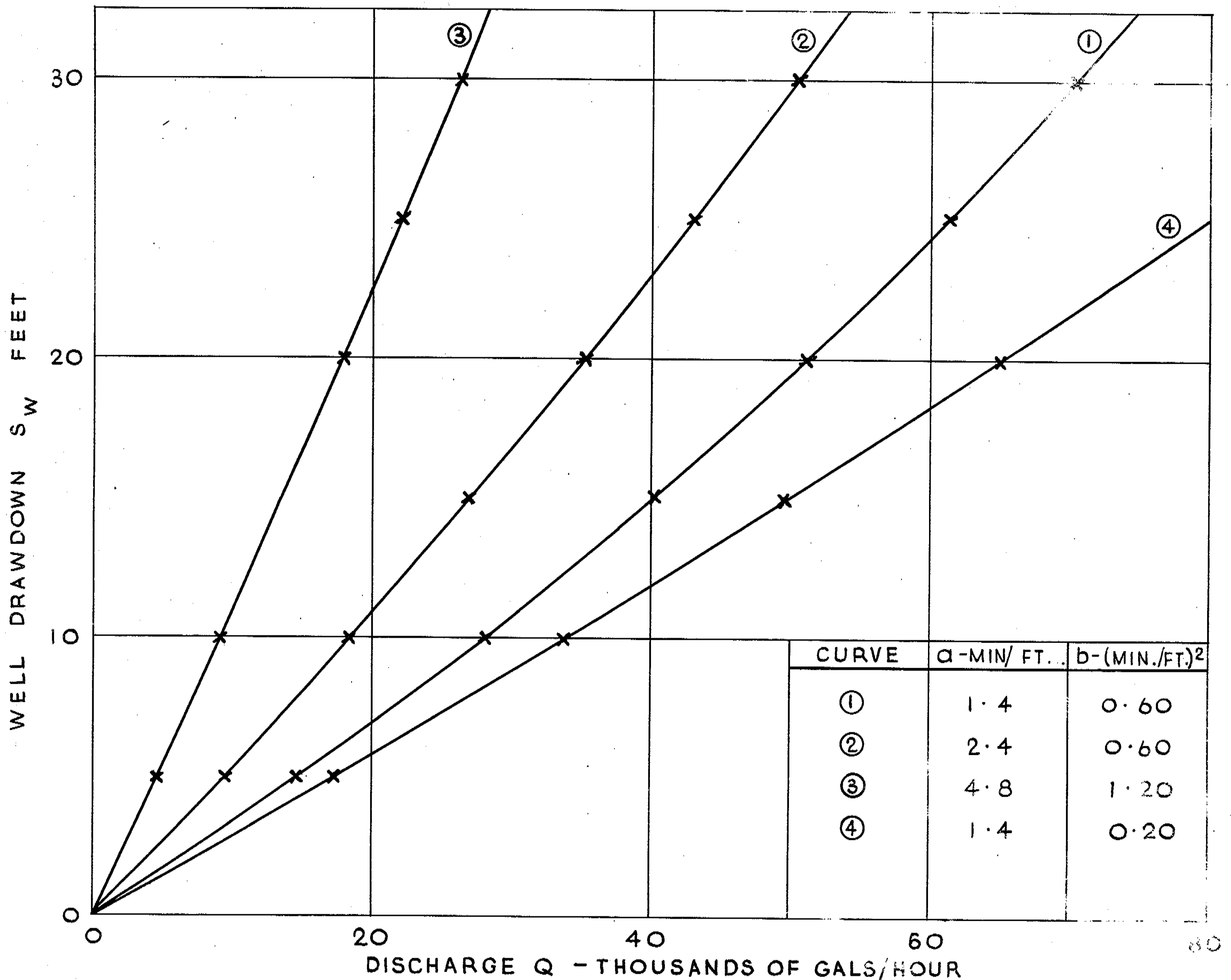


Fig. (3-15): Drawdown-discharge curves showing effect of material properties.

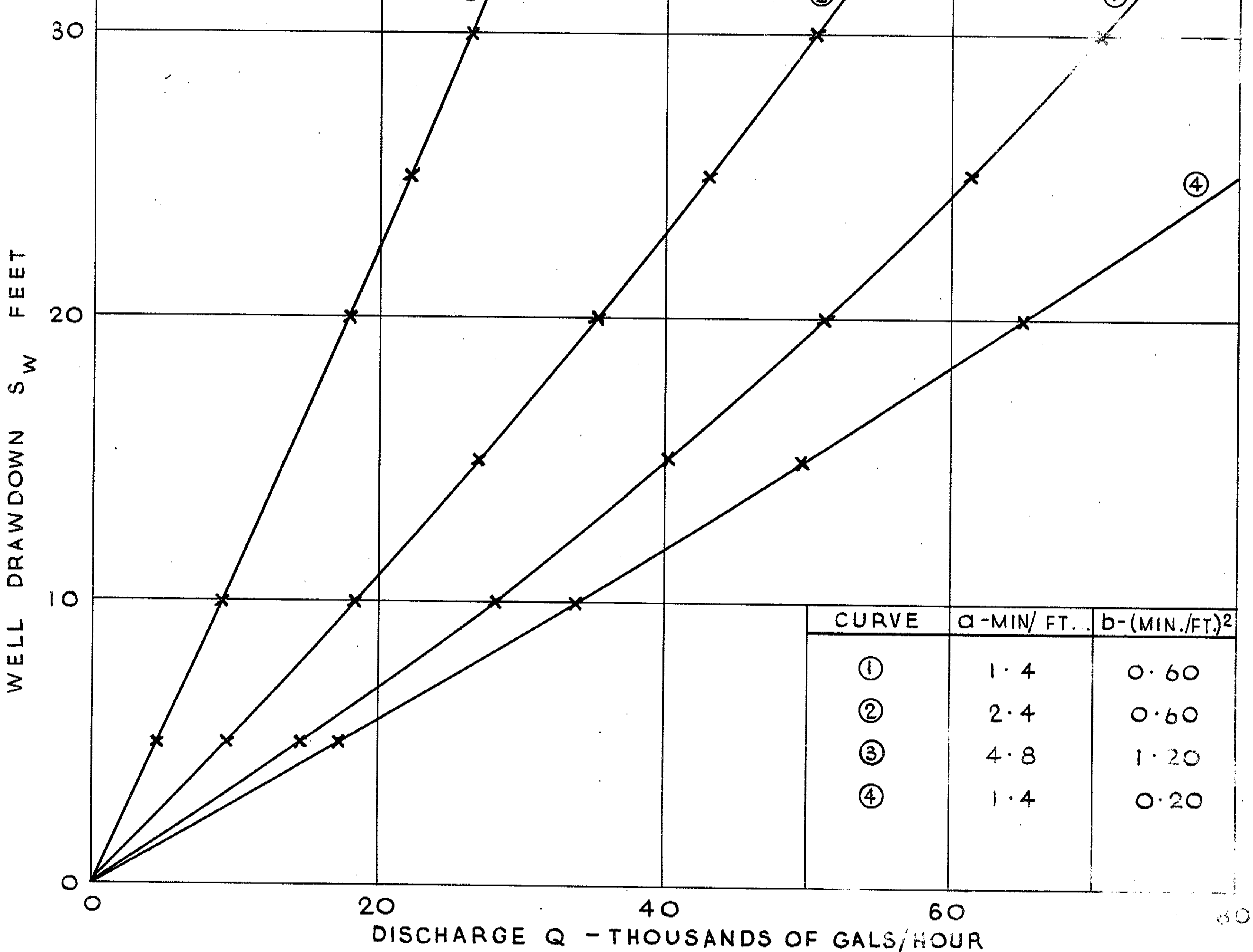


Fig. (3-15): Drawdown-discharge curves showing effect of material properties.

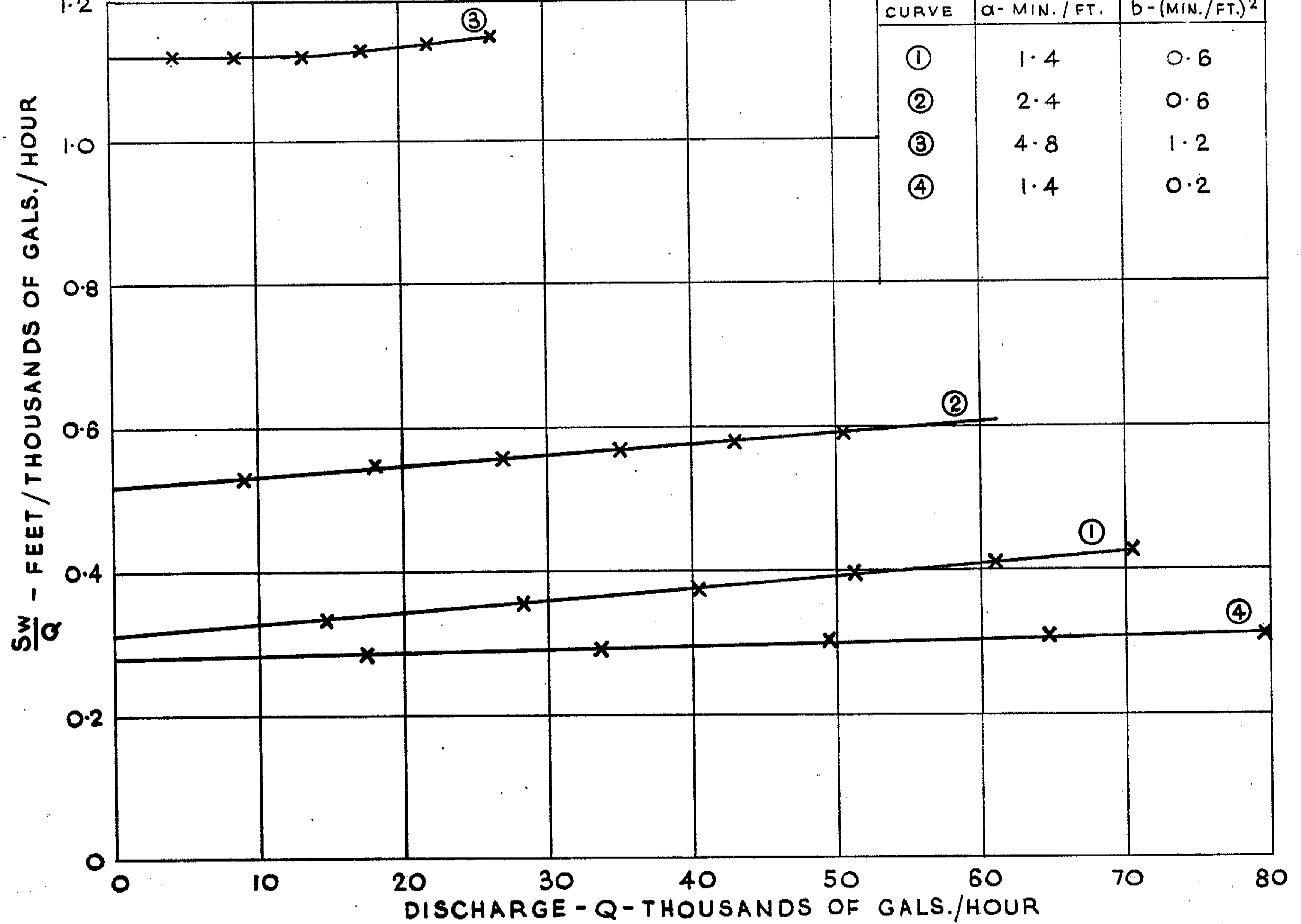


Fig. (3-16): $^{s}w/_{Q}$ Vs Q curves showing effect of material properties.

Table 9: Effect of Gravel Pack Properties

| Well No. | Type of Gravel Pack Material (Table 4) | Hydraulic Coefficients | | | Discharge at $s_w$=30 ft. (cfm) | Sp. C. (cfm/ft) |
|---|---|---|---|---|---|---|
| | | a (min./ft.) | b (min.$^2$/ft.$^2$) | K (ft./min.) | | |
| 1 | $\frac{1}{4}$" River Gravel | 0.337 | 0.069 | 2.800 | 169.08 | 5.636 |
| 2 | 3/16" Pea Gravel | 0.102 | 0.055 | 8.600 | 169.31 | 5.644 |
| 3 | 1/4" Uniform Gravel | 0.026 | 0.0155 | 32.6 | 170.41 | 5.680 |
| 4* | Aquifer material | 2.400 | 0.600 | 0.362 | 138.02 | 4.601 |
| 5** | Clogged 1/4" gravel | 4.900 | 5.400 | 0.153 | 86.37 | 2.879 |

* Non-gravel packed well

** Sand clogging results in high values of coefficients a and b steady flow analysis depend on the value chosen for the radius of influence. The results described previously are based on a value of 100 ft.

To show how the discharge is affected if different radii are chosen, a semi-logarithmic plot of the discharge ratio and the ratio of the radius of influence to well radius are presented in Fig. (3-17). Each graph corresponds to a particular well radius of the fully screened well. It is evident that the discharge ratio decreases only slightly with a large increase in the radii ratio when the latter exceeds about 500. This indicates that the common practice of choosing a radius of influence between 2000 and 3000 ft., for confined aquifers of large radial extent, is quite satisfactory.

### 3.5 Proposed Empirical Discharge-Drawdown Relationship

The $\frac{s_w}{Q}$ - Q plots for fully and partially screened wells may be approximated over a wide range of discharge by a straight line (Figs. 3-10 and 3-12). Thus an empirical relationship between $s_w/Q$ and Q may be written in the form

$$\frac{s_w}{Q} = A + BQ \tag{3-1a}$$

or

$$s_w = AQ + BQ^2 \tag{3-1b}$$

where A and B may be referred to as coefficients of formation loss.

The drawdown $s_w$ given by equations (3-1a) and (3-1b) does not include the head loss resulting from flow into and inside the well, referred to as well loss. The total drawdown in the well $s_o$ is given by

$$s_o = s_w + CQ^n \tag{3-2}$$

where C is referred to as coefficient of well loss and n is an exponent having a value between 1 and 2.

The estimation of well loss is discussed in Section 4.2.3.

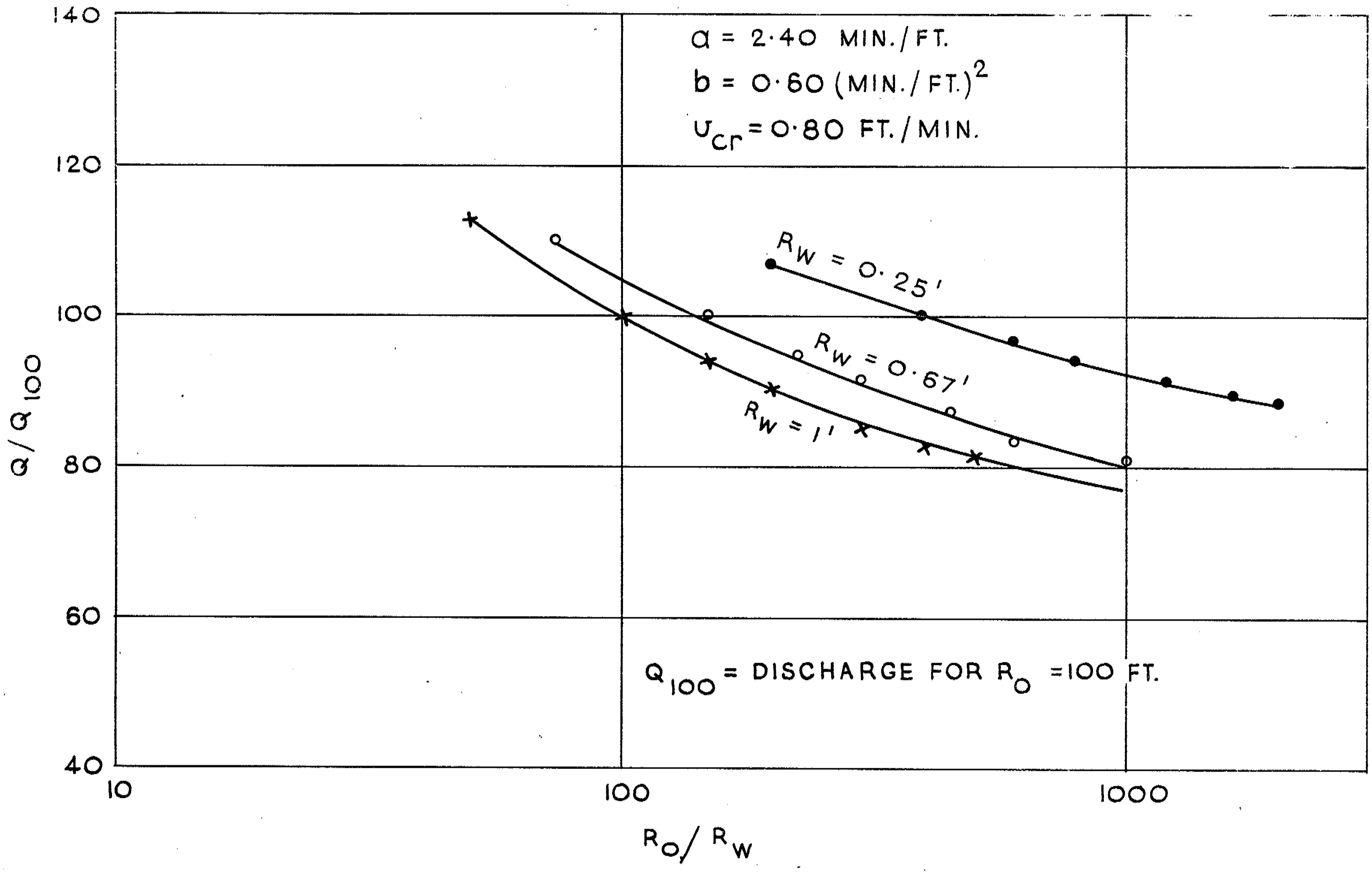


Fig. (3-17): Discharge ratio Vs radius ratio for a fully screened well.

# 4. Hydraulic Consideration and Procedures in Well Design

## 4.1 General

Well design involves the determination of the dimensional factors and selection of materials for the well structure. Good design aims to obtain at a reasonable cost a hydraulically efficient well that will yield a required discharge and have a long service life. To accomplish this, it is necessary to give careful consideration to factors influencing the well performance, and establish criteria for assessing and comparing the performance and efficiency of various selected designs. On the basis of the comparison and consideration of other technical and cost factors, the optimum well design feature can be selected.

There are several well design procedures and criteria available in the literature, most of which are based on elementary hydraulic analysis and empirical allowances, particularly regarding the complication resulting from non-Darcy flow in the near well zone, the complex design feature of the well and variability of the aquifer material.

The purpose of this section is to establish hydraulic criteria for assessing and comparing the well performance and to propose some procedures which may lead to improved well design. The proposed design procedures and guide-lines are intended for screened wells in unconsolidated formations. However, the basic concepts and principles are also applicable to non-screened wells in consolidated rock.

## 4.2 Hydraulic Performance of Well

### 4.2.1 Specific Capacity

The term "specific capacity" of a well is defined as the ratio of the discharge and the corresponding drawdown in the well.

The total well drawdown is made up of:-

(i) formation loss resulting from the head loss associated with non-Darcy flow in the near well zone and Darcy flow in the remaining portion of the aquifer,

(ii) well loss resulting from turbulent flow of water through screen openings into the well and axial flow inside the well from the screen to the pump intake.

For a well in an unconsolidated confined aquifer, the specific capacity, Sp. C, and the well discharge, Q, are related by

$$Sp.C = Q/s_o = Q/(AQ+BQ^2+CQ^n) \qquad (4\text{-}1)$$

where $s_o$ is the total drawdown in the well, and the coefficients A, B and C and the exponent n are as defined previously.

Equation (4-1) shows that the specific capacity of a well decreases with increasing discharge, and that the practice of assuming a constant specific capacity may lead to a sizable error. For a particular well design, the coefficients A and B may be determined by performing hydraulic analysis of two regime well flow, using the computer programs described, for various prescribed values of the theoretical well drawdown $s_w$, and constructing $s_w/Q$ - Q curves.

In determining the dimensions of the well structure, the required safe specific capacity value at the maximum drawdown available should be computed. The size of the intake portion of the well should be chosen to be sufficiently large to yield at least this safe value.

4.2.2 Entrance Velocity

The entrance velocity of water through the well screen may be determined from the theoretical velocity at the screen boundary as computed by the programs. The following continuity equation holds -

$$V_n = VA_r \qquad (4\text{-}2)$$

where $V_n$ is the entrance velocity, V is the theoretical velocity, ignoring the presence of the screen, and $A_r$ is the ratio of the effective open area and the gross area of the screen.

For the simplest case of steady radial flow toward a fully screened well in a single confined aquifer, V may be obtained directly from

$$V = Q/(2\pi r_w m) \qquad (4\text{-}3)$$

where $r_w$ is the well radius, and m is the aquifer thickness.

However, for more complicated flow patterns such as that of flow through multi-layered aquifers or flow toward a multiple screened well, equation (4-3) is not applicable.

The effective open area of a screen usually averages at a value considerably less than that of the actual opening area, as finer sediment particles settle around the screen and block the slot openings. For the purpose of general well design, the open area ratio $A_r$ is usually taken as 60%.

To avoid excessive blockage of the screen openings and hence a high screen loss, the value of $V_n$ should be properly selected. An average value between 6 to 15 ft/min. is recommended for the design of well screen and gravel pack. The design value chosen depends largely on the grain size distribution of the aquifer material in the close vicinity of the well. Laboratory tests and field experience indicate that if the entrance velocity is less than 6 ft./min., friction losses through screen openings will be negligible and the rate of incrustation and corrosion will be at a minimum. Generally, a safe entrance velocity is the velocity that is less than that necessary to carry the finest particle of the aquifer material to the well.

### 4.2.3 Well Loss and Hydraulic Efficiency

#### (i) Well Loss

Well loss results from flow through the well screen and inside the well. For high entrance velocity and partial blockage of screen openings, the loss may be a sizable fraction of the total well drawdown. It is usually represented approximately by the following equation:

$$s_{wl} = CQ^n \qquad (4\text{-}4)$$

where $s_{wl}$ denotes well loss, and C,Q and n are as previously defined.

For the general purpose of well design, an estimate of $s_{wl}$ may be made by calculating the loss through the screen, $s_{sc}$, and the loss inside the well, $s_{iw}$, and summing the two losses.

If the screen openings are approximated by a series of orifices, the streamline pattern as water enters the screen is as shown in Fig. (4-1). Theoretical analysis (Petersen, J.S. et al; 1955) yields a relationship between $s_{sc}$ and the screen characteristics of the form

$$s_{sc} = K_{sc} \frac{V_n^2}{2g} \qquad (4\text{-}5a)$$

where $\frac{V_n^2}{2g}$ is the entrance velocity head and $K_{sc}$ is a loss ceofficient characterising the screen as given by the expression

$$K_{sc} = 2 \frac{\cosh(\frac{CL}{D}) + 1}{\cosh(\frac{CL}{D}) - 1} \quad (4\text{-}5b)$$

where L and D are the screen length and diameter respectively, and C is given by

$$C = 11.31\, C_c\, A_r \quad (4\text{-}5c)$$

in which $C_c$ is the coefficient of contraction of the slot openings, and $A_r$ is the open area ratio of the screen.

Equations (4-5a) to (4-5c) have been confirmed by extensive laboratory tests on screens surrounded by a gravel envelope and placed in an open body of water. A plot of $K_{sc}$ against $\frac{CL}{D}$ is shown in Fig. (4-2). It is seen that for $\frac{CL}{D} > 6$, $K_{sc}$ is a minimum and equal to 2.

Flow inside the well may be considered as pipe flow as the water moves along the vertical axis of the well. Accordingly, the resulting head loss, $s_{iw}$, may be computed from the Darcy-Weisbach resistance equation for pipe flow.

The total well loss is now obtained as

$$s_{wl} = s_{sc} + s_{iw} = CQ^n \quad (4\text{-}6)$$

where the coefficient C and the exponent n are determined from a plot of $s_{wl}$ against Q.

(ii) Hydraulic Efficiency of Well

Fig. (4-3) shows the graphs of well loss against well discharge and total well drawdown against discharge for a hypothetical well in an unconsolidated confined formation. The various drawdown components are also indicated.

The hydraulic efficiency $\eta$ of the well may be defined as

$$\eta = \frac{AQ}{AQ+BQ^2+CQ^n} \times 100 \quad (4\text{-}7)$$

The value of hydraulic efficiency may be used as an index for assessing and comparing the performance of selected well designs. At high discharges, non-Darcy flow near the well and turbulence into and

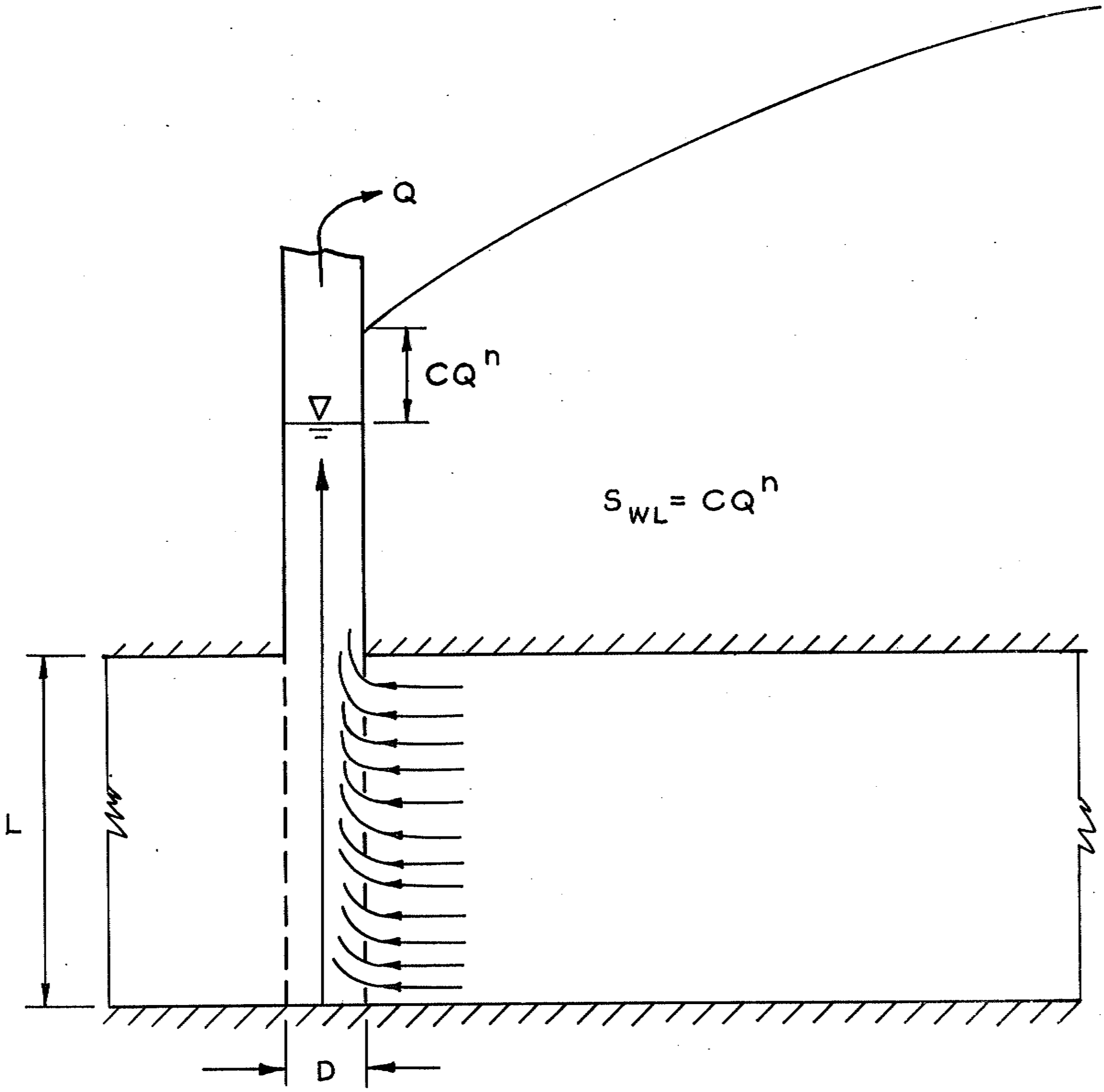


Fig. 4. 1: Flow through screen openings and well loss.

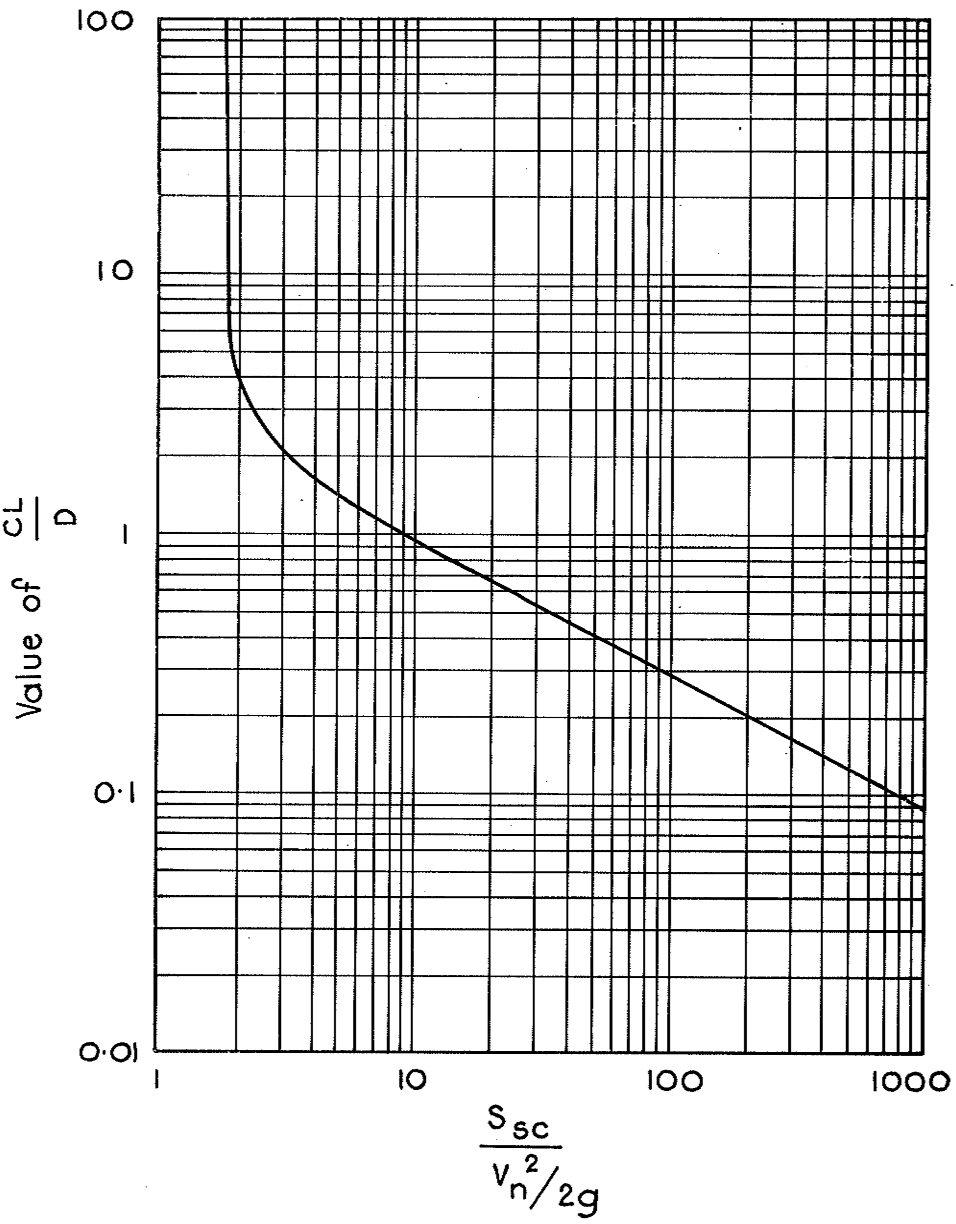


Fig. (4-2): Adjusted value of screen loss coefficient as a function of $\frac{CL}{D}$ (after Petersen, et al).

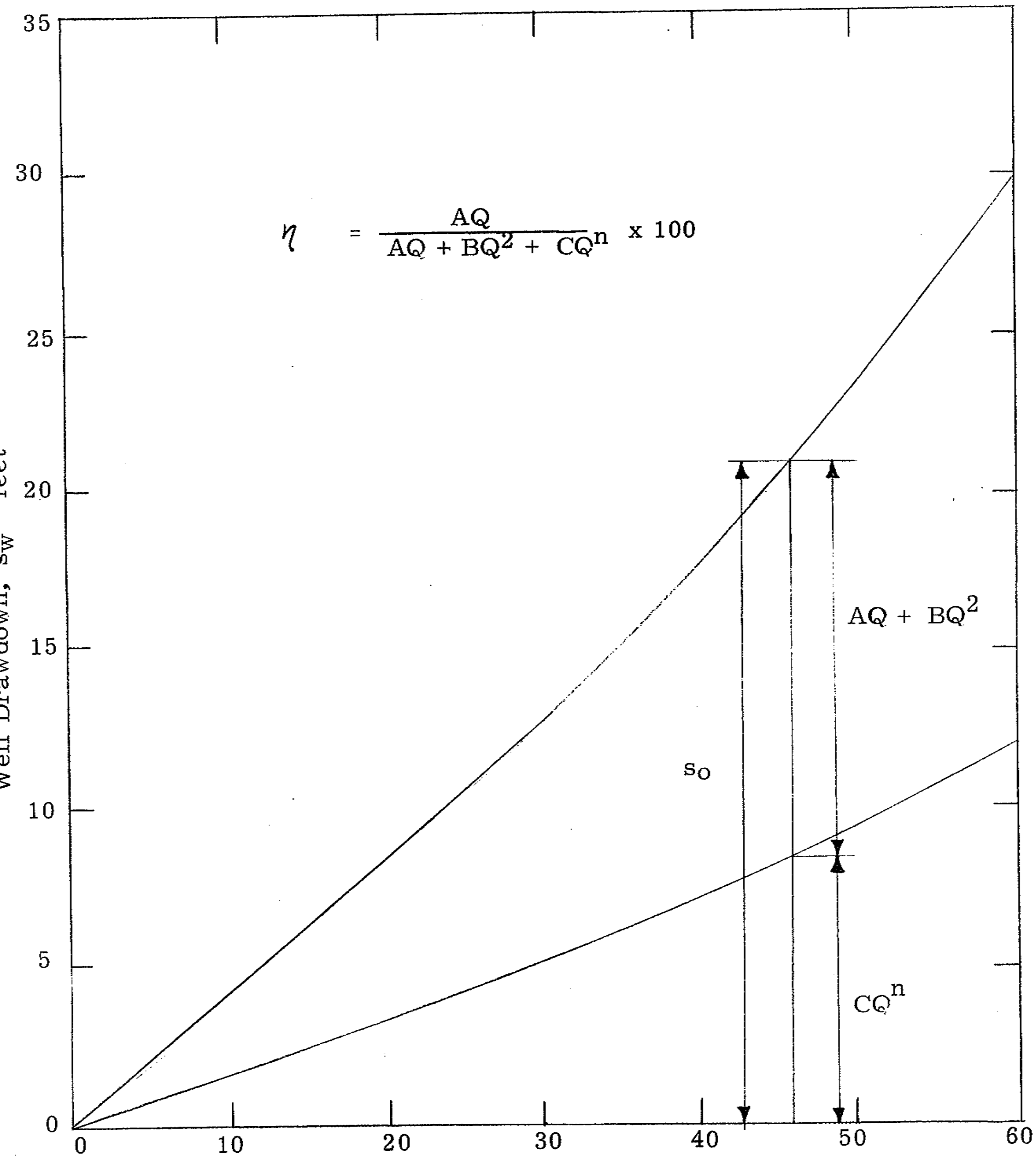


Discharge, Q - Thousands of Gals./Hour

Fig. (4-3): Discharge Vs. Well Drawdown showing Components of Losses.

inside the well will reduce the hydraulic efficiency. A plot of hydraulic efficiency against discharge enables these factors to be assessed in the design of the well.

The efficiency of a well can be improved by

(i) well development to improve the hydraulic properties of material in the near well zone;

(ii) use of gravel pack to reduce non-Darcy and well losses;

(iii) increasing the screen length or diameter to reduce the entrance velocity.

### 4.3 Selection of Screen and Casing Dimensions

#### 4.3.1 Screen Diameter

The diameter of the screened section of the well must be sufficiently large to ensure good hydraulic efficiency at the required specific capacity and to keep the entrance velocity safely below the permissible upper limit. Hydraulic analysis has shown that enlarging the diameter results in an appreciable reduction in the non-Darcy effect and well loss and a close to proportional percentage reduction of the entrance velocity.

To enable proper selection of the screen diameter, graphs of $s_W/Q$-$Q$ for selected values of the well radius and graphs relating the well radius to $s_W/Q$ at a prescribed value of the well drawdown should be prepared with the aid of the two computer programs previously described. Well loss should also be estimated and the graphs adjusted to include this loss. Hydraulic efficiency should then be computed and graphs relating the efficiency to the well discharge obtained. To avoid the problem of clogging and incrustation of the screen, an average entrance velocity of between 6 and 15 ft/min. should be adopted as a criterion in deciding the optimum diameter. Cost and other technical factors associated with the well construction should also be taken into account.

#### 4.3.2 Casing Diameter

The diameter of the well casing must be sufficiently large to accommodate the pump with proper clearance for installation and efficient pumping operation. The optimum casing diameter recommended by Edward E. Johnson, Inc., is two nominal sizes larger than the bowl size of the pump.

Under no circumstance should the casing diameter be less than one nominal size larger than the pump bowl. Smaller diameters may cause binding of the pump shaft and excessive head loss. The casing diameter may be reduced below the maximum anticipated pumping depth. Table 10 lists casing sizes suggested for various pumping rates.

Table 10: Suggested Casing Diameters (after Johnson, E.E. Inc.)

| Anticipated Well Yield, in gpm | Nominal Size of Pump Bowls, in inches | Optimum Size of Well Casing, in inches | Smallest Size of Well Casing in inches |
|---|---|---|---|
| < 100 | 4 | 6 ID | 5 ID |
| 75 - 175 | 5 | 8 ID | 6 ID |
| 150 - 400 | 6 | 10 ID | 8 ID |
| 350 - 650 | 8 | 12 ID | 10 ID |
| 600 - 900 | 10 | 14 OD | 12 ID |
| 850 - 1300 | 12 | 16 OD | 14 OD |
| 1200 - 1800 | 14 | 20 OD | 16 OD |
| 1600 - 3000 | 16 | 24 OD | 20 OD |

For the pump sizes and pumping rates shown in Table 10, the head losses resulting from the axial flow are small and may be neglected in the calculation of well loss.

### 4.3.3 Screen Open Area and Slot Size

(i) Open Area

Selection of open area is based on a safe average entrance velocity between 6 to 15 ft./min., depending on the grain size distribution of the formation material immediately surrounding the screen and whether or not an artificial gravel pack is used. On the assumption of 60% of the open area being effective, the total open area may be computed from the following equation:

$$A_o = \frac{\pi DLV}{0.6V_n} \qquad (4\text{-}8)$$

where $A_o$ is the total open area, D and L are the length and diameter of screen, $V_n$ is the design average entrance velocity, and V is the velocity at screen as obtained from the computer programs.

The open area per unit length of commercial screen is related to slot size. Table 11 lists the figures of open area for various aperture sizes of stainless steel screen as manufactured by Surescreen Co. in Brisbane. It is seen that the open area increases with the increasing

Table 11: Surescreen, Stainless Steel Standard and Medium Pattern Screens (by courtesy of Surescreen Manufacturing Co., Brisbane, Australia).

| Casing or Pipe Size | Screens 5" O.D. | 6" O.D. | 8" O.D. | 10" O.D. | 12" O.D. | |
|---|---|---|---|---|---|---|
| Maximum O.D. | 4-5/16" | 5-3/16" | 7-1/16" | 9" | 11-1/4" | |
| Minimum I.D. | 3" | 4-3/8" | 6-1/4" | 8-3/16" | 10-5/16" | |
| Number and diameter of longitudinal rods | 12 x .203 | 13x.203<br>26x.203 | 18x.203<br>36x.203 | 40x.203 | 54x.203 | |
| Aperture size (inches) | Open area in square inches per foot of screen | | | | | % Open area |
| .007 | 9.56 | 11.45 | 16.05 | 20.6 | 25.9 | 6.25 |
| .010 | 13.30 | 15.96 | 22.3 | 28.65 | 36.0 | 8.69 |
| .015 | 19.12 | 23.30 | 32.1 | 41.25 | 51.75 | 12.5 |
| .020 | 24.5 | 29.4 | 41.1 | 54.7 | 66.2 | 16.0 |
| .025 | 29.45 | 35.4 | 49.4 | 63.5 | 79.6 | 19.25 |
| .030 | 33.8 | 40.8 | 57.0 | 73.2 | 92.0 | 22.25 |
| .035 | 38.3 | 46.0 | 64.2 | 82.6 | 103.5 | 25.0 |
| .045 | 45.8 | 55.2 | 77.0 | 99.0 | 124.2 | 30.0 |
| .055 | 52.5 | 63.2 | 88.1 | 113.2 | 142.1 | 34.4 |
| .065 | 58.5 | 70.2 | 98.1 | 126.0 | 158.2 | 38.2 |
| .080 | 66.0 | 79.5 | 111.0 | 142.4 | 179.0 | 43.3 |
| .105 | 76.5 | 92.0 | 128.3 | 165.0 | 206.5 | 50.0 |
| .125 | 84.2 | 100.0 | 139.4 | 179.0 | 225.0 | 54.4 |
| .140 | 87.3 | 105.0 | 146.6 | 188.4 | 236.5 | 57.2 |

Triangular wrapping wire section: 0.105" wide, 0.100" deep slot size.

(ii) Slot Size

Determination of the slot size is made from sieve analysis data on samples of material immediately surrounding the screen. The permissible slot size is usually the largest that will maintain the stability of the aquifer material. As a general guide for a homogeneous formation consisting of fine uniform sand, the proper slot size should be the size that will retain about 40% to 50% of the sand. For stratified aquifers, slot openings of different sections of the well screen are chosen according to the gradation of the materials of the different strata. Each section of screen is made with openings to retain about 40% to 50% of the material of each stratum. If fine material overlies coarse material, the slot size for the screen section to be installed in the coarse stratum should not be more than double the size for the overlying layer, and at least 2 ft. of the smaller slot screen should be extended down into the coarse layer. These precautions are necessary to avoid the possibility of fine sand entering the upper part of the larger screen.

For a gravel packed well, the selection of slot size should also be based on a careful study of sieve analyses of the pack material. For the case in which the pack and aquifer materials are uniform, as a guide, the slot size should retain at least 90% of the aquifer material.

4.4 Selection of Gravel Pack

4.4.1 General

Artificial gravel pack is required for aquifers consisting of fine materials as it is not practicable to use very small slot sizes. The use of a pack of particles of larger size not only results in a larger allowable size of slot openings but also a reduction in non-Darcy and well losses and a general improvement in well performance.

The basic requirements of gravel pack are as follows:-

(i) Suitable grading that will ensure sand-free operation after well development and hence stability of the aquifer formation.

(ii) Good hydraulic characteristics which lead to a general improvement in well performance.

(iii) Long service life.

### 4.4.2 Grading of Pack

Selection of pack grading is based on sieve analyses of samples of aquifer material in the immediate vicinity of the well screen. Several methods are available in the literature. The method presented here is that recommended by Kruse (1960).

The following definitions are necessary:-

(i) $D_x$ size is the size such that x% of the material in the sample (by weight) is smaller.

(ii) Pack-Aquifer ratio or P-A ratio is the ratio of $D_{50}$ size of the gravel pack to the $D_{50}$ size of the aquifer.

(iii) Uniformity coefficient is the ratio of the $D_{60}$ size to $D_{10}$ size of the material.

Test results carried out by Kruse on gravel packs at Colorado State University indicated the following values as the upper limits of P-A ratio if a stable filter action is to be maintained.

| Aquifer | Gravel Pack | Limiting P-A Ratio |
|---|---|---|
| Uniform | Uniform | 9.5 |
| Non-uniform | Uniform | 13.5 |
| Uniform | Non-uniform | 13.5 |
| Non-uniform | Non-uniform | 17.5 |

The test data also indicated:

(i) less aquifer movement occurs with non-uniform gravel packs than with uniform gravel packs at the same P-A ratio;

(ii) at low P-A ratios, increasing aquifer uniformity coefficient increases initial sand movement;

(iii) at high P-A ratios, increasing aquifer uniformity coefficient decreases sand movement.

The procedures in design of the grading are summarised as follows:-

(i) Construct sieve-analysis curves for samples of all strata comprising the aquifer. Determine the stratum composed of the finest sand and use this curve as a basis for selection of pack grading.

(ii) Determine $D_{10}$, $D_{50}$, $D_{60}$, $D_{90}$ and the uniformity coefficient, $C_u$, for the aquifer material.

(iii) If the aquifer is reasonably uniform, choose a P-A ratio of less than 9.5 for a uniform gravel pack and a ratio of less than 13.5 for a non-uniform gravel pack. If, on the other hand, the aquifer is non-uniform, choose a P-A ratio of less than 13.5 for a uniform pack and a ratio of less than 17.5 for a non-uniform pack.

(iv) From the selected P-A ratio, calculate $D_{50}$ for the gravel pack. The value obtained represents the first point on the sieve analysis curve for the gravel pack Decide on the value of $C_u$ for the pack material and draw a free-hand smooth curve through the initial point representing a material with $C_u$ equal to the desired value. It is suggested that a value of $C_u \leqslant 2$ should be chosen for a uniform pack and $C_u \leqslant 3.5$ for a non-uniform pack. In general $C_u$ for the pack is chosen to be of the same magnitude as that for the aquifer material.

(v) Prepare specifications for the pack material by first selecting 4 or 5 sieve sizes that cover the spread of the curve and then set down a permissible range of % retained on each of the selected sieves.

Having selected the desired pack material according to the above procedures, the designer should then obtain the values of the hydraulic coefficients in the head loss relations. The most reliable method of doing this is to carry out permeameter tests. Alternatively, their values may be estimated from available data on pack materials of similar grain size distribution. The hydraulic coefficients thus obtained are used in the computation of well flow and losses by the computer programs.

### 4.4.3 Thickness of Gravel Pack

The optimum thickness of a pack depends on several factors. To ensure that the entire screen will be surrounded by the gravel envelope, a minimum thickness of 3 inches is considered practical for placing in the field. Under most conditions, the maximum thickness should not exceed 9 inches. A thicker envelope is considered uneconomical as it does not materially increase the specific capacity of the well nor reduce the possibility of sand pumping. Moreover, too thick a pack makes it difficult to remove drilling mud and cuttings from the aquifer face during well development.

Since the use of clean gravel pack results in considerable improvement in the well performance, selection of the designed pack thickness should also be based on the results of hydraulic analysis obtained from the computer programs. Graphs of well drawdown-discharge, should be obtained for various values of the thickness. From the comparison of the hydraulic performance and cost of the wells, the optimum thickness may be selected.

## 5. Conclusions and Further Work

Steady flow behaviour of wells in a thin unconsolidated confined aquifer has been analysed by two finite element programs written in Fortran IV computer language to solve one- and two-dimensional two regime well flow respectively.

The effects of well design factors and non-Darcy flow on the well discharge and specific capacity have been closely examined. It has been shown that non-Darcy flow only occurs in the immediate vicinity of the well screen, and that the non-Darcy effect may be reduced by:-

(i) well development to improve hydraulic properties of aquifer material in the near well zone;

(ii) the use of clean gravel pack material of good hydraulic characteristics;

(iii) increasing screened diameter and length and proper positioning of screen.

Graphical and tabulated data on the discharge-drawdown relationship for a limited range of possible well design factors and hydraulic characteristics of aquifer material have been presented. To cover a wider range of these parameters is only a matter of additional labour and computer time.

Well performance, losses and efficiency and other hydraulic considerations in well design have been discussed. By the use of the computer programs to analyse steady two-regime well flow, procedures and criteria for designing screened wells in unconsolidated confined formations have been proposed, the usefulness of which remains to be demonstrated by the well design engineer.

Additional work envisaged in the near future is briefly outlined as follows:-

(i) Extension of the two finite element programs to solve transient two regime confined flow and study of transient flow behaviour of various well designs.

(ii) Comparison of computed results for transient flow with test results obtained from the experimental facility described in Section D of this report.

(iii) Field study, already described in Section A, to allow the results of computer analysis and laboratory experiments to be verified.

(iv) Development of insitu methods for predicting hydraulic coefficients of material in the immediate vicinity of the well screen.

## Appendix I

## Mathematical Solution of Steady Radial Flow toward a Fully Screened Well.

### I-1 General Solution

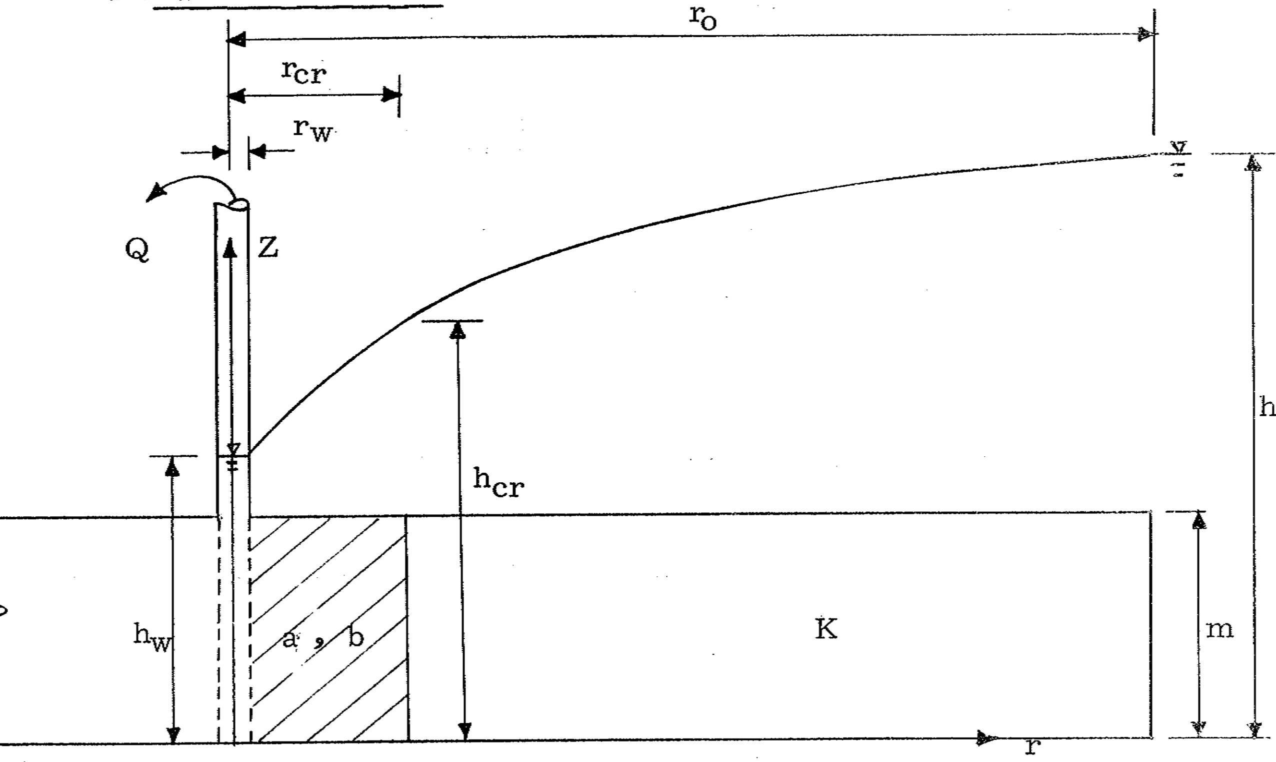


Fig (I-1): A mathematical model of confined well-aquifer system.

A mathematical model of a confined well-aquifer system is as shown in Fig. (I-1). The well, fully penetrating the single confined aquifer, is screened over the entire aquifer thickness. Non-Darcy flow is assumed to occur in the shaded subregion extending from the well radius $r_w$ to the critical radius $r_{cr}$. The equation relating hydraulic gradient to velocity is given by :-

$$-\frac{dh}{dr} = aV + bV^2 \qquad (I-1)$$

The flow velocity and well discharge are related by

$$V = -\frac{Q}{2\pi rm} \qquad (I-2)$$

Substituting equation (I-2) into equation (I-1) gives

$$\frac{dh}{dr} = \frac{aQ}{2\pi mr} - \frac{bQ^2}{4\pi^2 m^2 r^2}$$

which may be integrated to yield

$$\int_{r_w}^{r} \frac{dh}{dr}\, dr = \int_{r_w}^{r} \frac{aQ}{2\pi m} \frac{dr}{r} - \int_{r_w}^{r} \frac{bQ^2}{4\pi^2 m^2} \frac{dr}{r^2}$$

$$h - h_w = \frac{aQ}{2\pi m} \ln\left(\frac{r}{r_w}\right) + \frac{bQ^2}{4\pi^2 m^2}\left(\frac{1}{r_w} - \frac{1}{r}\right) \qquad \text{(I-3)}$$

Equation (I-3) describes the hydraulic head variation over $r_w \leqslant r \leqslant r_{cr}$

The critical radius $r_{cr}$ is given by

$$r_{cr} = \frac{Q}{2\pi m V_{cr}} \qquad \text{(I-4)}$$

where $V_{cr}$ is the critical flow velocity corresponding to the critical Reynolds number.

Now the equation describing Darcy flow in the remaining portion of the aquifer may be written as

$$K\frac{dh}{dr} = \frac{Q}{2\pi m r} \qquad \text{(I-5)}$$

which may be integrated to give

$$\int_{r}^{r_o} K\frac{dh}{dr}\, dr = \int_{r}^{r_o} \frac{Q}{2\pi m} \frac{dr}{r}$$

$$h_o - h = \frac{Q}{2\pi m K} \ln\left(\frac{r_o}{r}\right) \qquad \text{(I-6)}$$

Equation (I-6) describes the head variation over $r_{cr} \leqslant r \leqslant r_o$

## I-2 Well Drawdown-Discharge Relationship

The theoretical well drawdown is obtained by substituting $r = r_{cr}$ into Equations (I-3) and (I-5) and adding. Hence

$$h_o - h_w = \frac{aQ}{2\pi m} \ln \left(\frac{r_{cr}}{r_w}\right) + \frac{bQ^2}{4\pi^2 m^2} \left(\frac{1}{r_w} - \frac{1}{r_{cr}}\right) + \frac{Q}{2\pi mK} \ln \left(\frac{r_o}{r_{cr}}\right) \qquad \text{(I-7)}$$

On letting $s_w = h_o - h_w$, equation (I-7) may be written in the following form

$$s_w = AQ + BQ^2$$

or

$$s_w/Q = A + BQ \qquad \text{(I-8)}$$

where $A = \frac{a}{2\pi m} \ln \left(\frac{r_{cr}}{r_w}\right) + \frac{1}{2\pi Km} \ln \left(\frac{r_o}{r_{cr}}\right)$

and $B = \frac{b}{4\pi^2 m^2} \left(\frac{1}{r_w} - \frac{1}{r_{cr}}\right)$

For given values of the well radius, the hydraulic coefficients of aquifer and the radius of influence, it is seen that A and B slightly depend on the critical radius $r_{cr}$ which is related to the well discharge as given in Equation (I-4).

Fig. (I-2) shows a general plot of $s_w/Q$ against Q.

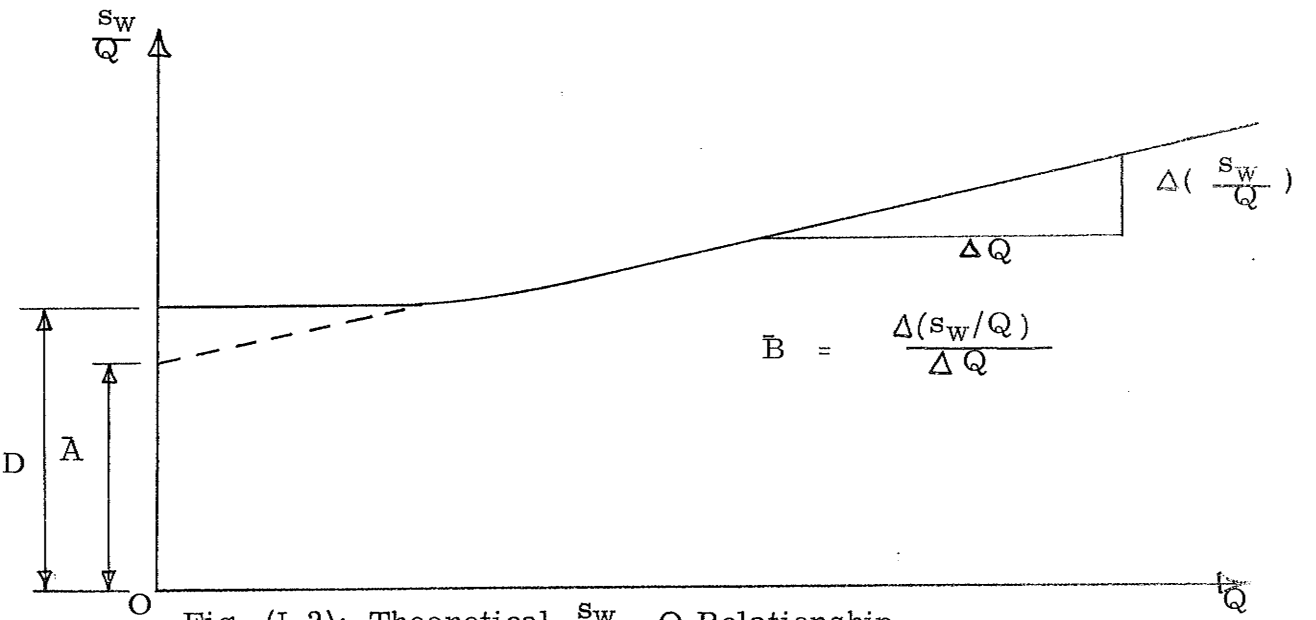


Fig. (I-2): Theoretical $\frac{s_w}{Q}$ - Q Relationship

The horizontal line corresponds to Darcy flow in the entire region of the aquifer, which occurs at low discharge values. For this line, the coefficient B is zero and A becomes

$$A_D = \frac{1}{2\pi Km} \ln \left(\frac{r_o}{r_w}\right) \tag{I-9a}$$

The remaining portion of the $s_w/Q$-$Q$ graph is a mild curve which is closely approximated by a sloping line at greater values of the well discharge. $\bar{A}$ and $\bar{B}$ are the intercept and slope of the line which are approximated by

$$\bar{A} = \frac{a}{2\pi m} \ln \left(\frac{\bar{r}_{cr}}{r_w}\right) + \frac{1}{2\pi Km} \ln \left(\frac{r_o}{\bar{r}_{cr}}\right) \tag{I-9b}$$

$$\bar{B} = \frac{b}{2\pi^2 m^2} \left(\frac{1}{r_w} - \frac{1}{\bar{r}_{cr}}\right) \tag{I-9c}$$

where $\bar{r}_{cr}$ is the critical radius value at a maximum safe discharge capacity of the well.

## List of References

1. Ahrens, T.P. - "Well design criteria, Parts I and II", Water Well Jour., Urbana, Illinois, (1957).

2. Aitken, R.R., Alexander, E.L. - "Optimum hole diameter for water wells", Water Well Jour., Jan. (1967).

3. Anandakrishnan, M., Varadarajula, G.H. - "Laminar and turbulent flow of water through sands", A.S.C.E., Jour., Proc., 89, SM5, pp. 1-15, (1963).

4. Blair, A.H. - "Well screens and gravel packs: A technical review of commercial and theoretical literature", Water Research Assoc., U.K., Tech. Paper No. TP 64, Oct. (1968).

5. Dudgeon, C.R. - "Flow of water through coarse granular materials", M.Eng. thesis, Univ. of New South Wales, (1964).

6. Erde lyi, M., et al - "Estimation of groundwater resources", Int. Post-grad. Course on Hydrological Methods for Developing Water Resources Management, Course III, Series of Manuals No. 11, pp. 163-171, (1970).

7. Forbes, C.F. - "Theory and appraisal of hydraulic conditions in wells", Water Research Lab., Univ. of New South Wales, Report No. 113, Proc. of Groundwater Symposium, Paper No. 3, pp. 28-49, August, (1969).

8. Irrigation and Water Supply Commission, Queensland - "Report on Extraction of Water from Unconsolidated Sediments", Australian Water Resources Council, Research Project 68/8, (1968).

9. Johnson, Edward E., Inc. - "Groundwater and Wells: A reference book for the water-well industry", Johnson, Edward E. Inc., St. Paul, Minnesota, U.S.A. (1966).

10. Kruse, G. - "Selection of gravel packs for wells in unconsolidated aquifers", Colorado Agriculture Experimental Station, Tech. Bull., 66 (1960).

11. Lane, K.S. - "Laminar and turbulent flow of water through sand", A.S.C.E., Jour., Proc., 90, SM3, pp. 171-176, (1964).

12. Linguist, E.-"On the flow of water through porous soils", 1st Congress des Grands Barrages, Stockholm, Vol. 5, pp. 81-101, (1933).

List of References (cont'd.)


13. Petersen, J.S., et al - "Effect of well screens on flow into wells" Trans. A.S.C.E., 120, pp. 563-607, (1955).

14. Peterson, D.F. (Jr.) "Hydraulics of Wells", A.S.C.E., Proc., 81, 708, pp. 1-23, June (1955).

15. Rao, K.V.R., Raju, T.S. - "Well characteristics and design criteria of water wells in the desert tracts of Jaisalimer District, Rajasthan", Dept. of Geology and Geophysics, Univ. of Roorkee, U.P., Proc. of the Symposium on Groundwater Studies in Arid and Semi-arid Regions, Paper No. 18, pp. 243-269, (1966).

16. Smith, R.C. - "Relation of screen design to the design of mechanically efficient wells", A.W.W.A., Jour., 55, 609-714, May (1963).

17. Sunada, D.K. - "Turbulent flow through porous media", Hydraulic Lab., Univ. of California, Berkeley, Contribution No. 103, (1965).

18. Walton, W.C. - "Groundwater resource evaluation", McGraw-Hill Book Co., New York, Chapter 5, pp. 291-259, (1970).

19. Ward, J.C. - "Turbulent flow in porous media", A.S.C.E., Jour., Proc., 90, HY5, pp.1-12, (1964).

20. Zienkiewicz, O.C., Phillips, D.V. - "An automatic generation scheme for plane and curved surfaces by 'isoparametric' coordinates", Int. Jour. for Numerical Methods in Engineering, Vol. 3, pp.519-528, (1971).

# SECTION D

## DESIGN, CONSTRUCTION AND OPERATION OF THE EXPERIMENTAL FACILITY

by

C.R. Dudgeon and W.H.C. Swan.

SECTION D

Table of Contents


| | Page No. |
|---|---|
| 1. Introduction | D1 |
| 2. Design Selected | |
| 2.1 General Layout | D2 |
| 2.2 Location | D2 |
| 2.3 Structural Design | D7 |
| 2.4 Instrumentation Annexe | D7 |
| 2.5 Instrumentation and Inspection Holes | D7 |
| 2.6 Overhead Shelter | D8 |
| 2.7 Water Supply and Pipework | D8 |
| 2.8 Electric Hoist | D8 |
| 2.9 Outer Aquifer Retaining Barrier | D8 |
| 2.10 Inner Aquifer Retaining Barrier | D13 |
| 3. Instrumentation | |
| 3.1 Piezometer Tappings | D13 |
| 3.2 Pressure Gauge and Transducers | D14 |
| 3.3 Orifice Plate Meters | D14 |
| 3.4 Contact Electrode Gauge for Measuring Water Levels | D14 |
| 3.5 Multiple Observation Well | D14 |
| 4. Operation of Experimental Facility | |
| 4.1 Calibration | D17 |
| 4.2 Placement of Aquifer Material | D17 |
| 4.3 Flooding of Aquifer Material | D17 |
| 4.4 Determination of Effective Porosity of Aquifer | D17 |
| 4.5 Confined Aquifer Testing | D18 |
| 4.6 Unconfined Aquifer Testing | D18 |
| 5. Laboratory Tests - Confined Aquifer | |
| 5.1 Objectives | D19 |
| 5.2 Test Procedures | D19 |
| 5.3 Experimental Results - Confined Aquifer | D20 |
| 5.3.1 Laboratory Test Results | D20 |
| 5.3.2 Sieve Analyses | D20 |
| 5.3.3 Effective Porosity Measurements | D20 |
| 5.4 Analysis of Experimental Results | D29 |
| 5.4.1 Determination of the Coefficient of Hydraulic Conductivity 'K' | D29 |

Table of Contents (cont'd.)


| | Page No. |
|---|---|
| 5.4.2 Determination of Forchheimer Coefficients 'a' and 'b'. | D30 |
| 5.4.3 Determination of the Critical Reynolds Number $\mathbb{R}_{cr}$ | D31 |
| 5.5 Discussion of Results | D32 |
| 5.6 Conclusions and Further Work | D33 |

## 1. Introduction

The well simulation tank was designed and constructed specifically for use in studying the hydraulics of flow into wells and practical aspects associated with well drilling and development.

The immediate uses envisaged for the experimental facility were:-

(i) verification of the theoretical and numerical methods developed to study the pattern of flow through the aquifer in close proximity to wells and to predict flow rates and drawdowns:

(ii) verification of design graphs and tables to be prepared using a digital computer;

(iii) study of the flow phenomena in the well and in the vicinity of the well boundary (e.g. at screens);

(iv) study of the effects of drilling and development techniques on the hydraulic properties of the aquifer material near the well.

Future uses might include the testing of new types of commerical screens, pumps and other types of equipment.

It was considered that to meet current and future needs the facility should be designed:-

(i) to be as flexible in operation as possible;

(ii) to allow various types of instrumentation to be installed without difficulty or structural modification;

(iii) to allow confined and unconfined flows to be studied with velocities at the screen up to those met in high yielding wells in the field;

(iv) to allow model or small size prototype studies to be carried out for either -

(a) a full circle portion of a well and surrounding aquifer,

(b) a quadrant portion of a well and surrounding aquifer;

(v) to allow observation of flow along a radial plane for the quarter well case;

(vi) to be relatively maintenance free;

(vii) to minimise material handling problems;

(viii) to allow experiments to proceed regardless of weather conditions.

Because of scaling problems involved in non-linear flow through porous media, the larger the tank the better but the greater the problem in handling aquifer material. It was clear that as regards size, a compromise, governed mainly by the cost, materials handling and available space would be necessary.

## 2. Design Selected

### 2.1 General Layout

As a compromise between the conflicting requirements, a square tank in plan, with internal dimensions of 16' x 16' x 11' was selected. The general layout of the tank and associated structures is shown in Figures 2.1 and 2.2 .

The square section was selected as it allowed tests to be performed either on a quadrant of an aquifer of 16 ft. radius with the well located in one corner of the tank or on a circular aquifer of 8 ft. radius with the well located in the centre of the tank. Provision of inspection windows in the wall of the tank common to the instrumentation annexe allow observation of flow along a radial plane for the quarter well case.

Other advantages of a square section were the ease of forming for construction, the existence of space for stilling areas at the corners and the ease of fitting a pressure resisting cover to allow confined flow cases to be studied under high flow rate conditions.

The pressure resisting cover was located approximately 5 ft. above the floor of the tank. The design head on the cover was 55 ft., applied through a recirculating pump with provision for damping pressure fluctuations.

A major design problem was to allow for the transfer of the upthrust on this cover to the walls of the tank.

### 2.2 Location

The tank was sited in the grounds of the Water Research Laboratory on a rock ledge adjacent to a bank of convenient height.

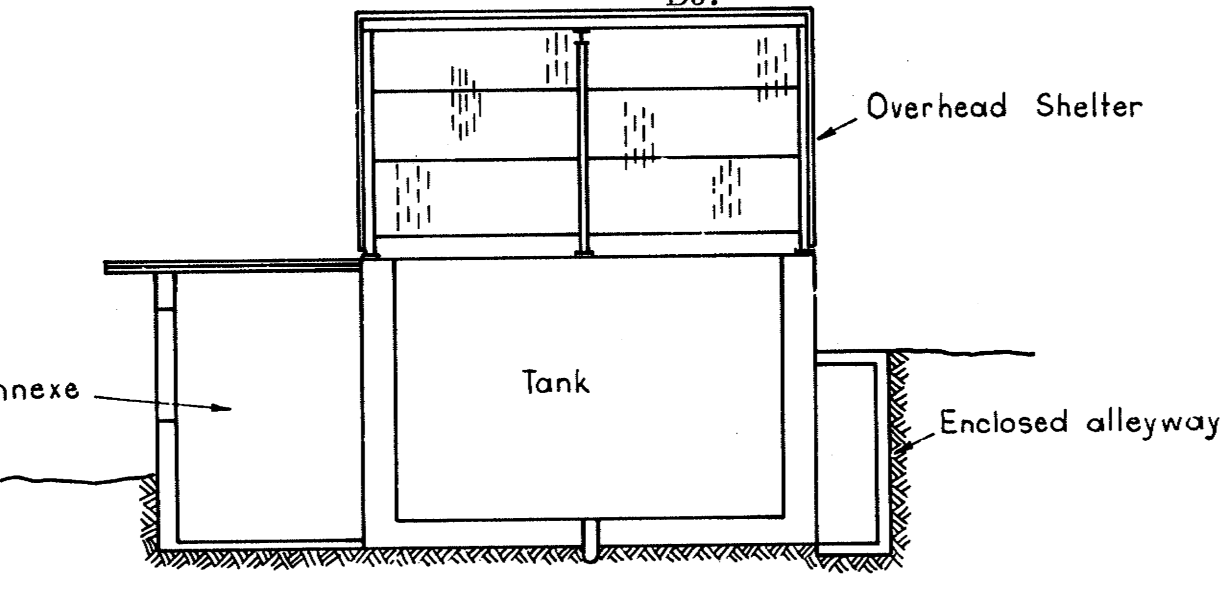


ELEVATION A-A

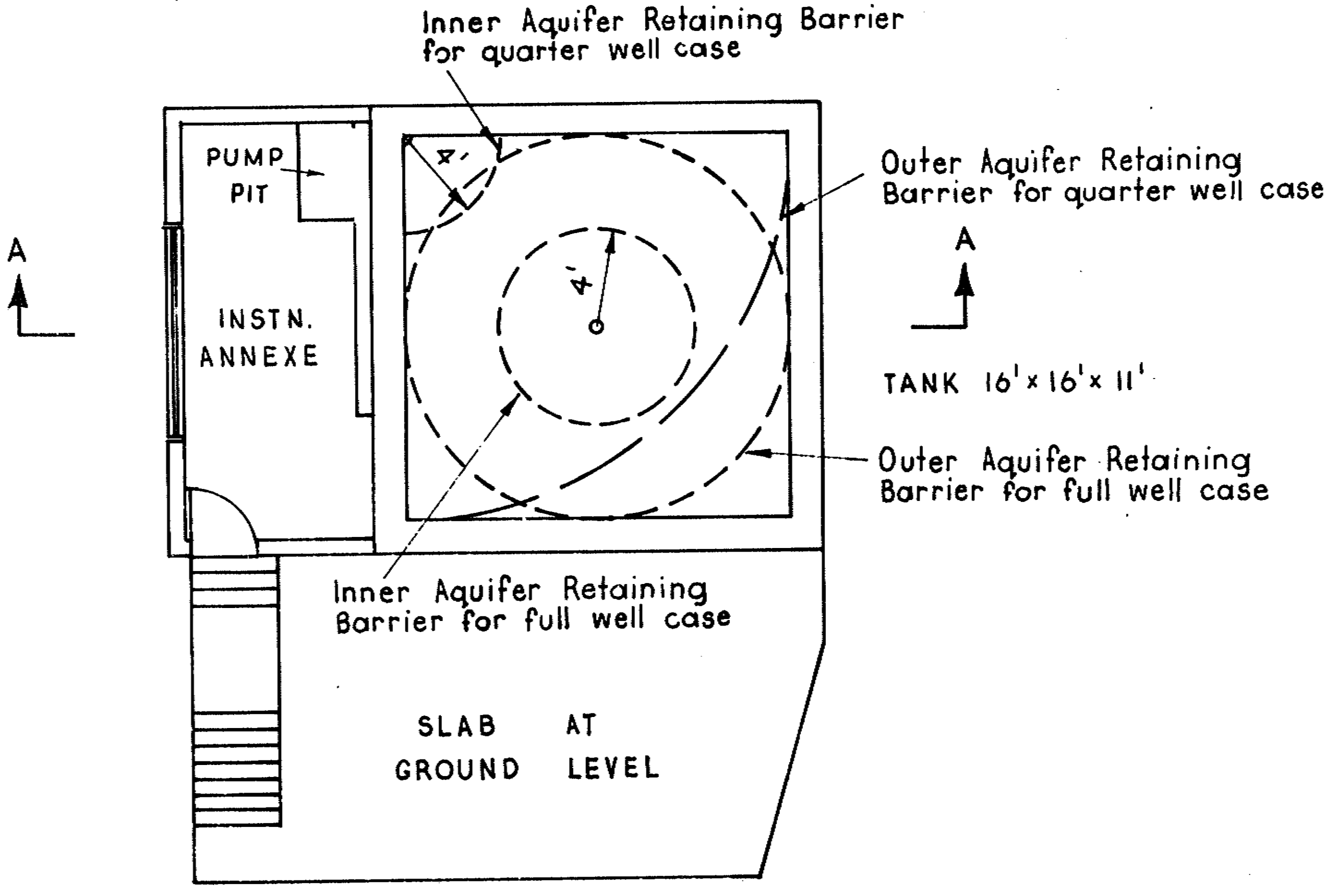


FLOOR PLAN

Scale : 1/8" = 1' 0"

FIGURE 2·1 : WELL TESTING FACILITY

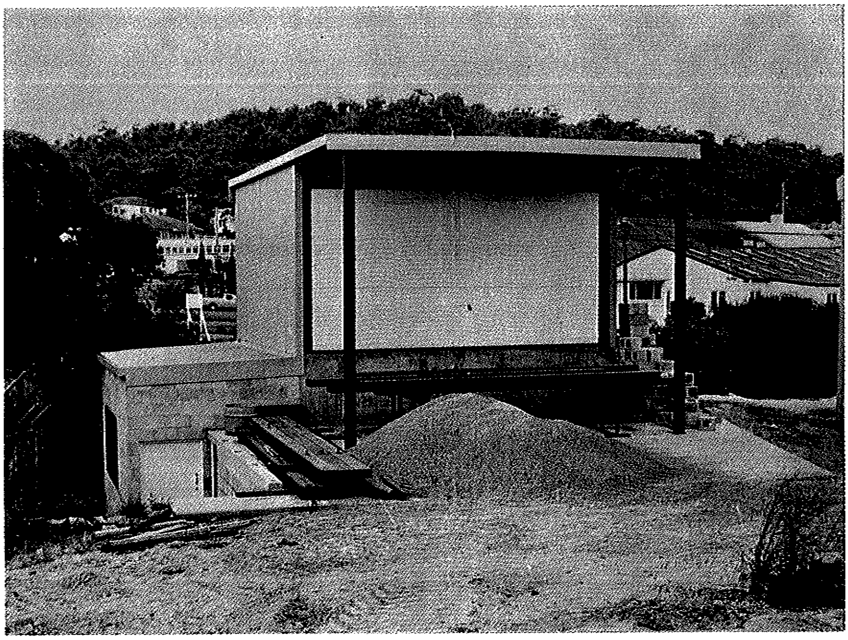

Figure 2.2: Well Testing Facility.

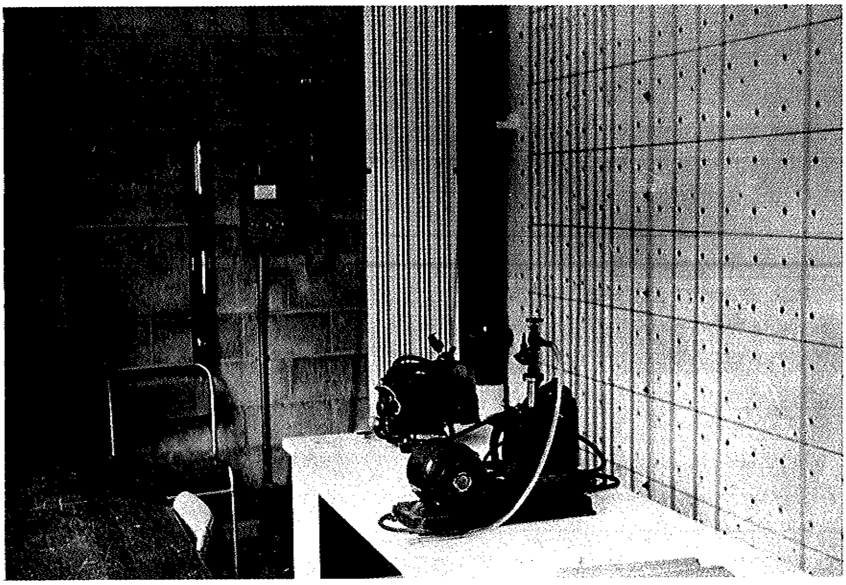

Figure 2.3: Internal view of Instrumentation Annexe showing Orifice Manometer Panel (centre) and Piezometer Tubes (right)

As can be seen from Figure 2.1 this allowed the base of the tank to be placed below the level of the adjoining working area. A covered walkway between the tank and the masonry wall retaining the bank allowed access to all sides of the tank and the pipe system. The concrete roof of the walkway formed part of a paved area approximately 4 feet below the top of the tank walls at the level of the main working area. The arrangement allowed easy access to the top of the tank for transferring materials and equipment and afforded a sheltered paved working area in front of the tank.

A large concrete bin for storing aquifer material was located immediately in front of the tank.

## 2.3 Structural Design

Design calculations for the confined case design head of 55 feet resulted in a base and wall thickness of 15 inches with heavy reinforcement in both floor and walls to resist the upward thrust on the confining lid.

It was initially intended to have the pressure cover at the top of the tank but because of the high shear stresses in the concrete the cover was placed nearer the bottom. A removable flange is provided around the inside of the walls to take the weight of the cover. Upthrust is transferred to the reinforced concrete walls by a system of steel beams and trusses. The lower level of the cover in no way hampers the operation of the tank for either confined or unconfined aquifer tests. To have increased the thickness of the tank walls to resist the shear with a full height cover would have increased the cost considerably and made the provision of access and inspection holes through the walls impracticable.

## 2.4 Instrumentation Annexe

An instrumentation annexe approximately 9 feet wide extends the full length of one side of the tank. Masonry block walls, a concrete floor and insulated roof prevent rapid fluctuations of temperature within the annexe.

## 2.5 Instrumentation and Inspection Holes

A mosaic of $\frac{1}{2}$ inch diameter holes at 1 foot centres left in the walls of the tank allow access for instrumentation wires and tubes. The holes were formed by P.V.C. tubes through which form tie bolts passed during construction. Each tube had its own waterstop cast into the concrete and can be plugged at its inner or outer end.

In the wall common to the tank and annexe, 1 inch diameter holes at 6 inch centres were provided in addition to the instrumentation holes. (Fig. 2 The P.V.C. tubes which lined these holes were fitted with transparent windows at their inner ends to allow flow through the aquifer material at the wall to be observed when a corner well was being tested. The diameter of inspection hole selected was considered the smallest which would allow scrutiny of typical zones of the coarsest aquifer material likely to be used. A small illuminating telescope was required for detailed observation.

Part of the interior of the instrumentation annexe with manometers and observation holes at the corner well position is shown in Figure 2.3.

## 2.6 Overhead Shelter

A portal frame enclosure was constructed over the tank and covered with steel sheeting to protect models in the tank from the weather. Double doors fitted to the accessible side of the enclosure opened out to combine with a roof extension to form a sheltered working area in front of the tank.

## 2.7 Water Supply and Pipework

The flexible arrangement of 6 inch and 4 inch pipes selected allows gravity driven or pumped water supplies to be fed to and drawn from wells placed at the centre or corner of the tank. Figure 2.4 shows the layout in diagrammatic form. Gravity flows up to 2 c.f.s could be drawn from the laboratory's reservoir at inlet heads of up to 20 feet. A 6 inch centrifugal pump fitted with a 20 H.P. motor and capable of delivering 2 c.f.s. against a head of 60 feet was used to recirculate water through the tank. The head-discharge characteristics of the pump were such that the pump could be used to supply maximum discharge at the tank's design head.

## 2.8 Electric Hoist

With a view to easing the materials handling problem a movable hoist rail was hung from the overhead shelter structure. An electric hoist with a safe working load of 1 ton moving on this rail allows items of equipment, sections of the cover and aquifer material to be transferred to and from the tank.

## 2.9 Outer Aquifer Retaining Barrier

Initially it was intended to use only 16 gauge perforated steel sheets, joined together to form a circular barrier, to retain the aquifer material,

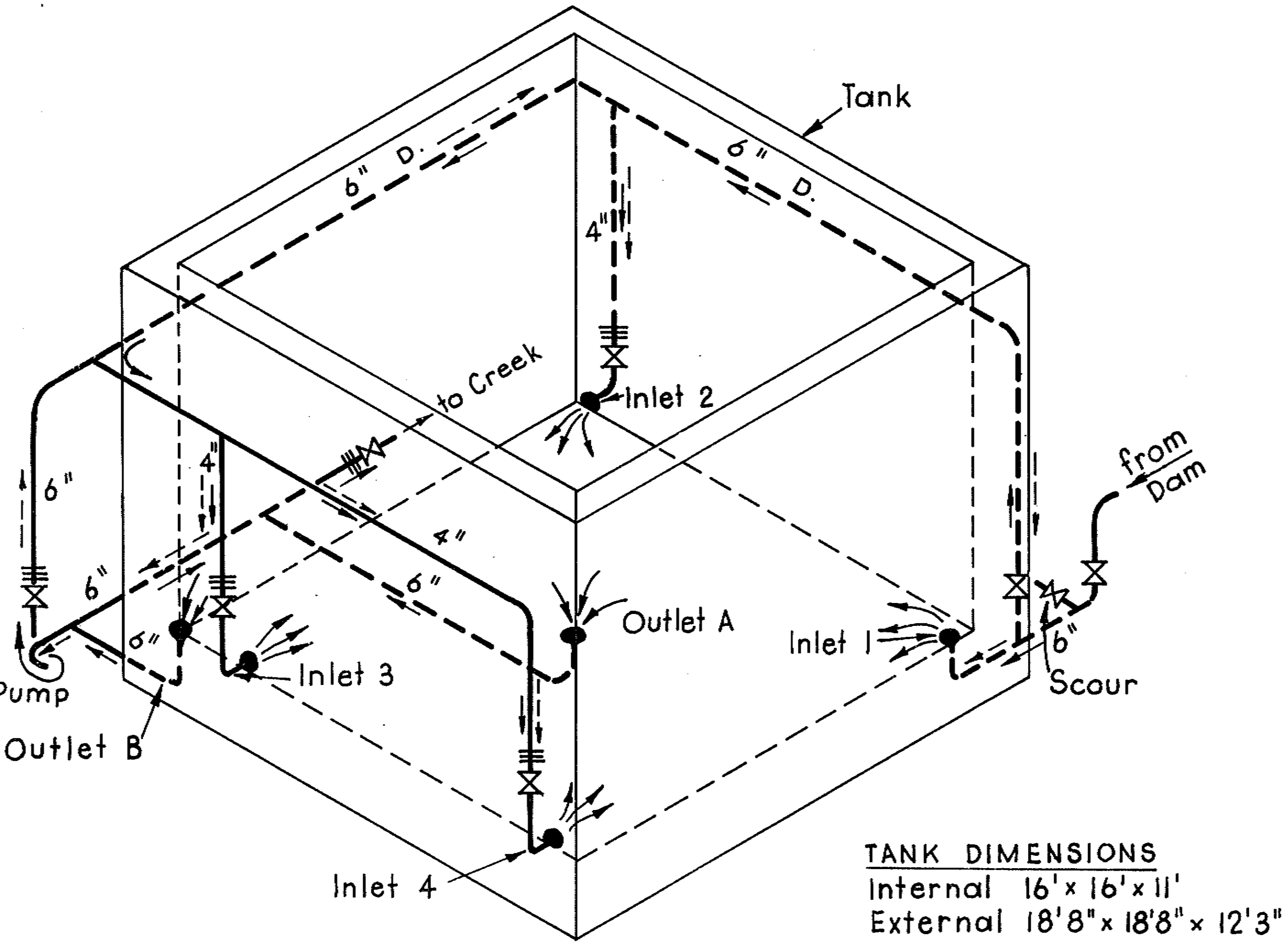


≡ Orifice Plates shown thus

1. With ¼ well under investigation Inlet 1 only to be used and Outlet A, to be blank flanged; valves on Inlets 2,3,4 to be enclosed.
2. With full well under investigation use all Inlets and blank flange outlet B
3. With pump in operation flow shown – – –►; gravitate ———►

FIGURE 2·4: EXPERIMENTAL FACILITY PIPEWORK AND FLOW DIAGRAM

Figure 2.5: Internal View of Observation Wall.

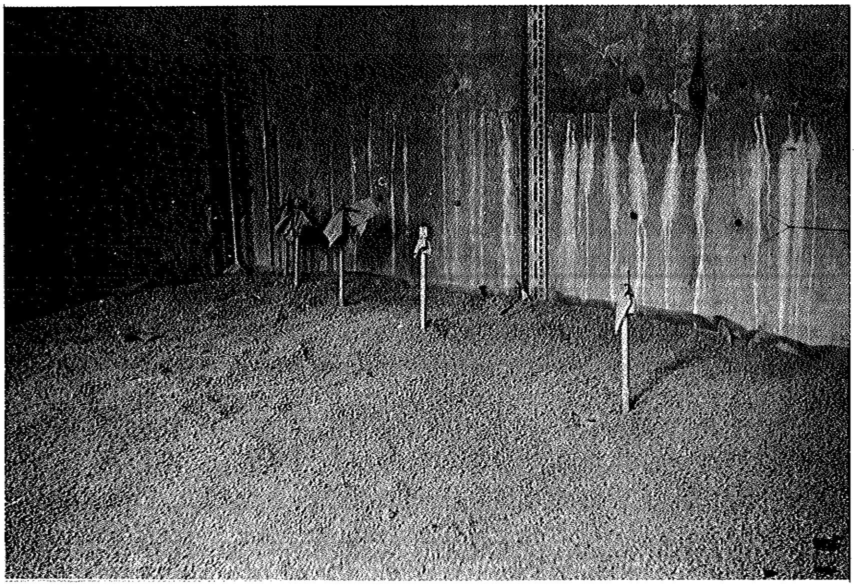

Figure 2.6: View of Aquifer Material in Tank showing Location of Inner Aquifer Retaining Barrier and Multiple Observation Wells.

allowing the load to be taken by the metal in hoop tension. However, difficulties arose in transferring the load between sheets, and to the tank wall in the case of a quadrant aquifer, as it was decided to limit the aquifer thickness to 5 feet until suitable connections could be developed. The solution adopted was to connect the sheets to prefabricated curved steel frames bolted together to form a cylindrical barrier. Connection of these frames together and to the walls by bolts can be done quickly and easily with the aid of the hoist.

### 2.10 Inner Aquifer Retaining Barrier

A 4 feet radius inner barrier was provided to allow aquifer material close to the well to be removed without disturbing the bulk of the aquifer. This allowed the task of changing screens and gravel pack material to be speeded up and the packing of the major part of the aquifer to remain unchanged. The barrier was made from perforated 16 gauge steel sheet, curved and corrugated to allow it to resist compressive loading without buckling. The open area of the barrier was 52% which was considered great enough to prevent additional flow resistance being introduced at this point. This view was confirmed by observation of the hydraulic grade line through the aquifer in the vicinity of the barrier.

A view of part of the interior of the tank showing the positions of the corner well and inner retaining barrier is shown in Figure 2.6.

## 3. Instrumentation

### 3.1 Piezometer Tappings

Copper tubes were set into the tank floor during construction on a radial line from the corner well outlet to the diagonally opposite corner. The spacing was varied as shown in Figure 3.1 to allow for the greater rate of variation of pressure towards the well locations. The tubes were led to the outer edge of the tank base, those originating between the corner and centre well positions terminating in the annexe, the remainder in the covered space on the opposite side. A screwed brass tee fitted to the end of each tube allowed permanent connections to be made to a bank of manometer tubes and additional connections to pressure gauges or transducers as required.

Additional piezometers can be inserted at any point required by taking advantage of the access holes in the walls.

### 3.2 Pressure Gauge and Transducers

A "Precision Pressure Gauge", Model 145, was purchased from Texas Instruments Inc., U.S.A., to allow rapid and accurate measurements of pressure to be made for both steady and unsteady flow conditions. It is also intended to use capacitance pressure transducers for unsteady flow work in future studies in the tank.

### 3.3 Orifice Plate Meters

Discharges were measured by D and D/2 orifice plate meters manufactured according to the specifications of the British Standard Code for Flow Measurement, B.S. 1042, Part I, 1964. The upstream and downstream lengths of adjacent straight piping specified by the code could not be provided because of the short piping runs but the deviations from the standard were not great. Calibration runs showed no significant differences between computed and actual discharge coefficients for all flow conditions.

Meters were provided on the discharge side of the pump and at each of the corner inlets so that the total flow and distribution of flow could be measured.

### 3.4 Contact Electrode Gauge for Measuring Water Levels

A relatively inexpensive stainless steel contact electrode using a low voltage battery, transistorised amplifying circuit and indicator light was developed for measuring water levels in the main and observation wells. It proved to be accurate and reliable and warrants development as a field instrument.

### 3.5 Multiple Observation Well

To allow measurement of piezometric heads to be made at various levels at a given point in the aquifer a multiple observation well was developed. This consisted of a length of P.V.C. tube with holes drilled at 1 foot intervals and a series of sliding valves which allowed the holes to be covered or uncovered as required without disturbing the piezometer tube or the surrounding aquifer material. The valves were operated by a rod inserted from the top of the well.

These observation wells were placed in the aquifer on a line radiating from the pumped well.

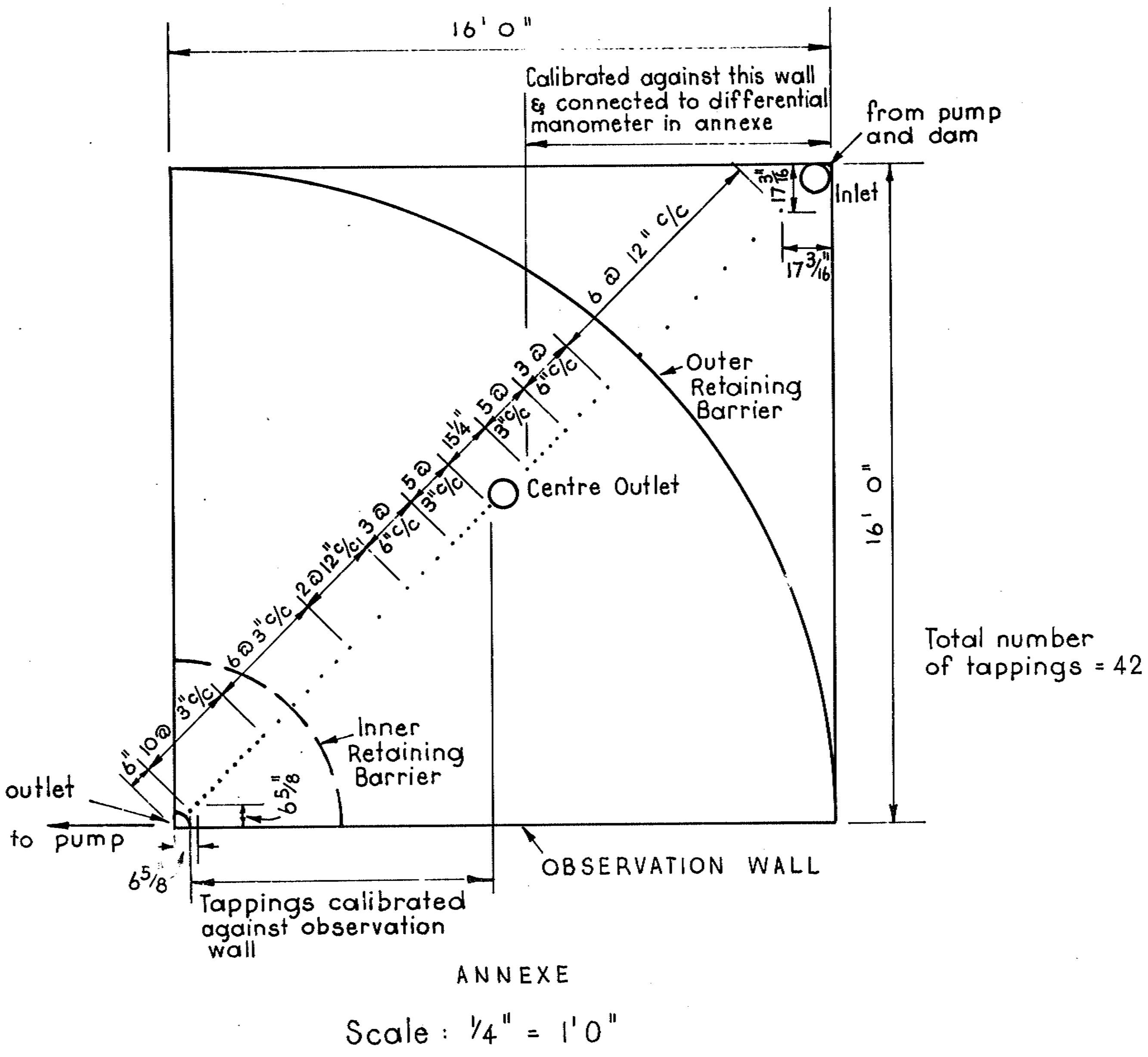


FIGURE 3·1 : LOCATION OF PIEZOMETER TAPPINGS AND AQUIFER RETAINING BARRIERS

## 4. Operation of Experimental Facility

### 4.1 Calibration

The manifolds which linked the manometer tubes on each side of the tank were joined through a connecting manometer so that levels on each side could be inter-related. Since the roofs of the instrumentation annexe and walkway were at different levels it was found necessary to depress the water levels in the manometer tubes in the walkway below the corresponding levels in the annexe. Horizontal lines at 1 foot vertical intervals were drawn on the tank walls behind the manometers to allow readings to be compared. Distances between calibration lines were measured with a 12 inch rule to an accuracy of 1/16 inch.

The tappings of the orifice plate meters were connected to a panel of manometers provided with scales graduated to 1/8 inch. Calibration runs using the best, worst and intermediate combinations of flow rate and orifice diameter showed that differential heads measured on these scales did not differ significantly from values computed according to the flow code B.S. 1042 despite the upstream and downstream pipe lengths being somewhat shorter than specified by the code. The tank served as a volumetric measuring tank for flow meter calibration. Water was run into or out of the tank through the meters over measured time and depth intervals.

### 4.2 Placement of Aquifer Material

Aquifer material was placed in the tank by tipping it from buckets carried by the hoist. Care was taken to avoid uneven compaction.

### 4.3 Flooding of Aquifer Material

The tank was filled slowly to allow time for air to escape in advance of the wetting front. There was no indication of appreciable volumes of air trapped between the aquifer particles.

### 4.4 Determination of Effective Porosity of Aquifer

After initial wetting, the aquifer was allowed to drain for a week. The tank was then re-filled slowly. The volumes of water required to fill the pores in the aquifer were determined over successive depth increments. Effective porosity values were calculated from the measured volumes of gross space occupied by the aquifer and water added.

## 4.5 Confined Aquifer Testing

Initial confined tests were made by covering a 5 feet thick aquifer with polythene sheeting held down by several inches of aquifer material and sealed to the edges of the tank. Water above the confining layer applied additional force to hold the sheeting down and at the same time provided head to drive water through the aquifer from the outer perforated metal boundary to the well which was left open to the atmosphere.

Because of the shortage of time between completion of construction of the tank and the completion of the current project it was decided to defer the use of the pressure resisting lid until experiments on development processes were performed in the succeeding project. Further confined tests at higher flow rates could be carried out at that time in conjunction with determining the effects of development on the hydraulic characteristics of the aquifer material near the well.

It was found that, even with the relatively small heads available with the open tank, non-Darcy flow occurred near the well, allowing sufficient data to be obtained for comparison with computed values.

## 4.6 Unconfined Aquifer Testing

Priority was given to confined aquifer tests as by far the greatest proportion of aquifers throughout Australia are of this type. However, by drawing down the water surface in the well sufficiently, the confined aquifer could be used for unconfined flows as the aquifer material was coarse enough to allow ready entry of air and make capillary fringe effects negligible. It was thus possible to obtain experimental data for comparison with computed values for unconfined flow. Measurements of the vertical variation in head at various distances from the well were also made for comparison with computed values.

# 5. Laboratory Tests

## 5.1 Objectives

The ultimate objectives of the laboratory tests in the experimental facility are to investigate under controlled conditions flow through well screens and the surrounding zone of the aquifer which is affected by construction and development of the well. Losses can then be identified, calculated and minimised and flow rates maximised.

In the laboratory tests performed to date, the objectives included verification of the steady state flow analysis postulated in the numerical studies for a confined aquifer , the determination of the coefficient of hydraulic conductivity 'k', the determination of the Forchheimer coefficients 'a' and 'b', the determination of the critical Reynolds Number $\mathbb{R}_{cr}$ for the transition from the linear flow regime to the nonlinear flow regime and the determination of the effect of the inner aquifer retaining barrier on the flow.

## 5.2 Test Procedures

Before the commencement of tests the experimental tank was allowed to fill slowly in order to allow the vast majority of the air in the pores of the aquifer to escape. Once the water level in the experimental tank had covered the top of the aquifer model the remainder of the volume of the tank was filled rapidly.

Careful examination of all piezometer and manometer tubes was carried out to ensure no airlocks were present. Any airlocks were subsequently removed by flushing.

The recirculating pump was then started and run for a period of approximately 15 minutes to ensure that all air trapped in the recirculating pump, pipeline and aquifer material near the well screen was removed as evident from the lack of air bubbles in the recirculated water entering the tank in the stilling area outside the outer aquifer retaining barrier. During this time the desired flow rate was set by means of a throttling valve on the opposite side of the tank to the instrumentation annexe.

When all air had been removed, the pump was shut off and the system allowed to settle down. This afforded time to recheck all the piezometer and manometer tubes.

The differential manometer levels for the orifice plate meter above the pump were then depressed and the pump started. Careful manipulation in depressing the levels of the manometer was required after the starting of the pump in order to keep the levels on scale. The depression of the manometer levels was accomplished with the aid of compressed air from a small cylinder.

Upon attaining steady state conditions the orifice manometer was then observed, followed by the observation of the connecting manometer between the piezometer manifolds, the well drawdown and then the piezometer tubes. Periodic checks were made of the levels in the orifice manometer, the connecting manometer of the piezometer manifolds and the well drawdown to ensure that steady state conditions were attained. Any major fluctuations resulted in the test being discarded and a new test re-run at the same discharge.

At the completion of the test, the throttling valve was reset to a new discharge and the test procedure repeated.

## 5.3 Experimental Results - Confined Aquifer

### 5.3.1 Laboratory Test Results

All results obtained from the laboratory tests were tabulated, and later prepared for inclusion as data into a Fortran IV computer programme for processing. A tabulation of the results from twentyone tests is given in Table 1. A semi-logarithmic plot of drawdown against radial distance from the well for six of these tests is shown in Figures 5.1 and 5.2.

### 5.3.2 Sieve Analyses

Sieve analyses were performed on the aquifer material used in the laboratory tests. The results of the analyses using the British standard sieve series are given in Figure 5.3.

### 5.3.3 Effective Porosity Measurements

The effective porosity of the aquifer material was determined by volume measurement during the slow filling of the tank and aquifer model. Results of the tests are tabulated in Table 2.

Table 1: Experimental Results - Confined Aquifer

| Test | Discharge Q (cusecs) | Well Draw-down $s_w$ | Drawdown at Radius r from Well, s(ft) | | | | | | | |
|---|---|---|---|---|---|---|---|---|---|---|
| | | | r=0.50 | 0.75 | 1.00 | 1.50 | 3.00 | 5.00 | 7.00 | 10.00 |
| 1 | 0.052 | 0.080 | 0.070 | 0.062 | 0.057 | 0.046 | 0.026 | 0.010 | 0.002 | 0.000 |
| 2 | 0.083 | 0.18 | 0.164 | 0.143 | 0.133 | 0.112 | 0.081 | 0.055 | 0.039 | 0.029 |
| 3 | 0.129 | 0.31 | 0.253 | 0.212 | 0.191 | 0.160 | 0.108 | 0.066 | 0.045 | 0.019 |
| 4 | 0.183 | 0.47 | 0.364 | 0.309 | 0.270 | 0.228 | 0.161 | 0.109 | 0.077 | 0.041 |
| 5 | 0.204 | 0.59 | 0.466 | 0.403 | 0.356 | 0.294 | 0.205 | 0.143 | 0.101 | 0.052 |
| 6 | 0.213 | 0.73 | 0.533 | 0.486 | 0.419 | 0.346 | 0.247 | 0.174 | 0.116 | 0.070 |
| 7 | 0.222 | 0.76 | 0.541 | 0.437 | 0.382 | 0.314 | 0.221 | 0.142 | 0.093 | 0.043 |
| 8 | 0.272 | 0.80 | 0.606 | 0.518 | 0.450 | 0.366 | 0.257 | 0.179 | 0.127 | 0.070 |
| 9 | 0.282 | 0.99 | 0.740 | 0.594 | 0.516 | 0.417 | 0.292 | 0.193 | 0.130 | 0.066 |
| 10 | 0.313 | 1.23 | 0.890 | 0.708 | 0.609 | 0.489 | 0.328 | 0.219 | 0.140 | 0.068 |
| 11 | 0.341 | 1.37 | 1.005 | 0.796 | 0.677 | 0.546 | 0.369 | 0.244 | 0.161 | 0.083 |
| 12 | 0.367 | 1.57 | 1.146 | 0.896 | 0.766 | 0.615 | 0.422 | 0.281 | 0.182 | 0.094 |
| 13 | 0.399 | 1.75 | 1.25 | 0.99 | 0.834 | 0.666 | 0.454 | 0.308 | 0.198 | 0.099 |
| 14 | 0.433 | 2.03 | 1.453 | 1.130 | 0.964 | 0.716 | 0.516 | 0.349 | 0.219 | 0.115 |
| 15 | 0.484 | 2.38 | 1.696 | 1.336 | 1.115 | 0.875 | 0.589 | 0.391 | 0.250 | 0.125 |
| 16 | 0.550 | 2.95 | 2.065 | 1.086 | 1.336 | 1.042 | 0.693 | 0.464 | 0.292 | 0.146 |
| 17 | 0.593 | 3.35 | 2.353 | 1.792 | 1.511 | 1.177 | 0.774 | 0.520 | 0.328 | 0.167 |
| 18 | 0.608 | 3.46 | 2.385 | 1.823 | 1.526 | 1.187 | 0.778 | 0.521 | 0.328 | 0.169 |
| 19 | 0.624 | 3.55 | 2.454 | 1.871 | 1.563 | 1.214 | 0.787 | 0.522 | 0.334 | 0.167 |
| 20 | 0.633 | 3.60 | 2.525 | 1.943 | 1.641 | 1.287 | 0.886 | 0.568 | 0.334 | 0.188 |
| 21 | 0.708 | 4.40 | 3.048 | 2.334 | 1.933 | 1.503 | 0.975 | 0.654 | 0.417 | 0.214 |

Table 2: Effective Porosity Measurements

| Depth (ft.) | | Effective Porosity (percent) |
|---|---|---|
| From | To | |
| 0 | 0.5 | 33.75 |
| 0.5 | 1.0 | 31.36 |
| 1.0 | 1.5 | 32.40 |
| 1.5 | 2.0 | 30.80 |
| 2.0 | 2.5 | 30.50 |
| 2.5 | 3.0 | 30.50 |
| 3.0 | 3.5 | 36.75 |
| 3.5 | 4.0 | 38.68 |
| | | Mean Porosity 33.1 per cent |

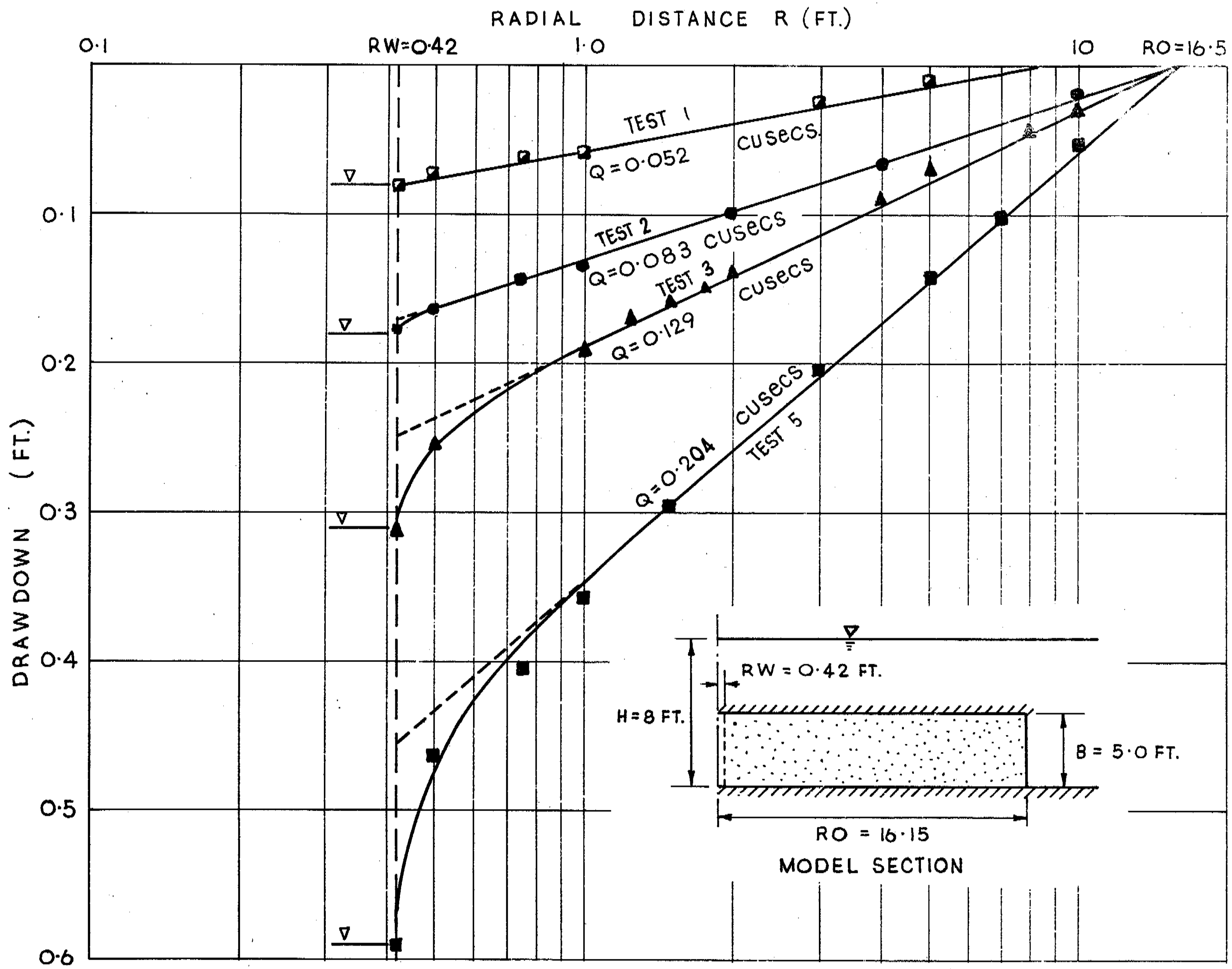


Figure 5.1: Typical Drawdown Curves - Confined Aquifer.

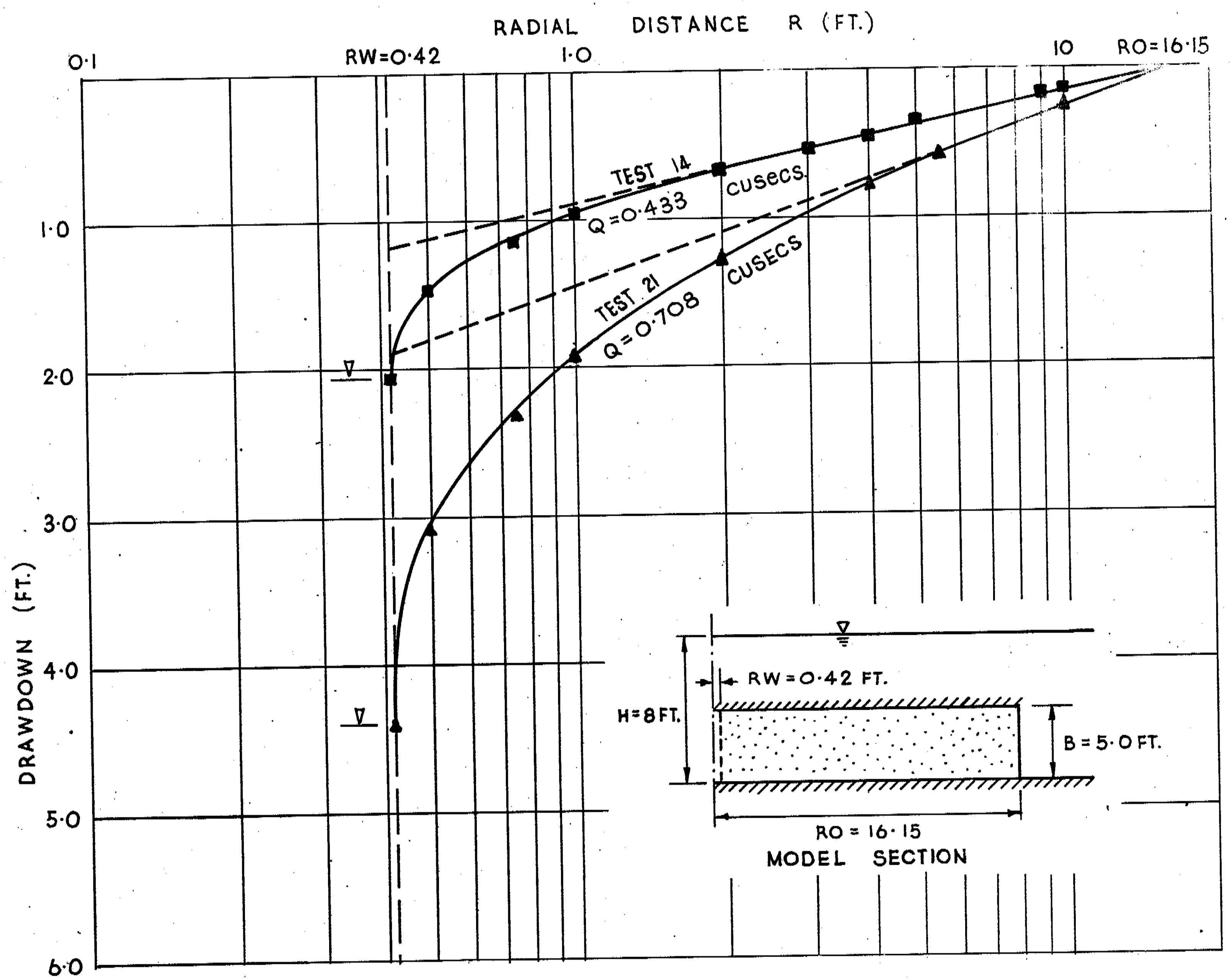


Figure 5.2: Typical Drawdown Curves - Confined Aquifer.

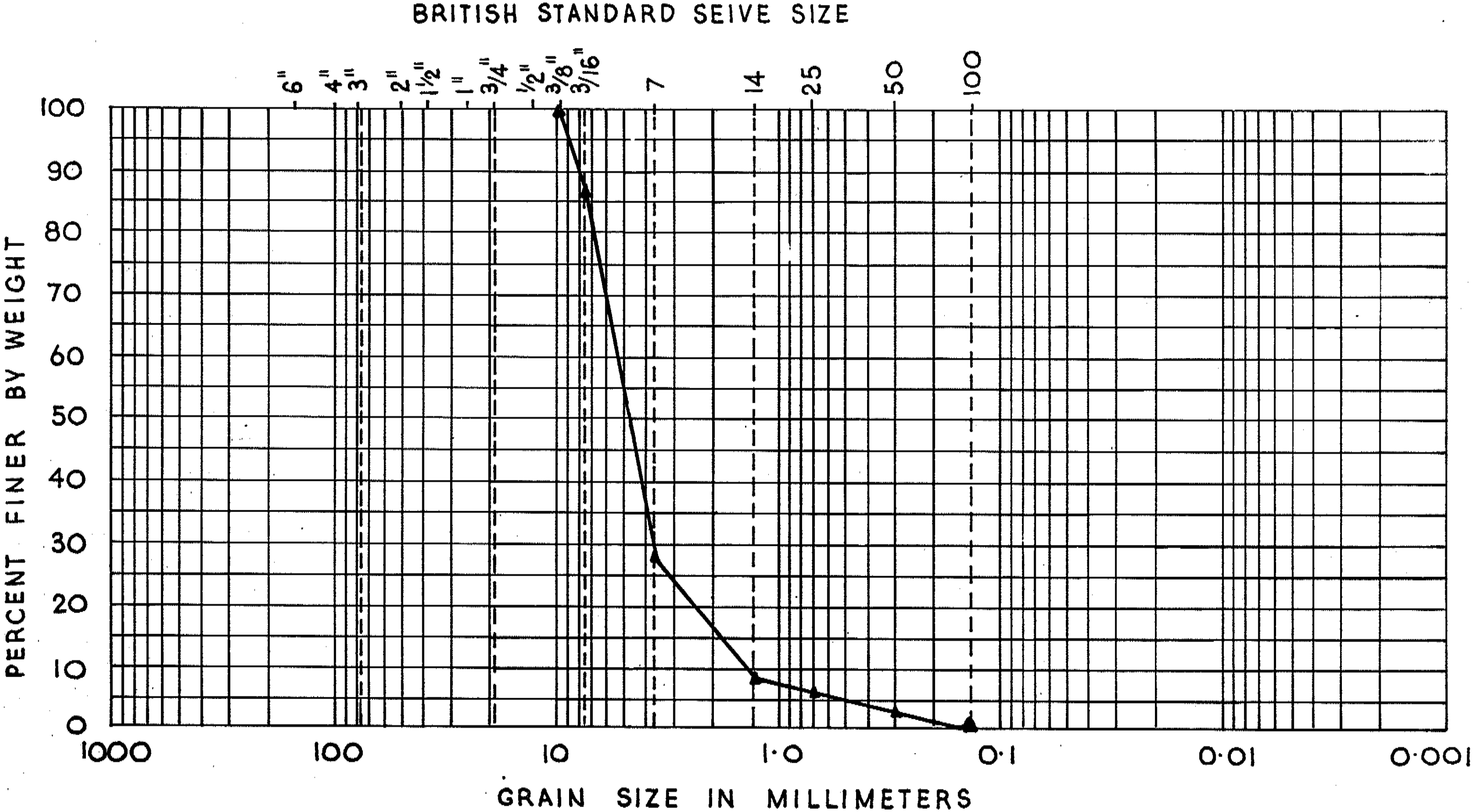


Figure 5.3: Size Grading Aquifer Material - Confined Aquifer.

## 5.4 Analysis of Experimental Results

### 5.4.1 Determination of the Coefficient of Hydraulic Conductivity 'K'

The value of the coefficient of hydraulic conductivity 'K' was determined from the slope of the straight line portion of the drawdown curves, in conjunction with the use of equation (5.1).

$$K = \frac{2Q}{\pi m \Delta s} \ln \left( \frac{r_2}{r_1} \right) \tag{5.1}$$

The results of the analysis are shown in Table 3. Test 21 was not included as there was some dewatering of the aquifer due to the water level in the well being below the top of the aquifer model.

Table 3: Coefficient of Hydraulic Conductivity 'K'

| Test | $\Delta s$ (ft) | $\ln \frac{r_2}{r_1}$ | Q (cusecs) | K (ft/sec) |
|---|---|---|---|---|
| 1 | 0.08 | 3.65 | 0.052 | 0.2437 |
| 2 | 0.17 | 3.65 | 0.083 | 0.2268 |
| 3 | 0.25 | 3.65 | 0.129 | 0.2397 |
| 4 | 0.345 | 3.65 | 0.183 | 0.2464 |
| 5 | 0.455 | 3.65 | 0.204 | 0.2083 |
| 6 | 0.52 | 3.65 | 0.213 | 0.1913 |
| 7 | 0.53 | 3.65 | 0.222 | 0.1946 |
| 8 | 0.56 | 3.65 | 0.272 | 0.2257 |
| 9 | 0.62 | 3.65 | 0.282 | 0.2113 |
| 10 | 0.75 | 3.65 | 0.313 | 0.1939 |
| 11 | 0.85 | 3.65 | 0.341 | 0.1863 |
| 12 | 0.93 | 3.65 | 0.367 | 0.1833 |
| 13 | 1.00 | 3.65 | 0.399 | 0.1854 |
| 14 | 1.15 | 3.65 | 0.433 | 0.1749 |
| 15 | 1.25 | 3.65 | 0.484 | 0.1799 |
| 16 | 1.50 | 3.65 | 0.550 | 0.1703 |
| 17 | 1.70 | 3.65 | 0.593 | 0.1620 |
| 18 | 1.75 | 3.65 | 0.608 | 0.1614 |
| 19 | 1.77 | 3.65 | 0.624 | 0.1638 |
| 20 | 1.80 | 3.65 | 0.633 | 0.1633 |

Mean value of linear hydraulic coefficient K = 0.1956 ft/sec.

### 5.4.2 Determination of Forchheimer Coefficients 'a' and 'b'

The calculation of the Forchheimer coefficients 'a' and 'b' was performed using the theory proposed in Appendix 1 of Section C. For the purposes of the calculation the relationship between the drawdown and the discharge is assumed to be of the form

$$\frac{s_w}{Q} = A + BQ \tag{5.2}$$

where

$A$ = intercept on the $\frac{s_w}{Q}$ axis of the $\frac{s_w}{Q}$ versus Q plot

$B$ = slope of the linear $\frac{s_w}{Q}$ versus Q plot

also $A = \left( \frac{a}{2\pi m} \ln \frac{r_c}{r_w} + \frac{1}{2\pi Km} \ln \frac{r_o}{r_{cr}} \right)$

$B = \frac{b}{4\pi^2 m^2} \left( \frac{1}{r_w} - \frac{1}{r_{cr}} \right)$

The significance of equation (5.2) is illustrated in Figure 5.4. The horizontal portion of the curve corresponds to linear flow regime existing up to the critical radius. The $\frac{s_w}{Q}$ value of this horizontal line will be denoted by D and is given by Equation (5.3).

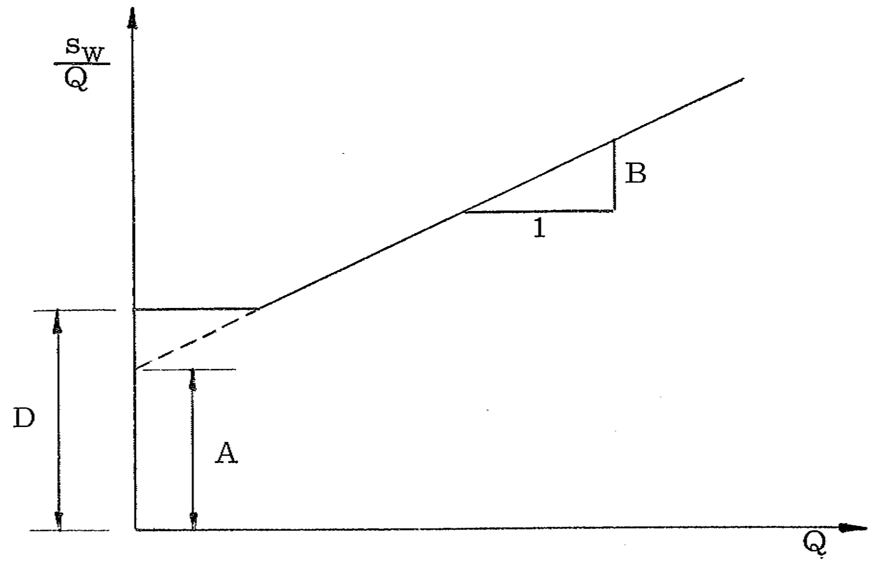


Figure 5.4: Significance of $\frac{s_w}{Q} = A + BQ$

$$D = \frac{1}{2\pi Km} \ln \left(\frac{r_o}{r_w}\right) \qquad (5.3)$$

It is assumed further that the ratio of a to 1/K is in the same ratio as A to D, consequently

$$\frac{D}{A} = \frac{1}{Ka} \qquad (5.4)$$

From the $\frac{s_w}{Q}$ against Q plot (Figure 5.5) for the aquifer model tested and the knowledge of the value of K

$$D = 0.593$$

$$A = 0.52$$

Hence $\frac{1}{Ka} = \frac{0.593}{0.52} = 1.14$

then

$$a = \frac{1}{1.14K}$$

$$= 4.475 \text{ sec/ft.}$$

$$= 0.075 \text{ min/ft.}$$

Also the slope $B = \frac{0.5}{4 \times 0.34} = 0.365$

and $b = \frac{C\, 4\, \pi^2\, m^2}{\frac{1}{r_w} - \frac{1}{r_{cr}}}$

For a typical test which lies close to the line of best fit, for example test 20, $r_{cr} = 3.7$ and,

$$b = \frac{0.365 \times \;^{2} \times 5^{2} \times 4}{2.1}$$

$$= 173 \text{ sec}^2/\text{ft}^2 = 0.048 \text{ min}^2/\text{ft}^2$$

A drawdown discharge curve for all test results has been included for the sake of completeness (Figure 5.6).

### 5.4.3 Determination of the Critical Reynolds Number $\mathbb{R}_{cr}$

The critical velocity $V_{cr}$ was calculated from the knowledge of the coefficient of hydraulic conductivity 'K' and the Forchheimer coefficients 'a' and 'b' and relationship (5.5)

$$V_{cr} = \frac{1}{b}\left(\frac{1}{K} - a\right) \tag{5.5}$$

For values of $K = 0.196$ ft/sec.
$a = 4.475$ sec/ft.
$b = 173$ sec$^2$/ft$^2$

then $V_{cr} = 0.0037$ ft/sec.

The critical Reynolds Number $\mathbb{R}_{cr}$ was then calculated by relationship (5.6)

$$\mathbb{R}_{cr} = \frac{V_{cr}\ \bar{d}}{\quad} \tag{5.6}$$

Adopting a temperature of $68^{\circ}$F for the purposes of the calculation

$$= 1.94 \text{ slugs/ft}^3$$

$$= 2.1 \times 10^{-5} \text{ lb sec/ft}^2$$

and $\bar{d} = d_{90} = 4.92 \times 10^{-3}$ ft.

Hence $$\mathbb{R}_{cr} = \frac{0.0037 \times 0.00492 \times 1.94}{0.000021} = 1.7$$

### 5.5 Discussion of Results

The drawdown curves obtained in Figures 5.1 and 5.2 provide verification of the two flow regime adopted in the theoretical analysis.

In the drawdown curves of Figures 5.1 and 5.2 there appears to be an additional drawdown in the well, over and above the formation losses which increases with increasing discharge. The additional drawdown is more than likely the result of screen losses although this has not been fully substantiated. At this point it should be noted that all of the computations performed neglected the existence of screen losses.

During the tests it was assumed that no increase in permeability resulted from development of the aquifer material surrounding the screen.

With regard to the coefficients, 'a', 'b', and 'K' it should be borne in mind that the values obtained from the experimental results are at best only approximate values. The degree of certainty that can be assigned the calculated value of K is reasonably high as this has been obtained directly from the slope of the straight line portion of the drawdown curve. However, the degree of certainty which can be assigned to the values of 'a' and 'b' is not as high. The values of 'a' and 'b' are estimated to be within 10 per cent of their correct values. It should be realised that this estimated error and the values of 'a', 'b' and 'K' require verification by permeameter tests on the aquifer material. This will be carried out shortly.

The values for 'K', 'a', 'b', and '$\mathbb{R}_{cr}$' obtained by the methods outlined, compare favourably with the values obtained for similar size materials tested and tabulated in Section C.

Finally, any effect of the inner aquifer retaining barrier upon the flow profile through the aquifer model from the drawdown curves appears to be negligible.

## 5.6 Conclusions and Further Work

The analysis of the experimental results presented shows that the flow of water towards a heavily pumped well is of a two flow regime nature, the two flow regimes being

(a) linear; governed by a hydraulic gradient velocity relationship

$$v = Ki \tag{5.7}$$

(b) non-linear; governed by a hydraulic gradient-velocity relationship

$$i = av + bv^2 \tag{5.8}$$

The extent of the non-linear flow regime can be specified indirectly by the critical Reynolds number $\mathbb{R}_{cr}$.

The existence of increasing screen losses appearing in the drawdown curves for increasing discharge warrants further investigation. Further studies will include the effects of partial penetration, well radius, drilling and development and different screen types under transient and steady state conditions for confined and unconfined aquifers.

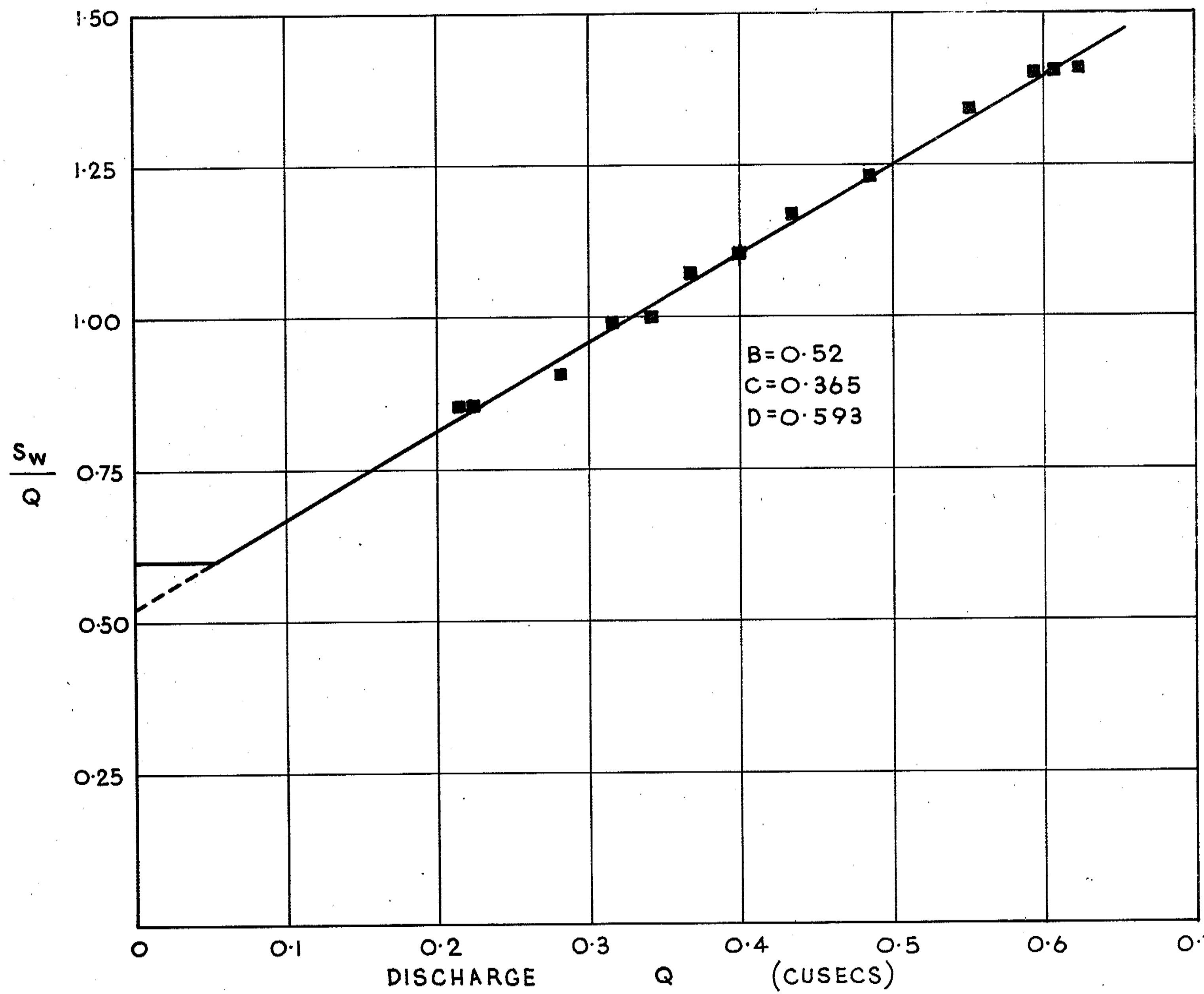


Fig. 5.5: $\frac{S_W}{Q}$ versus Q plot.

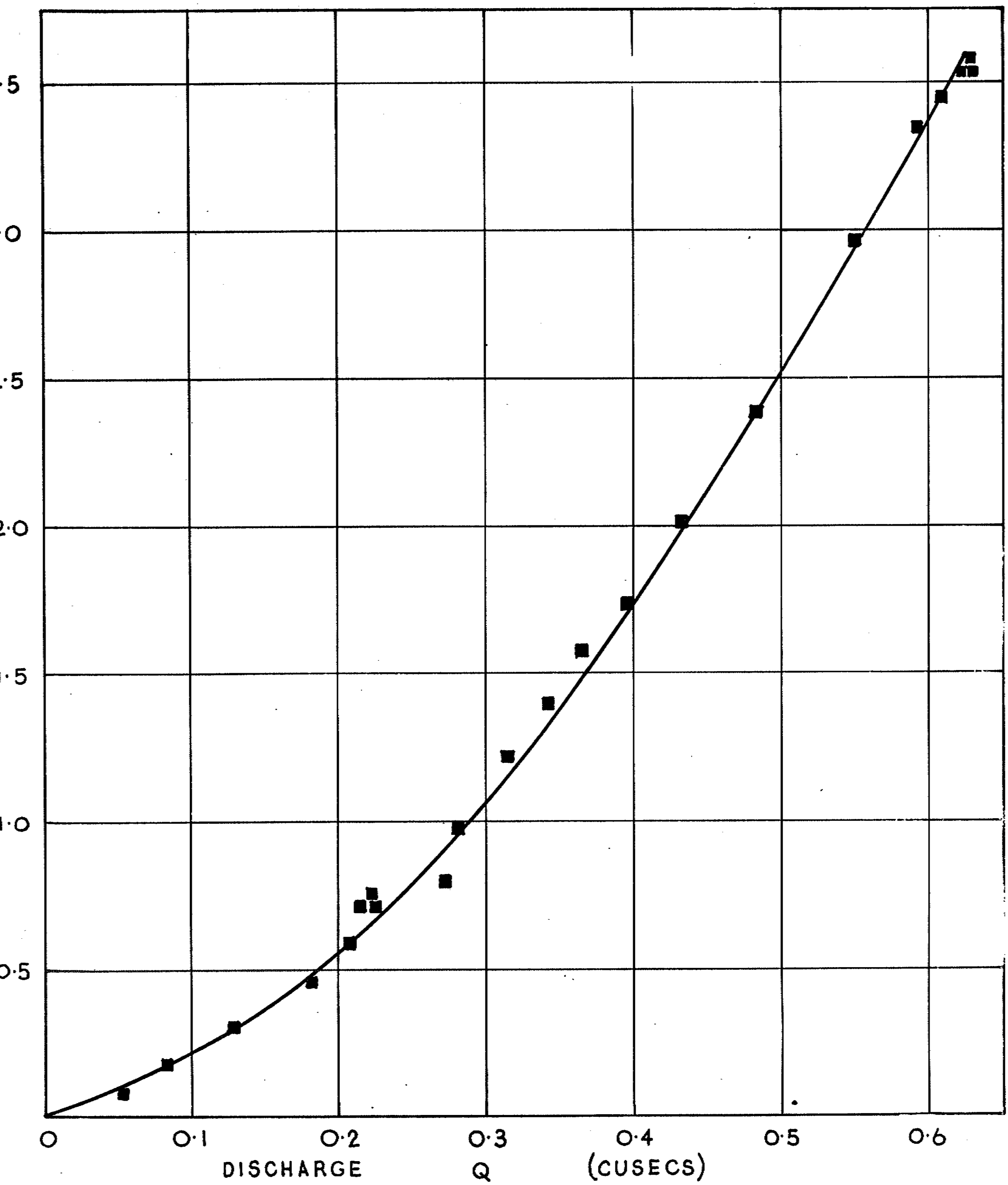


Fig. 5.6: $S_W$ versus Q plot.